THE ROLES OF PHOSPHORYLATION IN MUMPS VIRUS RNA SYNTHESIS AND REPLICATION

by

JAMES ZENGEL

(Under the Direction of Biao He)

ABSTRACT

Mumps virus (MuV) is a paramyxovirus with a negative-sense non-segmented, negative-strand RNA-genome. MuV infects humans causing acute infection with hallmark enlargement of the parotid gland [1]. Although in incidence of mumps has greatly decreased since introduction of vaccines in the late 1960's, there have been large outbreaks in highly vaccinated population [2–6]. To better control these outbreaks, we need to better understand the replication of MuV and the role of MuV proteins in replication and pathogenesis. It has been known for over 30 years that many of the MuV proteins are phosphorylated, but until recently the role of phosphorylation of these proteins had not been studied [7]. In the follow body of work, we aim to better understand the role of phosphorylation in MuV RNA synthesis and replication and apply these finding to enhance the yield of a candidate vaccine in cell culture. We determined the major phosphorylation site in the nucleoprotein (NP) to be at position S439, and show that phosphorylation at this site has a negative effect on RNA synthesis and peak viral titers. We also build on previous research on phosphorylation of the phosphoprotein (P) [8] by determine the kinase involved in the phosphorylation of the MuV P protein to be

PLK1 and showing the NP is important for P phosphorylation. The binding site for P was determined to be at residue T147, and mutation of this residue to prevent PLK1 binding and phosphorylation of other residues in P resulted in increased MuV growth in cell culture. We used what was learned in the basic research into the phosphorylation of MuV proteins to enhance the growth of a novel MuV vaccine candidate previously developed in our lab [9]. By introducing an alanine substation mutation at position T147 and rescuing a vaccine virus containing the T147A mutation, we increased vaccine yield 10-fold in vero cells. This work allows for a better understanding of how phosphorylation effects MuV RNA replication and growth and the findings advanced the development of a next generation MuV vaccine candidate.

INDEX WORDS: Mumps; MuV; paramyxovirus; vaccine; phosphorylation; nucleoprotein; phosphoprotein; kinase; polo-like kinase 1; PLK1

THE ROLES OF PHOSPHORYLATION IN MUMPS VIRUS RNA SYNTHESIS AND REPLICATION

by

JAMES ZENGEL

BS, University of California, Berkeley, 2008

A Dissertation Submitted to the Graduate Faculty of The University of Georgia in Partial Fulfillment of the Requirements for the Degree

DOCTOR OF PHILOSPHY

ATHENS, GEORGIA

2017

THE ROLES OF PHOSPHORYLATION IN MUMPS VIRUS RNA SYNTHESIS AND REPLICATION

by

JAMES ZENGEL

Major Professor:	Biao He
Committee:	Melinda Brindley
	Kimberley Klonowski
	Ming Luo
	Ted Ross

Electronic Version Approved:

Suzanne Barbour
Dean of the Graduate School
The University of Georgia
August 2017

ACKNOWLEDGEMENTS

I would like to thank my major professor, Biao He, for his help and support through my time in his lab. I would like to thank my committee for their advice and guidance while I was working on my thesis work. I would like to thank all my lab members, past and present, for their help with experiments, writing, and friendship throughout my graduate career. I would like to thank all my friends and colleagues for making my time at UGA a great experience. I would like to thank my family for always supporting me. And I would like to thank Shannon for always supporting me, and making every day better.

TABLE OF CONTENTS

Page

LIST OF TABLES

Page

LIST OF FIGURES

Page

CHAPTER 1

INTRODUCTION

Mumps virus (MuV) is a paramyxovirus with a negative-sense, non-segmented RNA-genome. MuV infects humans causing acute infection with hallmark enlargement of the parotid gland [1]. Widespread vaccination in the United States with the Jeryl Lynn vaccine strain, which began in the late 1960s, has led a large reduction in the number of infections. While the number of cases has been greatly reduced , there have been multiple large outbreaks (>1000 cases) in the United States and Europe over the past decade [2–5]. In these outbreaks at least 90% of the individual infected received the measles, mumps, and rubella (MMR) vaccine [6]. New strategies to control these outbreaks are needed. Understanding the roles of each of the MuV proteins in virus replication and pathogenesis will aid in the development of countermeasures for MuV.

While there is a general understanding of the roles of the various MuV proteins based on previous studies or inferences from closely related viruses, such as PIV5. There are still many aspects of MuV replication and pathogenesis that are not well understood. Our lab has previously shown that phosphorylation of P plays a critical role in viral RNA synthesis [8]. The hypothesis for the proposed research is transcription and replication of MuV is controlled by phosphorylation of NP and the NP-dependent phosphorylation of P. The following specific aims will be addressed:

Specific Aim 1: Determine the phosphorylated residues in MuV NP that are critical for viral transcription and replication. Phosphorylation of NP was demonstrated

through radioactive labeling MuV infected chicken cells [7], but the role of this phosphorylation is still not understood. Phosphorylation sites in NP will be predicted through the use of *in silico* prediction and mass spectrometry. The role of phosphorylation at selected sites will be determined using a minigenome system and incorporation of mutations at selected sites into rescued MuV. The working hypothesis is that phosphorylation of residues in MuV NP play a role in viral RNA transcription and replication.

Specific Aim 2: Determine host kinases that are involved in the phosphorylation of MuV proteins. We have found that many of the MuV proteins are phosphorylated, yet the kinases responsible for the phosphorylation have not been identified. Because MuV is not thought to encode kinase activity, we believe that we can identify host kinases responsible for the phosphorylation of viral proteins. We will first identify potential phosphorylation sites through sequence based prediction, mass spectrometry, and mutagenesis. We hypothesize that we can use kinase motif prediction algorithms and siRNA screening to determine which host kinases are important for viral replication and transcription.

Specific Aim 3: Improve the lead MuV vaccine candidate by altering NP and P phosphorylation sites. A vaccine candidate based on the genotype G mumps virus (MuV/Iowa/2006) was modified to prevent transcription of V and delete the SH gene (MuV-dVdSH). This vaccine was shown to be immunogenic in mice and have a good safety profile [9], but the replication of the vaccine candidate in cell culture was attenuated. We hypothesis that growth of the vaccine candidate may be enhanced

through the incorporation of mutations in NP and P, which increase virus growth in cell culture, while maintaining attenuation of pathogenesis *in vivo*.

A sub aim for this project is to determine if vaccination with MuV-dVdSH can produce an immune response to currently circulating mumps genotype better than vaccination with the current Jeryl Lynn vaccine. It has previously been shown that the Jeryl Lynn vaccine (genotype A) produces lower neutralizing titers to the major genotype circulating in the United States (genotype G). We would also like to determine if there are differences in heterologous neutralization between other genotype, specifically genotype F, which is currently the major circulating genotype in China. The working hypothesis is that the MuV-dVdSH vaccine candidate based on the genotype G virus, MuV/Iowa/06, will produce a better immune response to currently circulating strains in the United States and China when compared to the Jeryl Lynn vaccine.

CHAPTER 2

LITERATURE REVIEW

Classification, history, and impact

Mumps is believed to first be described by Hippocrates in the 5th century BC [1] and the virus is predicted to have entered the human population no sooner than 4000-5000 years ago based on population densities required to sustain transmission [10]. Mumps infection can result in serious complications and often involves the CNS. Involvement of the CNS during mumps disease progression was first demonstrated by Hamilton, a physician in 1790 [11], reviewed in this publication [12]. The detection of an infectious agent in the CNS during mumps infection was able to confirm this in 1943 [13].

In the early 20th century, there were many publications that suggested mumps was caused by a transmissible agent that was present in bacteria free filtrate of saliva from patients with mumps. When inoculated into various animals, some characteristics of mumps infection were recapitulated, namely swelling of the parotitis, fever, mononuclear cell infiltration, orchitis, and meningitis [14–19]. In the first of these studies, in 1908, Granata demonstrates that filterable agents isolated from patients with mumps caused disease in rabbits. Inoculation of the filtered saliva resulted in fever in infected rabbits when infected intravenously. When it was directly inoculated into the parotid gland he reported some amount of swelling. This was the first demonstration the mumps may be caused by a virus. Following this research, another group used material isolated from the

children with mumps to inoculate monkeys [18]. This caused fever and an apparent immune response, but not the classical swelling observed in people. Mumps was known to be associated with meningitis since early characterization of the disease. This included description of meningitis described in a mumps patient as early at 1758 by Hamilton. There were many other descriptions of meningitis that were summarized at the time of this early research [20,21]. This was likely the impetus for the next animal studies that were performed that looked into the neurovirulence of the filterable agent isolated from individuals with mumps [17]. Researchers found that both rhesus macaques and cynomolgus macaques developed meningitis when injected intracerebrally with the filtered agent. Over half of the cynomolgus macaques died and one of the rhesus macaques died. The same study was the first to show swelling of [14–16]the parotid glands of monkeys injected by intraperitoneal and intravenous inoculation. These results suggested that similar symptoms could be demonstrated in monkeys and that these might be a good model for further research.

Cats were another model that looked promising for mumps research and could recapitulate some of the disease seen in humans. Wollstein had multiple studies that explored aspects of mumps disease using injection of filtered lysate for patients with mumps [14–16]. Cats would develop symptoms including fevers, parotitis, meningitis, and orchitis, which are some of the major clinical symptoms seen in patients. The orchitis was associated with a decrease in spermatogenesis, which is also seen in humans. During passage of the virus over multiple generations in cats, there was an increase followed by a decrease in virulence, although specific changes in the virus could not be assessed at the time. The studies were limited by the age and route of infection with only

young cats showing disease and direct inoculation being required. Overall, this research showed that cats could be a good model for studying mumps disease.

Although up to this point, there was a large body of research showing the mumps was likely caused by a filterable agent, there was still some debate as to whether the cause could be bacterial [22–24]. Kermorgant's research found that there were spirochetes that could be isolated from mumps patients, and suggested that these were the actually causative agent for mumps. Because of the debate at the time, there needed to be conclusive evidence that demonstrated the causative agent of mumps and showed that Koch's postulates could be met.

The first study considered to conclusively show that mumps was caused by a virus agent was published in 1934 by Johnson and Goodpasture. The authors show that Rhesus macaques inoculated with filtered saliva from individuals with clinical symptoms of mumps developed symptoms consistent with those seen in humans. They also showed the saliva from healthy individuals did not cause any disease, suggesting that a virus is the causative agent of mumps [25]. These studies allowed for an early basis for MuV research. Using filtration, they established that mumps was caused by a virus. They also developed that early large animal model using Rhesus macaques that is still being pursued as one of the most relevant animal models for symptomatic MuV infection [26].

The same researchers were then able to fulfill Koch's postulates through the experimental infection of children with or without prior mumps disease. Virus isolated from infected monkeys was used to infect children. Upon clinically apparent disease, saliva from one of the children was used to infect naïve monkeys, resulting in parotitis [25,27]. In these sets of experiments published in 1934-1935, Johnson and Goodpasture

advanced the understanding of causative agent of mumps and set up basic research needed to develop a vaccine. Although the use of human subjects in the manner they were used in this study would not occur today, these experiments were important for the understanding of MuV infection and pathogenesis. Showing that a filterable agent was able to cause mumps in humans was able to initiate further research into the development of a vaccine for protection.

By 1945, multiple groups were able to show that the virus could be propagated in embryonated chicken eggs, which allowed for further characterization of the virus [28,29]. This also allowed for attenuation through serial passage in eggs, which would be later used for the development of vaccines against mumps [30].

Mumps virus properties

MuV is an enveloped, non-segmented, negative-sense RNA virus with a standard genome size of 15,384 nucleotides. It belongs to the order *Mononegavirales*, family *Paramyxoviridae*, subfamily *Paramyxovirinae*, and genus *Rubulavirus*. The MuV genome is comprised of seven transcriptional units in the order 3'-NP-V/P/I-M-F-SH-HN-L-5', with RNA synthesis initiating at a single site at the 3' end. These gene encode for nine viral proteins, with three proteins being produced by the V/P/I gene through RNA editing, where V is the faithful transcript, two guanine (G) residues are inserted to produce the P mRNA, and 4 G residues are inserted to produce the I mRNA [31]. The alternate editing of the V/P/I gene allows for proteins with multiple different functions to be transcribed using a single portion of the genome. The ability to produce multiple transcripts from a single portion of the genome allows for more functionality while not

needing to increase the size of the genome. This allows for a more efficient genome organization.

Like other paramyxoviruses, there is a transcription gradient, with the highest levels of transcription for the genes at the 3' end of the genome. The most abundant protein is the nucleocapsid protein (NP), which encapsidates the viral RNA genome, forming the ribonucleoprotein (RNP). The mumps replication complex consists of NP, the phosphoprotein (P), and the large polymerase protein (L), with P and L forming the viral RNA-dependent RNA polymerase (vRdRp) [32–34]. In the early 1970's, MuV were found to have a RNA polymerase very similar to other paramyxoviruses. Further characterization showed that both the NP and P proteins are important for replication of the viral RNA.

The P transcript was described in 1988 as containing a single open reading frame, which encoded a protein of 391 amino acids in length [35]. It was later found that there were multiple transcripts made from the P gene, and the P was not actually the faithful transcript [31]. The faithful transcript of the gene encodes the V protein, and two additional proteins are expressed when there were two and four G residues inserted during mRNA transcription, producing mRNA encoding the P and I proteins, respectively. The phosphoprotein (P) interacts with NP and L, acting as an adapter between the RNP and viral polymerase to allow for RNA synthesis [36]. P is also though to play a regulatory role in transcription and replication [8].

The structural proteins of the mumps virus are the matrix protein (M), and the two glycoproteins, the fusion (F) and the hemagglutinin-neuraminidase (HN) proteins. The matrix protein is required for viral budding and linking of the RNP with the glycoproteins

during viral assembly. Co-transfection experiments show that only M is required for budding of virus like particles (VLPs), but that the efficient budding requires other viral proteins. The maximal production of VLPs resulted when M, NP, and F were present [37]. The HN protein is a membrane-anchored, highly glycosylated protein with a globular head. HN is involved in receptor binding, through interaction with sialic acid on the cell surface, required for virus-cell attachment. It also has neuraminidase activity required for virus release [38,39]. HN is also required for efficient virus-cell and cell-cell fusion by the F protein [40]. The F protein is also glycosylated and is produced in an inactive F0 form. Host proteases are required for cleavage of F0 into the active F1 and F2 heterodimers, which are linked by two disulfide linkages [41,42].

There are also three non-structural proteins produced during MuV infection, the V, I and small hydrophobic (SH) proteins. The V protein of mumps plays a critical role in pathogenesis and is involved in host immune regulation. When expressed in cell culture, the V protein is able to block both interferon (IFN) expression and interleukin-6 (IL-6) signaling. Preventing mumps virus from expressing V through directed mutagenesis also results in attenuation [43,44]. Recent work also shows that the V protein is involved in transcription and replication in the closely related virus parainfluenza virus 5 (PIV5), which is also able to interact with the mumps virus replication complex [45]. V likely interacts with P in the shared N-terminal domain, which is involved in P oligomerization [46]. Currently the role of the I protein is unknown, but it is not required for virus replication. It likely also interacts with V and P through their shared N-terminal domain, so it could play a role through interaction with those proteins. The SH protein is a small membrane bound protein, which while not

required for viral replication [47], is involved in mediating the host immune response. SH has been shown to block the signaling of tumor necrosis factor alpha (TFN-α) [48] in transfected cells, and this effect was no longer present in cells infected with mumps virus lacking the SH ORF [49].

Transmission and symptoms

As previously discussed, MuV is present in the saliva of infected patients [27] and can be transmitted between individuals through the upper respiratory tract or conjunctiva. The virus is thought to be spread by droplet transmission. The virus has an incubation period of 12 to 25 days, with an average of 16-18 days [50,51]. Upon onset of illness, virus can be isolated from the saliva, cerebrospinal fluid, and urine. Virus could be recovered as soon as symptom onset and up to two weeks after symptom onset [52,53]. MuV is usually found in the urine of infected patients and infection of the kidneys is common yet does not cause overt pathology in the organ [54]. The characteristic symptom of mumps infection is the swelling of the parotid gland, although this swelling does not always occur and other symptoms, such as meningitis and orchitis, may occur without apparent parotitis [55,56].

Mumps is often found in the CNS, with immune cell infiltration into the CSF found in at least one third of clinically attended mumps cases. Even with this high level of CNS involvement, symptomatic CNS infection is not common and encephalitis occurs in less than 0.5% of cases [12,13,57,58]. Mumps infection can also cause hearing loss in one or rarely both ears and was the most common infectious cause of unilateral deafness before widespread vaccination [59,60]. Mizushima et. al. explored the pathogenic cause of deafness in 55 patients. They found that there was no relation between the severity of

the MuV infection and deafness. There was also a wide spread in the ages of individuals at the time of infection and no difference in the male to female ratio, suggesting that anyone infected with mumps may be at risk for more severe outcomes. The large number of cases of deafness caused by mumps illustrates that large total number of cases, since the incidence of deafness after infection was low at about 1 in 20,000 infections [60].

Although mumps is classically considered a disease of children, there are also many cases of infections in postpubertal individuals, which lead to additional symptoms and areas of infection. One major issue is orchitis, which occurs in many males that are infected with mumps after puberty [61,62]. Although it is less common, oophoritis and mastitis can occur in postpubertal females, with oophoritis possibly leading to premature menopause [63,64]. MuV infection can cause spontaneous abortion in pregnant women [65], although pregnant women do not suffer more severe disease. Another earlier study showed that infection could result in spontaneous abortion in about 25% of women, usually when infection occurred during the first trimester [66].

Although sterility due to orchitis is considered rare [67], there are many cases of sterility or decreased sperm count described [68] and the pathology behind sterility is being researched [69]. Wang et. al. showed that there was a difference in the expression of geranylgeranyl diphosphate synthase 1 (GGPPS). In infertile patients that had a previous MuV infection, there was a decrease in the GGPPS expression in the testis comparted to infertile patients that did not have a history of infection. Decrease expression of GGPPS was shown to be important for regulation of prenylation in Sertoli cells in mice, a cell type that is critical for spermatogenesis. This research suggests that these changes may result in immune responses in the testis, resulting in infertility.

Treatment and vaccination

There is currently no effective therapeutic for treatment of mumps. The administration of mumps-specific immunoglobulins has been attempted with limited success [70], but the best way to prevent mumps disease is prophylactic treatment through the use of vaccination. The current mumps vaccines are all live attenuated vaccines from various origins. Table 2.1 lists the current and past MuV vaccines (adapted from [1] Table 43.2). The most common mumps strain used in vaccines worldwide in Jeryl Lynn, which was developed through the serial passage in embryonated hen's eggs and chick embryo cell culture of a virus isolated from a child for which the virus is named [71]. There have been other vaccines produced by similar methods, including Leningrad-3 [72] and later L-Zagreb [73] in the former Soviet Union, Rubini in much of Europe [74], and Urabe in Japan, Europe, and Canada [75]. The use of many of these early vaccines was halted or scaled back due to issues with aseptic meningitis after vaccination or a lack of vaccine efficacy. Leninigrad-3 [76], Leningrad [77] and Urabe [78] vaccines all have a significant risk of aseptic meningitis of about 20-100 cases per 100,000 vaccinated individuals. This compares to a rate of less than 1 case per 100,000 vaccinated individual for the Jeryl Lynn vaccine [79]. Development of safer vaccines has in some cases led to a less effective vaccine, as was the case with the Rubini vaccine produced in the late 1980s [80]. This vaccine was later shown to have very limited efficacy compared to other vaccines and was withdrawn from use. The Rubini vaccine had a vaccine efficacy of 6.3%, compared to 61.6% for Jeryl Lynn and 73.1% for Urabe Am 9 over the same period [74].

Although the MMRV effectively decreased the total number of mumps cases in vaccinated populations, there continues to be MuV cases. The United States Department of Health and Human Services releases Healthy People objectives every ten years, looking forward at health goals in the United States over the next ten years. In 2000, there was a goal set to eliminate indigenous mumps cases by the year 2010 [81]. But, after numerous large outbreaks in the United States, this goal has now be updated to reduction of reported cases in the United States to under 500 per year [82]. The current vaccines are the best tool for preventing mumps disease, but there is debate about whether the current vaccines match the circulating MuV genotypes.

While MuV is considered to have a single serotype, there are 12 distinct genotypes. Genotyping of MuV was traditionally performed by sequencing the SH gene and corresponding non-coding gene start and gene end sequences, but was recently updated to included HN sequencing to better define genotypes [83]. In North America and parts of Europe, the most common outbreaks strains of MuVs are genotype G, while the most common vaccine strain, Jeryl Lynn, is genotype A [84,85]. Other strains have been associated with individual cases in the United States, but have not been connected to large outbreaks [83]. This may be due to differences in the infectiousness or antigenicity between the strains, although this has not been demonstrated experimentally.

In Korea, where the Jeryl Lynn (genotype A) and Urabe AM9 (genotype B) strains are used for vaccination, the most common circulating MuV are genotype H [86]. There is also concern that the genotype C virus circulating in India may not be neutralized effectively after immunization with the current vaccine strain used in the area, L-Zagreb (genotype N) [87]. In this study, the researchers show that a majority of the

circulating strains in India are of genotype C and that both vaccinated and unvaccinated individuals are infected.

In China, there is still circulating MuV in the population, even with widespread vaccination [88], most of which appears to be of genotype F [89]. The vaccine used in China is S_{79} strain (genotype A) [66]. This vaccine was derived from the same Jeryl Lynn strain used in the United States. Fu et. al. performed a study in 2004-2005, which showed an efficacy of 86% for one dose of vaccine. It was also shown that the efficacy was higher soon after infection (first 4 years), further from the time of vaccination.

There was another study, researchers characterized a large outbreak among vaccinated Palestinian refugees [90]. In this outbreak, there were just under 4,000 cases of mumps. Of the individuals, 68% had at least one dose of the MMR vaccine, and it was confirmed that most of the people infected did have an IgG response from the initial vaccination. They feel that this suggests a lack of protection from the current vaccine. When the virus causing the outbreak was sequenced, they found that the virus was of genotype H, and suggested that a better matched vaccine may be needed.

Although there are changes in the genotype, MuV is still considered to only have one serotype. There are researchers that argue against immune escape as a reason for the recent, large outbreak of mumps in vaccinated populations [91]. While this research did not find a significant difference in the neutralizing titer against a range of viruses for individuals vaccinated with Jeryl Lynn, there was at least a 2-fold decrease in the titer when neutralizing the most commonly circulating genotype in the United States (genotype G). There was also a large spread in the neutralizing titer for these individuals, so although the titer required for protection from MuV infection has not been established,

it is possible that even this decrease is sufficient to allow for the increase in infections seen in the United States over the past decade.

Mumps virus transcription and replication

The RNA genome associates with NP to form the helical ribonucleoprotein (RNP), which protects the genome from degradation, and serves as the template for RNA synthesis. The NP also associates with the phosphoprotein (P) and indirectly with the large protein (L), which form the viral RNA-dependent RNA polymerase (vRdRp) [33]. The vRdRp uses NP-encapsidated RNA as a template for both replication of the vRNA genome and production of mRNA [1]. The vRdRp transcribes the NP-encapsidated RNA into 5' capped and 3' polyadenylated mRNAs in cytoplasm [92]. Although the exact details of mRNA production are not known, the process is currently believed to involve termination and reinitiation (stop and start) at each gene junction. The vRdRp also replicates viral RNA genome [92–96]. It is thought that vRdRp transcribes mRNA first and replicates vRNA at a later stage after entry into host cells. The regulation of the switch from transcription to replication by vRdRp is not clear. It is thought that phosphorylation state of the P protein plays a critical role. Interestingly, P interacts with NP in RNP as well as free NP [36,97–99].

Some structural studies have been carried out to look at how NP, P, L, and RNA interact with themselves and one another to form the complex required for both vRNA and mRNA synthesis. The morphology of many paramyxovirus nucleocapsid proteins have been characterized, while sharing some commonalities, there are also many differences that allow for the nucleocapsid structures to be differentiated [100]. There are differences in the number of subunits that it takes to make a full turn in the structure, the

width of the ring structure, and the distance between turns of the ring. Each of these may impact the way in which RNA is accessed by the polymerase complex and the stability of the RNA regarding temperature and RNase exposure. The mumps NP was found to not require its C-terminal tail in order to form nucleocapsid structures [99]. This same study demonstrated that the N-terminal domain of NP binds to the P protein of MuV, and that there was no domain on the C-tail that strongly binds the P protein. A nucleocapsid binding domain (NBD) in P was also found to be from residues 343-391. Understanding how the various components of the MuV replication complex interact is important when designing possible treatments or preventative measures.

The use of bacterially expressed nucleoprotein allowed for better characterization of the MuV nucleocapsid complex. It was found the when NP was co-expressed with P in *E. coli*, there was a production of NP-RNA rings that contained 13 NP subunits [101]. The ring structure did not require the presence of RNA, and the RNA contained in the ring could be readily removed through the use of RNase treatment. When RNA was incorporated, it was found to be of 78 nucleotides in length, matching the size that would be expected based on the rule of six. Further research by the same group produced a more detailed structure of the MuV nucleocapsid, using cyro-electron microscopy [36]. To visualize the MuV nucleocapsid in a more natural setting, nucleocapsid was purified from infected cells. The nucleocapsid had a traditional herringbone structure, which is seen in many related viruses. The researches also wanted to better understand the role of P and its interaction with the nucleocapsid. To do this, the components of the RNP structure were co-transfected and the resulting nucleocapsid structure was visualized. They found that when only the C-terminal domain of P was co-expressed with NP, there

was little change in the overall structure of the nucleocapsid. When the N-terminal domain of P was co-expressed with NP, there was an uncoiling of the nucleocapsid structure, suggesting that this interaction may be important for accessing of the RNA by the polymerase during RNA synthesis. Functional testing of the P truncations in this paper also show that there is a requirement for both the C-terminal and N-terminal domains for RNA synthesis. The P protein has been shown to have an effect on RNA replication and it appears that there may be a regulatory role [8]. When mutations were introduced into the P protein, there can be an increase or decrease in the transcriptional activity of the MuV RdRp when assessed using either a minigenome system or when introduced into the virus. The ability of these mutations to change the rate of RNA synthesis suggests a regulatory role. This research gave better insight into how the RNA may be accessed and the role the P may be playing. The minigenome system (Fig. 2.1) and rescue system (Fig. 2.2) for MuV used in this work is also critical to ongoing work into the mechanisms of MuV replication.

Building on the previous structural information about NP of the closely related virus parainfluenza virus 5 (PIV5) [102], a high resolution (10.4-Å) cyro-EM structure for the N-terminus of NP was modeled [103]. The cryo-EM structure of MuV NP lacked RNA, while there was RNA crystalized with PIV5-NP. There were also some differences among residues that may interact with the RNA or L. The lack of RNA leads to an opening of the RNA binding groove, which may be similar to the changes needed for the RdRp to access the RNA during synthesis. Neither group was able to get structural information about the C-terminal tail, likely due to the unstructured nature of the tail. It is important to note that when the tail is removed, there is no activity in the

minigenome system, suggesting that this region is critical to act as a temple for RNA synthesis, either through its role in interacting with RNA or the RdRp.

The structure of the oligomerization domain of the P protein was crystalized, giving structural information for residues 213-277 [36]. It was found that the P protein oligomerizes in two pairs of parallel α-helices that align in an antiparallel orientation. This is in contrast to vesicular stomatitis virus (VSV) [104] and Sendai virus (SeV) [105], which both have four parallel α-helices that form the oligomerization domain. It was also discovered that there was a second NBD in P between residues 1 to 194, along with the previously discussed domain between residues 343 to 391 [36]. The multiple studies on the domains of MuV P have allowed for the identification of the oligomerization domain, two nucleotide binding domains, and a basic structure in regard to orientation of the tetramer. This has allowed for a general model of the P, NP, L structure to be proposed, although additional research will be needed to confirm this model [97].

There has also been some progress made in characterization and structure for the L protein. Due to the large size of the L protein, it is difficult to perform some critical experiments to determine the role of individual domains and find a structure for L. Although a molecular clone of L has been available since 1992, there has not been a published structure for any of MuV L [34]. There was recently a published structure for VSV, which is also a negative strand RNA virus, although it is a part of another family (rhabdoviridae), and more closely related to rabies virus [106]. Although this structure may give some insight into the MuV L protein, there are likely significant differences between the two proteins. A structure of the MuV L protein would be an important

addition to the field. Since RNA replication is a major target for drug discovery for the treatment of viral disease, it would be a very useful addition to the field.

Mumps virus fusion and budding

MuV is an enveloped virus that has two surface exposed glycoproteins, the fusion protein (F) and hemagglutinin-neuraminidase protein (HN). Cell-cell fusion requires both F and HN expression in the same cell [107]. F and HN are also both important for viral budding. Although only the matrix protein (M) is required for budding, F and HN proteins coordinate with M and the nucleocapsid proteins (NP) for optimal budding [108]. Besides M, F was shown to be the most critical for efficient budding in this study.

When SH is not able to identify the genotype of MuV isolates, HN is recommended to determine the genotype [83]. There are many different areas of the HN protein that have been identified to be involved in sialic acid (SA) binding, neurovirulence, and antigenicity [109]. Early studies looking at epitopes in HN using monoclonal antibodies (mAbs) to map different sites in HN, showing that there are at least 3 strongly inhibitory sites, as well as 5 less inhibitory sites, although the locations of these sites were not defined [110]. Using these antibodies, the researchers could decrease virus induced cellular toxicity. When trying to identify epitopes important for MuV neutralization, researchers found that monoclonal or polyclonal antibodies generated against a genotype A virus had decreased or no binding to genotype C and D viruses [111]. HN proteins with substitutions at positions 269, 252, and 354 were found to no longer bind some of the mAbs generated against genotype A virus. This type specific neutralization had also been described earlier [112]. Sialic acid and virulence were also found to be linked to differences in the HN sequence [113]. Vaccination with the Urabe

AM9 strain of MuV sometimes resulted in post-vaccination meningitis [78]. Further research showed that this may have been related to the mutation HN(E335K), which resulted in a shift from an α2,3 to and α2,6 sialic acid binding preference [113]. They also found that this mutation led to an increase in neuraminidase activity. Later research showed that in rescued virus there was no difference in virulence in neuronal cell lines or the rat neurovirulence model [114]. Around the same time another group demonstrated that there was a difference in the accessibility of the HN receptor binding motif due to this change [115]. It appears that there are multiple genes that may be involved in the neurovirulence of MuV [116], and that a single point mutation is not likely to be the cause of neurovirulence [117]. The rat model seems to be a good predictor for neurovirulence, although the underlying mechanisms and residues important for neurovirulence still need further study. This suggests that testing of potential vaccines for neurovirulence will be critical, and that lack of known neurovirulence markers will not be sufficient.

Before there was a structure for the MuV HN protein, researchers used the structure of HN for Newcastle disease virus (NDV) [118] and PIV5 [119,120]. While these structures were helpful in mapping important residues and creating models for MuV HN structure, the recently published MuV HN structure will be a very useful tool for mapping sites onto HN [121]. The MuV HN structure was solved bound to a trisaccharide containing an α2,3-linked sialic acid in the receptor binding groove. This model will allow for better characterization of antigenic sites on MuV and may be important for determining residues that could be involved in differences in antigenicity between the current vaccines and circulating strains of MuV.

It has been demonstrated that changes in the F proteins can cause differences in viral growth characteristics and virulence. Previous studies have shown that increases in fusion correlated with increases in neuroinvasion [122] and neurovirulence [123]. This means that understanding how changes in MuV can affect fusion are very important. Understanding the viral proteins and host factors involved in fusion may allow for the development of treatment for severe cases of mumps and prevention of neurovirulent MuV infections. Although there is currently no structure for MuV F, the structure of the closely related virus PIV5 can be used to model MuV F [124,125]. Using these structures along with the MuV HN structure, we can map sites that may be critical for antigenicity, receptor binding, fusion, and F-HN interaction.

The F proteins of MuV is also critical for efficient viral budding [37]. Previous work showed that a leucine residue at position 383 in F was required for fusion in B95a cells [126]. This residue was mutated in the Hoshino vaccine strain (KO3), which resulted in decreased cell-cell fusion. Another residue at position 195 in F has been shown to affect the amount of cell-cell fusion in COS7 cells [127]. This residue is a serine in most viruses, but it has also been found to be a phenylalanine or tyrosine in other viruses. When the aromatic residues are present, there is a decrease in fusion. These aromatic residues are present in Urabe, Zagreb, and some circulating viruses, including the 2006 isolate from the outbreak in Iowa (Iowa/06) that was used in most of the following research.

The F cytoplasmic tail has previously been shown to play an important role in fusion and budding in related viruses. For the closely related virus parainfluenza virus 5 (PIV5), deletion of 18 amino acids from the cytoplasmic tail resulted in a small decrease

in fusion and had little effect on virion production and budding [128]. This same study showed that there was a defect when both the F and HN cytoplasmic tails were removed, suggesting that there may be a redundant role for the two cytoplasmic tails. Another study in PIV5 showed that a 19 amino acid deletion resulting in the full deletion of the F cytoplasmic tail resulted in impaired fusion pore enlargement [129]. The cytoplasmic tail of the human respiratory syncytial virus (RSV) was shown to be important for viral budding and F surface distribution [130]. Another group showed that the in Sendai virus (SeV) and human parainfluenza virus 1 (hPIV1) the F cytoplasmic tail was not involved in intracellular trafficking, but that it was important for coordinating the components required for budding at the plasma membrane [131].

Phosphorylation in viral replication and transcription

For all negative-sense non-segmented RNA viruses, their genomes are encapsidated with nucleoprotein to form RNP. It has been shown that phosphorylation of NP plays a role in transcription, replication, and genome stability. In measles virus, phosphorylation of NP has been shown to up-regulate transcriptional activity in a minigenome assay [132]. A similar phenotype has also been seen in rabies virus [133] and Nipah virus [134]. In measles virus, phosphorylation of N is involved in genome stability and phosphorylation of N affects genome stability [135]. In Marburg virus, only phosphorylated NP is incorporated into nucleocapsid complexes [136]. Similarly in measles virus, phosphorylated N is preferentially incorporated into the nucleocapsid [137]. Although it has been shown that NP is phosphorylated in MuV-infected chicken cells, the role of phosphorylation was unclear at the time [7].

The phosphoprotein (P) of paramyxoviruses is named as such because it is highly phosphorylated. It has been shown for multiple viruses that the P protein plays a critical role in viral RNA synthesis (2-7). The role of the P phosphorylation in mRNA synthesis was studied thoroughly for PIV5, and it was found that phosphorylation can play both a positive and negative role (3-5). Residue S157 in P was found to be phosphorylated in infected cells (3). This site was found to be the binding site for the host kinase polo-like kinase 1 (PLK1) and PLK1 was found to phosphorylated P at position S308 upon binding (3, 4). Phosphorylation at these residues resulted in reduced viral gene expression and this reduction correlated with a reduction in host innate response. Regulation of gene expression by phosphorylation is believed to be involved in evading the host immune response by controlling viral protein production (4). Using mass spectrometry, T286 was identified as an additional phosphorylated residue. Mutation of this site to prevent phosphorylation resulted in decrease reporter activity in a PIV5 minigenome system and resulted in delayed viral growth when incorporated into the PIV5 virus (5). These results show that phosphorylation at this site increases viral mRNA synthesis, demonstrating that phosphorylation can both be a positive or negative regulator of RNA synthesis in PIV5.

While PLK1 has been shown to be an important kinase for the P protein of PIV5, the role of many host kinases in the phosphorylation of other negative sense viruses have been studied [138]. Some of the other host kinases found to play a role in the phosphorylation of paramyxovirus P proteins include casein kinase II (CKII), protein kinase c isoform zeta (PKC-ζ), and protein kinase B (AKT). The P proteins of RSV and measles virus are thought to be phosphorylated by CKII [138–140]. The P protein of hPIV3 and Sendai virus are phosphorylated by PKC-ζ [141,142], and the P protein for

canine distemper virus is phosphorylated by both CKII and PKC-ζ [143]. Because host kinases have been shown to be critical for phosphorylation of viral proteins in order for efficient virus replication, it has been suggested that host kinases may be a valid target for antiviral drug development [144]. It is also possible that removing kinase that down regulate viral growth in vaccine production cell lines may increase vaccine yields [145].

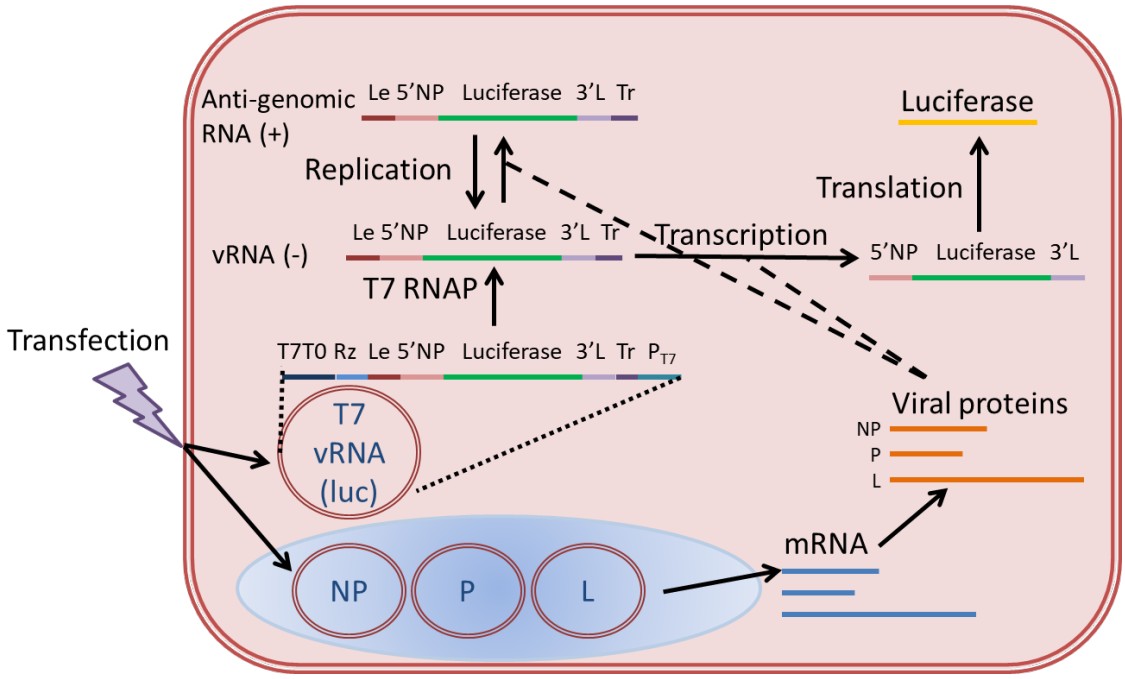

Figure 2.1. MuV minigenome system. In order to assess the ability of NP, P and L to support RNA replication in a simplified system, the MuV minigenome system is used. A minigenome plasmid containing the MuV leader and trailer sequences flanking a single Renilla luciferase ORF is co-transfected with plasmids encoding either the wild-type sequences or mutants of NP, P, and L. This results in the expression of NP, P and L with a viral RNA (vRNA) mimic encoding only luciferase. This is sufficient to allow for vRNA replication through a positive sense intermediate, and transcription to produce a single transcript encoding luciferase. This can be translated by host machinery to produces Renilla luciferase. RdRp activity is assessed using a luminescent reporter assay. Firefly luciferase encoding plasmid can be used as a transfection control.

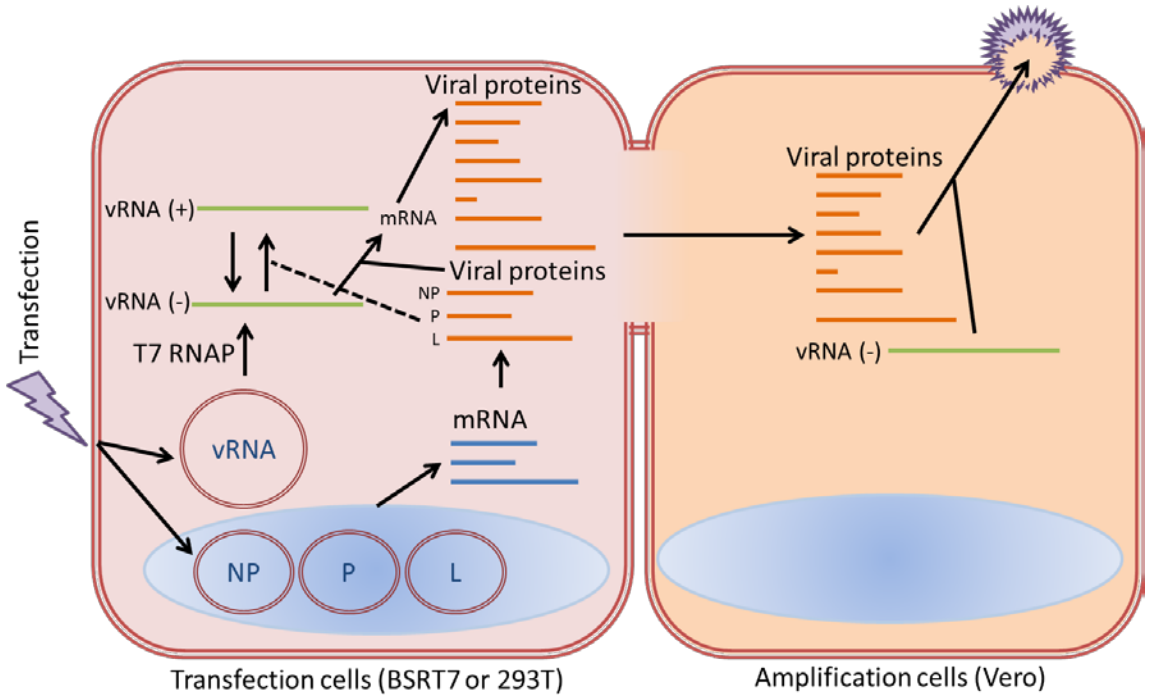

Figure 2.2. Rescue of MuV mutants. To produce MuV containing specific mutations, a reverse genetics system has been established. Plasmids encoding the MuV genome under a T7 promoter are engineered to contain mutation at specific sites. These plasmids are transfected with plasmids encoding NP, P, and L. Plasmid expressed T7 is co-transfected in rescues using 293T cells, and optionally co-transfected into BSRT7 cells, which constitutively express T7 polymerase. These plasmids are sufficient for gene transcription and genome replication, but a 2nd amplification cell line is required for virion production. Vero cells are co-cultured to allow for efficient virus production. All viruses produced using this method are clonally purified and fully sequenced.

Table 2.1: Mumps vaccine strain summary

Vaccine Strain	Manufacturer	Area of Use	Genotype
Hoshino	Kitasato Institute	Japan, Korea	**B** [3]
Jeryl Lynn (MumpsVax)	Merck and Co.	Worldwide	**A** [3]
Leningrad-3	Moscow State Facility for Bacterial Preparations	Former Soviet Union	**N** [83]
Leningrad-Zagreb	Institute of Immunology of Zagreb	Croatia, India, and Slovenia	**N** [83]
Miyahara	Chem-Sero Therapeutic Research Institute	Japan	**B** [146]
NK M-46	Chiba	Japan	
Pavivac	Sevapharma	Czech Republic	
RIT-4385	GlaxoSmithKline Biologicals	Europe	**A** [3]
Rubini (discontinued)	Swiss Serum Institute	Switzerland	**A** [3]
S-12	Razi State Serum and Vaccine Institute	Iran	**H** [147]
Sofia-6	Center for Infectious and Parasitic Diseases	Bulgaria [148]	
Torii	Takeda	Japan	**B** [3]
Urabe	GlaxoSmithKline Biologicals	Worldwide	**B** [3]
	Sanofi-Pasteur	Worldwide	
	Biken	Japan	
	Chiron Therapeutics and Vaccines	Germany, Italy, Asia, Latin America	

CHAPTER 3

THE ROLES OF PHOSPHORYLATION OF THE NUCLEOCAPSID PROTEIN OF MUMPS VIRUS IN REGULATING VIRAL RNA TRANSCRIPTION AND REPLICATION[1]

[1]Zengel J., Pickar A., Pei X., Lin A., He B. 2015. J Virol. 89:7338–47. Reprinted here with permission of the publisher.

Abstract

Mumps virus (MuV) is a paramyxovirus with a negative sense non-segmented RNA genome. The viral RNA genome is encapsidated by the nucleocapsid protein (NP) to form the ribonucleoprotein (RNP), which serves as a template for transcription and replication. In this study, we investigated the roles of phosphorylation sites of NP in MuV RNA synthesis. Using radioactive labeling, we first demonstrated that NP was phosphorylated in MuV-infected cells. Using both liquid chromatography-mass spectrometry (LC-MS) and in silico modeling, we identified nine putative phosphorylated residues within NP. We mutated these nine residues to alanine. Mutation of the serine residue at position 439 to alanine (S439A) was found to reduce the phosphorylation of NP in transfected cells by over 90%. The effects of these mutations on the MuV mini-genome system were examined. S439A was found to have higher activity, four mutants had lower activity and four mutants had similar activity compared to wild-type NP. MuV containing the S439A mutation had reduced phosphorylation of NP by 90% and enhanced viral RNA synthesis and viral protein expression at early time point after infection, indicating that S439 is the major phosphorylation site of NP and its phosphorylation plays an important role in down-regulating viral RNA synthesis.

Significance

Mumps virus (MuV), a paramyxovirus, is an important human pathogen that is re-emerging in human populations. Nucelocapsid protein (NP) of MuV is essential for viral RNA synthesis. We have identified the major phosphorylation site of NP. We have found that phosphorylation of NP plays a critical role in regulating viral RNA synthesis. The work will lead to a better understanding of viral RNA synthesis and possible novel targets for anti-viral drug development.

Introduction

Mumps virus (MuV) infects humans, causing acute infection with hallmark enlargement of the parotid gland (1). Before widespread vaccination in the late 1960s, mumps was the leading cause of aseptic meningitis and caused deafness in children (2). Although vaccination has greatly reduced the number of infections, large outbreaks have occurred recently in vaccinated populations. The largest recent outbreak in the United States originated at a university in Iowa in 2006, where over 5000 cases were reported, compared to approximately 250 cases per year in the preceding years (3). In 2014, there were over 1100 cases of mumps reported, mainly centered around universities (4). At least 90% of the individual infected received the Measles, Mumps, and Rubella (MMR) vaccine, and the majority of people received two doses (3). New strategies to control these outbreaks are needed. Understanding the roles of each MuV protein in virus replication and pathogenesis will aid development of countermeasures for MuV.

Mumps virus (MuV) is a member of the family Paramyxoviridae in the genus Rubulavirus (1). It has a negative sense, non-segmented, RNA genome of 15,384 nucleotides. The genome is comprised of seven transcriptional units that encode nine viral proteins in the following order: 3'-NP-V/I/P-M-F-SH-HN-L-5' with RNA synthesis initiating at a single site at the 3' end. The RNA genome associates with NP to form the helical ribonucleoprotein (RNP), which protects the genome from degradation, and serves as the template for RNA synthesis. The NP also associates with the phosphoprotein (P) and indirectly with the large protein (L), in which P and L forms the viral RNA-dependent RNA polymerase (vRdRp) (5). The vRdRp uses NP-encapsidated RNA as a template for both replication of the vRNA genome and production of mRNA (2). The

vRdRp transcribes the NP-encapsidated RNA into 5' capped and 3' polyadenylated mRNAs in cytoplasm (6). Although the exact details of mRNA production are not known, the process is currently believed to involve termination and reinitiation (stop and start) at each gene junction. The vRdRp also replicates viral RNA genome (7-10). It is thought that vRdRp transcribes vRNA first and replicates vRNA at a later stage after entry into host cells. The regulation of the switch from transcription to replication by vRdRp is not clear. It is thought that phosphorylation state of the P protein plays a critical role. Interestingly, P interacts with NP in RNP as well as free NP (11-14). Mumps NP is also involved in virus budding. It interacts with the matrix (M) protein, which is critical for virus egress (15).

For all negative-sense non-segmented RNA viruses, their genomes are encapsidated with nucleoprotein to form RNP. It has been shown that phosphorylation of NP plays a role in transcription, replication, and genome stability. In measles virus, phosphorylation of NP has been shown to up-regulate transcriptional activity in a minigenome assay (16). A similar phenotype has also been seen in rabies virus (17) and Nipah virus (18). In measles virus, phosphorylation of NP is involved in genome stability and phosphorylation of NP affects genome stability (19). In Marburg virus, only phosphorylated NP is incorporated into nucleocapsid complexes (20). Similarly, in measles virus, phosphorylated NP is preferentially incorporated into the nucleocapsid (21). Although it has been shown that NP is phosphorylated in MuV-infected chicken cells, the role of phosphorylation is unclear (22).

In this study, we used in silico modeling and mass spectrometry to determine phosphorylation sites in the NP of MuV. We studied the function of NP in RNA

transcription and replication using a minigenome system (23) and a reverse genetics system (24).

Materials and Methods

Plasmids and cells

All plasmids were constructed using standard molecular cloning techniques. Plasmid sequences were based on the sequence of a mumps virus isolated during an outbreak in Iowa from 2006 (GenBank: JN012242.1). MuV NP, P, and L were previously cloned into the pCAGGS expression vector (24, 25). Firefly-luciferase (pFF-Luc) and a MuV mini-genome plasmid expressing Renilla luciferase flanked by MuV-IA trailer and leader sequences and under a T7 promoter (pT7-MG-RLuc) were also previously produced (23). Mutations were introduced into pCAGGS-NP as previously described for introduction of pCAGGS-P mutations (23). Plasmids encoding the full-length genome of MuV-IA previously used to rescue virus were mutated as necessary. Plasmids and sequences are available upon request.

HEK293T cells were maintained in Dulbecco's modified Eagle medium (DMEM) supplemented with 5% fetal bovine serum (FBS) and 1% penicillin-streptomycin (P/S). BSR-T7 cells were maintained in DMEM supplemented with 10% FBS, 1% P/S, 10% tryptose phosphate broth (TPB), and 400 µg/ml G418 to maintain T7 RNA polymerase (RNAP) expression. Vero and HeLa cells were maintained in DMEM with 10% FBS and 1% P/S. All cells were cultured at 37°C and 5% CO_2. Cells were passaged the day before to achieve about 85-95% confluence for infection and 60-80% confluence for transfection.

Minigenome

BSR-T7 cells (1 day, 60-80% confluent, 24-well plate) were transfected with pCAGGS-P (80 ng), pCAGGS-L (500 ng), pT7-MG-RLuc (100 ng), pFF-Luc (1 ng), and varying amounts of pCAGGS-NP (wt or mutant at 0, 12.5, 25, 50, or 100 ng) using jetPRIME (Polyplus Transfection, France) following manufacture's protocol. Empty pCAGGS vector was used to maintain a constant amount of total plasmid transfected per well. After 48 hr, media was removed and 100 µl of passive lysis buffer (Promega, Madison, WI) was added to each well, followed by shaking on an orbital shaker for 15 min. 40 µl of lysate was transferred to a white 96-well plate and a dual luciferase assay (Promega) was performed according to the manufacturer's protocol. Luminescence was detected using a GloMax 96 Microplate Luminometer (Promega). The ratio of Renilla to firefly luminescence was determined for each well, and the average of 3-6 biological replicates was calculated. The peak activity for each NP plasmid was determined and each experimental data set was normalized to wt NP. The data reported is the combined data for a least 3 experimental replicates.

Virus Rescue and sequencing

BSR-T7 cells (1 day, 60-80% confluent, 6-well plate) were transfected with pCAGGS-NP (100 ng), pCAGGS-P (160 ng), pCAGGS-L (2000 ng), and full-length genome (2500 ng) using jetPRIME. After 48-72hr, transfected BSR-T7 cells were trypsinized and co-cultured with Vero cells at a ratio of 1:5 in a 10-cm dish. When CPE was observed (2-7 days), the media, likely containing virus, was collected and a plaque assay was performed using Vero cells. Single plaques were isolated 6-7 days later and cultured in fresh Vero cells in 6-well plates to produce passage 1 (P1). After titer

determination, P1 was passaged again in T75 or T150 flasks at an MOI of 0.01 to produce P2. After 72hrs, virus was collected, BSA was added to 1% final concentration, and aliquots were stored at -80°C. Titer was determined by plaque assay. Viral RNA was isolated using QIAamp Viral RNA Mini Kit (Qiagen, Valencia, CA) followed by synthesis of DNA templates using SuperScript III One-Step RT-PCR System with Platinum Taq (Life Technologies, Grand Island, NY) and 5 sets of primers were used to amplify the entire genome. Fragments were sent to Genewiz (South Plainfield, NJ) for sequencing using 6-10 primers per fragment. Only viruses matching the full-length plasmid sequence were used for further experiments. Primer sequences are available upon request.

Immunoprecipitation

Cells were lysed with whole cell extraction buffer (WCEB) (50mM Tris-HCl [pH 8], 280mM NaCl, 0.5% NP-40, 0.2mM EDTA, 2mM EGTA, and 10% glycerol) supplemented with protease inhibitors (1x protease inhibitor, 0.1mM phenylmethylsulfonyl fluoride OR 1x protease/phosphatase inhibitor cocktail for radioactive labeling experiments). Insoluble material was pelleted at 14000xg for 2 minutes and the supernatant was transferred to a new tube. Rec-Protein G-Sepharose 4B beads and anti-P or anti-NP mAb was added to each tube and nutated overnight at 4°C. The next day, tubes were spun at 600xg for 2 min and supernatant was aspirated. Three washes were performed with 1 ml of WCEB using the same process. The bead pellet was resuspended in 50-200 µl of 2x Laemmli Sample Buffer (Bio-Rad, Hercules, CA) + 5% β-Mercaptoethanol followed by heating at 95°C for 5 min.

Mass spectrometry

Vero cells in a 10-cm plate were infected with MuV-IA at an MOI of 0.5. After 24 hr, immunoprecipitation was performed as described above with an anti-MuV-P mAb. After overnight incubation, the sample was spun to pellet the beads and the supernatant was collected. The washes were continued and loading buffer was added as above. This produced the "anti-P" sample. The supernatant collected prior to the first wash was used for a second immunoprecipitation with anti-MuV-NP mAb. This produced the "anti-NP" sample. Both samples were resolved on a 10% acrylamide gel by SDS-PAGE. The gel was stained with Coomassie Blue G250 in 10% acetic acid and 45% methanol for 4 hours, followed by destaining with destain buffer (10% acetic acid, 40% methanol, 50% water). Bands were excised from the gel and sent to the MS & Proteomics WM Keck Foundation Biotechnology Resource Laboratory (Yale University, New Haven, CT) for further processing and mass spectrometry (MS). Briefly, the protein was digested with trypsin and enriched for phosphoproteins on a TiO_2 column (2x). Peptides were separated on a nanoACQUITY (Waters, Milford, MA) (75µm x 250mm eluted at 300nl/min, 80 minute run) with MS analysis on an Orbitrap Elite mass spectrometer (Thermo Scientific). Both the fraction enriched by the column and the flow-through were analyzed by LC-MS/MS, and peak lists were combined prior to a Mascot search against the NCBInr database with taxonomy restricted to viruses. Phosphorylated peptides were considered significant with a random probability score of less than 5%. For peptides with more than one possible phosphorylation site, the Mascot Delta Score and PhosphoRS score were used to determine which site was phosphorylated.

Radioactive labeling for phosphorylation analysis

In order to examine phosphorylation of NP expressed from transfected plasmid, 1 µg of pCAGGS-NP (wt or mutant) was transfected into HEK293T cells in a 6-well plate using JetPrime in duplicate. After 24 hr, cells were starved in 1 ml DMEM lacking methionine and cysteine for 30 min followed by labeling with about 50 µCi/ml ^{35}S-EasyTag Express35S Protein Labeling Mix (PerkinElmer, Waltham, MA) for 6 hr. Alternatively, the cells were starved with 1 ml DMEM lacking sodium phosphate followed by labeling with about 100 µCi ^{33}P-Orthophosphoric acid (Perkin Elmer) for 6 hr. The cells were then lysed and immunoprecipitation was performed with anti-NP mAb as described above. The samples were resolved on a 10% acrylamide gel by SDS-PAGE and gels were dried. Radioactivity was detected by exposing the gel to a Storage Phosphor Screen BAS-IP MS (Fuji) overnight. The screen was read on a Typhoon FLA 7000 (GE Healthcare Life Sciences, Pittsburgh, PA) and the densitometry analysis was performed using ImageQuant TL software (GE Healthcare). The ratio of ^{33}P/^{35}S was calculated and reported.

In order to determine NP phosphorylation in infected cells, Vero cells in a 6-well plate were infected with MuV (wt, S439A, S520A, or 542A) at an MOI of 0.1 for 1 hr. Media was replaced with DMEM containing 2% FBS and 1% P/S and incubated for 24 hr. After 24 hr, the cells were lysed, labeled, and immunoprecipitation and quantification were performed as above.

Growth Curves

Vero or HeLa cells in a 10-cm dish were infected with MuV (wt, S439A, S520A, or 542A) at an MOI of 0.01 or 5 in 5 ml of DMEM+2% FBS+1% P/S for 1 hr in

triplicate. Cells were washed four times with PBS and 10 ml of DMEM+2% FBS+1% P/S was added to the cells. One sample was taken immediately after the DMEM was added and labeled as 0 hpi (hours post infection). For MOI of 5, samples were collected at 0, 6, 12, 24, 48, and 72 hpi. For MOI of 0.01, samples were collected at 0, 24, 48, 72, 96, and 120 hpi. All samples were supplemented with 1% BSA after collection and stored at -80°C. Virus titers were determined by plaque assay on Vero cells. Results were confirmed in a second experiment. Significance was determined by two-way ANOVA using the Holm-Sidak method to correct for multiple comparisons.

Real-time PCR

Vero cells in a 6-well plate were infected with MuV (wt, S439A, S520A, or S542A) at an MOI of 0.1 for 1 hr, washed three times with PBS, and 2 ml of DMEM+2%FBS+1%P/S was added to each well. At 0, 6, 12, and 18 hpi, total RNA was collected using the RNeasy Plus Mini Kit with QIAshredder homogenization (Qiagen) according to the manufacturer's instruction. cDNA was generated using SuperScript III Reverse Transcriptase (Life Technologies) using 5 µl of RNA according to the manufacturer's directions. Oligo$(dT)_{15}$ (Promega) were used for mRNA cDNA synthesis and a primer specific for the negative sense genome (TGAACTAGCGAGGCCTATCCCCAAG) was used for genomic cDNA synthesis. 5µl of cDNA was used for real-time PCR using a MuV-F specific, FAM-tagged probe (Life Technologies) and TaqMan Gene Expression Master Mix (Life Technologies) according to the manufacturer's instructions. Real-time PCR was run on a StepOnePlus Real Time PCR System (Life Technologies). Biological triplicate samples were run for each sample. Ct values were normalized to genomic RNA at 0 hpi. Significance was

determined by two-way ANOVA using the Holm-Sidak method to correct for multiple comparisons.

Protein quantification

Cells were infected at an MOI of 0.1 for 6 hr or MOI of 5 for 24 hr. Cells were washed once with PBS and trypsinized. Cells were collected into a 1.5 ml tube and pelleted (all spins at 600 g), washed twice with DMEM+2% FBS, and fixed and permeabilized using Cytofix/Cytoperm solution (BD Biosciences, San Jose, CA) overnight at 4°C. The mAbs were conjugated using Zenon Alexa 488 (A488) or Allophycocyanin (APC) Mouse IgG_1 Labeling Kits (Life Technologies) according to the manufactures specifications. Cells were then washed twice with Perm/Wash buffer (BD Biosiences) followed by staining with anti-NP(A488) or anti-P(APC). After staining for 20 min at 4°C, samples were washed twice with Perm/Wash buffer and once with PBS+1%BSA. Cells were then resuspended in 500 µl of PBS+1% BSA. Flow cytometry was performed using the LSRII Flow Cytometer (BD) and data was collected and analyzed using FACSDiva (BD). The mean fluorescence intensity was calculated for the stained population.

Total protein was also measured by infecting cells at an MOI of 5 as above, lysing with 2x Laemmli Sample Buffer (Bio-Rad), and heating at 95°C for 5 min. Samples were then resolved on a 10% acrylamide gel by SDS-PAGE and transferred to Amersham Hybond LFP PVDF membranes (GE Healthcare Life Sciences). Immunoblotting was performed by incubating the membranes with anti-NP and anti-P mAb and anti-GAPDH [GT239] (Genetex, Irvine, CA) in 5% milk+PBS+0.1% Tween 20 (PBST) overnight at 4°C, followed by three washes with PBST, followed by incubation with Cy3 conjugated

goat anti-mouse IgG diluted 1:2500 (Jackson ImmunoResearch, West Grove, PA) in 5% milk+PBST for 1hr at room temperature. After the incubation, the membrane was washed four times with PBST and dried. The blot was visualized on the Typhoon FLA 7000 (GE Healthcare Life Sciences) and the densitometry analysis was performed using ImageQuant TL software (GE Healthcare)

Results

MuV NP is phosphorylated

Previously, it was shown that MuV NP was phosphorylated when mumps virus was grown in chicken embryo cells. In order to determine if NP is phosphorylated in mammalian cells, Vero cells were infected with the recombinant mumps virus, rMuV(Iowa/US/06) (referred to as MuV), at an MOI of 0.1 for 24 hr and labeled with ^{35}S-Met/Cys or ^{33}P- Orthophosphoric acid. Immunoprecipitation was performed using anti-NP mAb (24) and samples were resolved by SDS-PAGE. NP was detected in the ^{33}P labeling, indicating that NP was phosphorylated in infected cells (Fig. 3.1A, left panel). To determine if NP phosphorylation was dependent on other viral proteins, cells were transfected with a plasmid encoding MuV NP, labeled with radioactive reagents and immunoprecipitated as above (Fig. 3.1A, right panel). NP was detected in NP-transfected cells labeled with ^{33}P, indicating that NP was phosphorylated without any other viral proteins present.

Phosphorylation sites in NP were determined by *in silico* modeling and mass spectrometry

Potential phosphorylation sites within NP were first identified using NetPhos 2.0 (http://www.cbs.dtu.dk/services/NetPhos/), a sequence-based prediction (26). Using this

program, 12 phosphorylation sites were predicted above the cutoff value of 0.5. These sites are summarized in Table 3.1.

To identify the phosphorylated resides in MuV NP in infected cells, Vero cells were infected with MuV at an MOI of 0.1 for 48hr. In order to determine if there were differences in the phosphorylation state of NP interacting with P, two sequential immunoprecipitations were performed. Cells were first lysed and immunoprecipitated with a mAb specific for MuV-P, which pulled down all of the P protein in the sample, as well as NP that was associated with P (Fig. 3.1B, Sample 1). The unbound protein from the first immunoprecipitation was then immunoprecipitated again using a mAb specific for MuV-NP, which pulled down all of the non-P associated NP (Fig. 3.1B, Sample 2). These samples were resolved by SDS-PAGE and stained with Coomassie Blue. The labeled NP bands were excised from the gel. The samples were subjected to tryptic digestion, phosphopeptide enrichment, and analyzed by LC-MS/MS. The coverage was between 93-94% for each sample (Fig. 3.1C and 3.1D), with residues T387 and S439 found to be phosphorylated in both samples, and residues S25 and S542 phosphorylated in only in sample 1. The detected sites along with other sites that were below the defined cutoff for confirmed phosphorylation are summarized in Table 3.1.

The S439 residue in MuV NP was found to be the major phosphorylation site in transfected cells

To assess which serine and threonine residues contributed to NP phosphorylation, we chose to examine seven residues (S25, S94, T183, S298, T387, S439, and S542) based on identification by mass spectrometry and two residues (S67 and S520) based on high *in silico* prediction scores (0.990 and 0.979). Plasmids encoding NP were made

with mutations to convert the serine or threonine residues to alanine in the encoded protein. Effects of the mutations on phosphorylation were determined by transfection of cells with plasmids expressing wt NP or the NP with alanine substitutions in duplicate. After 24 hours, one replicate was labeled with ^{35}S and the other was labeled with ^{33}P. After 6 hours of labeling, the cells were lysed and immunoprecipitation with anti-NP antibody was performed. The samples were resolved by SDS-PAGE (Fig. 3.2A) and the ratio of ^{33}P to ^{35}S was calculated (Fig. 3.2B). NP-S439A had little or no phosphorylation, while there was no significant difference between wt NP and the other mutants. The addition of P and L in the transfection had no effect on the phosphorylation of wt NP during transfection (data not shown).

The role of NP residues was assessed with a MuV minigenome system

The role of NP in transcription and replication was studied using the MuV minigenome system previously developed in our lab (23). The minigenome system consists of plasmids required for transcription and replication of viral RNA (NP, P, and L), as wells as a plasmid that encodes a viral negative sense minigenome under a T7 promoter. When transfected into T7 RNAP-expressing BSR-T7 cells, the minigenome plasmid produces negative-sense RNA containing the sequence for Renilla luciferase flanked by the MuV leader and trailer. The MuV replication machinery (NP, P, and L) replicates this RNA through a positive sense intermediate and produces Renilla luciferase mRNA, which is translated by host machinery. Changes in Renilla luciferase activity are due to changes in the replicative and transcriptional activity of the MuV replication system. The plasmids encoding NP mutants were tested at four concentrations and the peak activity was reported for each (Fig. 3.3A). An example minigenome titration is

shown comparing wt NP and the S439A mutant (Fig. 3.3B). Western blots were performed for each minigenome set to examine NP expression levels (Fig. 3.3C). Two mutants and wt NP are shown, but all mutants had similar protein amounts when the same amount of plasmid was transfected, with some slight variation. The same plasmids showed no difference in protein levels when using radioactive labeling. The use of multiple concentrations of plasmid in the minigenome system also controls for any differences in expression. We found that the S439A mutant had a higher level of minigenome activity. Four of the substitutions (S25A, S94A, T183A, S298A) had lower activity and there was no change with the other four substitutions (S67A, T387A, S520A, S542A).

S439 was the major phosphorylation site in NP in virus

We have constructed plasmids containing full-length MuV genome with alanine substitutions in NP and produced seven plasmids (S25A, S94A, S183A, T387A, S439A, S520A, S542A). The reverse genetics system previously developed in our lab was used to successfully rescue three viruses (rMuV-NP-S439A, S520A, S542A) (24, 25). Complete genome sequences were confirmed as outlined in the methods. At least three rescue attempts were made to rescue the other viruses, without success, while wild-type viruses were consistently rescued. To examine the phosphorylation states of NP in these viruses, Vero cells were infected with wt MuV and the three mutant viruses. Radioactive labeling of infected cells and immunoprecipitation of cell lysates were performed, and phosphorylation was determined as in the previous experiment (Fig. 3.4A). After calculating the ratio of ^{33}P to ^{35}S (Fig. 3.4B), we found that there was a significant decrease in phosphorylation for MuV-NP-S439A, while there was no change in the other

two mutant viruses, indicating that S439 is the major phosphorylation site of NP. This is consistent with the results obtained using transfected NP.

rMuV(wt**), rMuV-NP-S439A, S520A, and S542A had changed gro**wt**h rates in cell culture**

To determine the effect of the NP mutations on virus growth in cell culture, single-cycle and multi-cycle growth curves were performed in Vero and HeLa cells. In a single-cycle growth curve, cells were infected with an MOI of 5 and supernatant was collected at 0, 6, 12, 24, 48, and 72 hours post infection (hpi). In a multi-cycle growth curve, cells were infected at an MOI of 0.01 and supernatant was collected every 24 hours until 144 hpi. During single-cycle replication in Vero cells (Fig. 3.5A), there was lower virus titer for rMuV-NP-S439A at 6 hpi when compared to rMuV(wt), but an increased titer at 12, 24, 48, and 72 hpi. rMuV-NP-S542A had decreased titers at 12, 24, 48, and 72 hpi and rMuV-NP-S520A had even lower titers at each of those time-points. During multi-cycle replication in Vero cells (Fig 3.5B), rMuV-NP-S439A had increased titers at 48, 96, and 120 hpi, while both rMuV-NP-S520A and S542A had reduced titers at 72 and 120 hpi when compared to rMuV(wt).

In HeLa cells, the growth characteristics of the viruses were similar to those in Vero cells for the single-cycle growth, but there were differences between HeLa and Vero for the multi-cycle growth. There still was a lag in single-cycle growth for MuV-NP-S439A (Fig. 3.5C), but the virus was able to reach a significantly higher titer than rMuV(wt) by 48hpi. During multi-cycle growth in HeLa cells (Fig. 3.5D), MuV-NP-S439A had lower titers from 72 to 144 hpi. MuV-NP-S542A has higher titers compared

to rMuV(wt) at 48 and 96hpi with slightly lower titers at 144hpi. MuV-NP-S520A had decreased titers compared to rMuV(wt) after 72hpi, similar to growth in Vero cells.

rMuV-NP-S439A had increased protein present at 6 and 24 hours post infection

To determine if there were differences in protein production for these viruses, the amount of protein produced during viral infection was examined by western blotting first (Fig. 3.6A). rMuV-NP-S439A had increased viral protein in cells (Fig. 3.6B). rMuV-NP-S542A also had a small increase in viral protein levels by western blot, although the increase was not significant. To determine if this difference was due to protein production on a per cell basis, flow cytometry was used to stain for viral protein expression after infection. In order to determine early protein production, cells were collected 6 hours after infection (MOI of 0.1) and stained with antibodies specific to MuV NP or P. The mean fluorescence intensity was determined for each of the stained populations (Fig. 3.6C). rMuV-NP-S439A produced more protein at 6 hpi, as seen by staining for NP, while amounts of P were not detectable at this time. Furthermore, rMuV-NP-S439A had an increase in both the amount of NP and P produced on a per cell basis using high MOI (MOI of 5) infection at 24 hpi (Fig. 3.6D). rMuV-NP-S542A had a trend toward higher protein levels by flow cytometry, but the difference was not significantly different from rMuV (wt) ($p=0.12$ to 0.4).

rMuv-NP-S439A had increased genome replication and mRNA production

To understand the difference in protein production and viral titer, the amount of genome RNA and mRNA were measured by quantitative real-time, reverse transcription PCR (qRT-PCR) in infected Vero cells (MOI of 0.1). The cDNA was generated using a genome specific primer to quantify genome RNA and oligo dT to quantify mRNA. The

probe used for all samples was specific to MuV F or HN. Data using the MuV F specific probe is reported. It was found that rMuV-NP-S439A had increased genomic RNA production at 6, 12, and 18 hpi, while rMuV-NP-S520A and S542A had decreased genomic RNA production at 12 and 18 hpi when compared to rMuV(wt) (Fig. 3.7A). rMuV-NP-S439A also had increased mRNA production at all timepoints, while rMuV-NP-S520A and S542A had decreased levels at 6, 12, and 18 hpi when compared to MuV(wt) (Fig. 3.7B). When comparing the ratio of mRNA to genomic RNA, rMuV-NP-S439A had increased relative mRNA levels at 0 and 6 hpi, rMuV-NP-S542A had reduced relative levels at 6 and 12 hpi, and rMuV-NP-S520A had no significant differences when compared to MuV(wt) (Fig. 3.7C).

Mutations in NP affect NP-P interaction during infection but not transfection

To investigate the mechanism of the phosphorylation of NP in regulating viral RNA synthesis, NP and P interaction was examined. Cells were transfected with plasmids encoding NP and P and immunoprecipitation was performed using either anti-NP (Fig. 3.8A) or anti-P (Fig. 3.8B) mAbs. After co-immunoprecipitation of NP and P when using plasmids encoding any of the mutant NPs, no difference was detected. To assess differences in NP and P association in infected cells, Vero cells were infected with MuV-wt, S439A, S520A, and S542A. Co-immunoprecipitation and total protein visualization was performed (Fig. 3.8C). The ratio of NP to P was calculated (Fig. 3.8D) and MuV-S439A had decreased amounts of NP co-immunoprecipitated with P during the anti-P pull down. While there was a difference in NP-P interaction during infection, there was no difference in the amount of NP or P in sucrose gradient purified virus from infected cells (data not shown).

Discussion

In this study, we identified and confirmed multiple phosphorylated residues in MuV NP by mass spectrometry and directed mutagenesis. We showed that S439 was the major site of phosphorylation. Mutating this residue to alanine caused an increase in minigenome activity and higher levels of viral RNA and protein expression in rMuV-NP-S439A-infected cells than wild type virus-infected cells at early time points after infection. This is in contrast to previous work on Measles, Rabies, and Nipah viruses, which have decreased activity in their respective minigenome systems when NP phosphorylation is reduced (16-18). To the best of our knowledge this is the only case in which decreased phosphorylation of the nucleoprotein of a virus resulted in increased activity, indicating that phosphorylation of NP down-regulate viral RNA synthesis. We hypothesize that phosphorylation can both up- and down-regulate activity and that these differences may depend on the site that is being phosphorylated.

The mechanism of down-regulation of viral RNA synthesis by S439 of NP is not clear. We assessed the RNA binding of S439A along with all other alanine substitution mutants, but no differences were found compared to any of the mutants and wt NP (data not shown). One interesting difference between wt NP and NP-S439A is their interaction with P. While we were not able to show any differences in interactions between NP and P or NP and M in transfected cells, we found that there was much less NP pulled down in cells infected with rMuV-NP-S439A by an anti-P mAb in co-immunoprecipitation. This result suggests that phosphorylation at S439 increases NP association with P in infected cells, although phosphorylation at S439 was found in both P-associated NP and free NP (Fig. 3.1B, Table 3.1). This is rather surprising because the domain of NP interacting

with P is located at N-terminal 400 amino acid residues of NP and mutation at residue 439 should not have affected binding with P (13, 14). The difference in expression levels of NP, P and L in transfection and infection may contribute to the difference observed in the NP-P binding. It is possible that a previous un-detected region of NP (C-terminal tail domain) can interact with P, in the presence of other viral protein such as L and M.

The fact that rMuV-NP-S439A caused a slight lag in virion production even though there was more RNA and protein at that time point when compared to the other viruses suggests that there may be some defect in packaging of RNA for production and release of progeny virus. The lag in virion production may be detrimental to virus growth *in vivo*, which could explain why this position is highly conserved among all MuV strains (data not shown). The lower titer of rMuV-NP-S439A in HeLa cells, a type I interferon (IFN) producing cell, compared to wt MuV is consistent with this residue being critical for MuV growth *in vivo*. It is possible that the rMuV-NP-S439A virus was more sensitive to type I IFN during HeLa infection, which is not observed in Vero cells, an IFN defective cell.

While mutations at other amino acid residues did not produce a significant decrease in phosphorylation in transfected cells, they did play critical roles. There was a small decrease in phosphorylation of the S542A mutant. There was also a small, but significant decrease in both genomic RNA and mRNA, although there was a slight increase in protein produced. It is possible that there may be some defect in budding for the rMuV-NP-S542A virus, which might have caused the decrease in RNA and increased protein in the cells. Less protein may be exported in progeny virions. In PIV5, a closely related paramyxovirus, it is known that negatively charged residues in the tail of NP are

important for NP-M interaction and virus budding (27). The impact of the mutation at S542 may also be attributed to the transient nature of phosphorylation at this site. This is consistent with the mass spectrometry data that shows S542 was only significantly phosphorylated in the P-associated sample. rMuV-NP-S520A had a lower virus titer when compared to MuV(wt), suggesting that there was some defect in virus growth, although there were only modest decreases in the amount of genomic RNA and mRNA produced. We were also unable to find any phosphorylation at this site by mass spectrometry and saw no decrease in phosphorylation when the residue was substituted for alanine. It is possible that phosphorylation at this residue per se does not have an impact on virus life cycle, but the residue itself is important for the virus life cycle. When amino acid residues at positions S94, T183, or S298 were substituted with alanine, there was a large decrease in minigenome activity. Viruses containing these mutations were not obtained after multiple attempts, likely due to the low level of replicative activity seen in the minigenome system, suggesting that these residues play important roles in the virus life cycle. It is surprising that viruses containing mutations at S67 and T387 were not obtained since these mutations did not affect minigenome activity. It is likely that these residues, not necessarily their phosphorylation status, may play a role beyond viral RNA synthesis. Interestingly, mutations at the unstructured C-terminus of NP allowed rescue of infectious virus and we were unable to rescue infectious viruses containing mutations at the N-terminal of NP, suggesting that residues in the more structure N-terminus need to be preserved.

Understanding the roles of phosphorylation of MuV NP will not only contribute to our knowledge on viral RNA synthesis, but also aid design of novel anti-virals and the

next generation of vaccines. Since MuV is not known to encode its own kinase to phosphorylate NP, the host kinases responsible for NP phosphorylation may be viable drug targets. While host kinase responsible for phosphorylation of NP's S439 residue is not likely a good target for antiviral drug development, kinases responsible for phosphorylation of N-terminal of NP may be good targets since mutating these residues resulted in difficulties in obtaining infectious viruses. Identifying of the host kinases responsible for phosphorylating these critical sites of NP may lead to development of small molecule inhibitors of the kinases as anti-MuV drugs, which do not exist at present. Preventing phosphorylation at NP-S439 was able to increase viral replication in Vero cells. This mutation can be incorporated into vaccine viruses enabling faster growth and higher titer viruses, which will reduce the cost of future vaccines.

Acknowledgements

We appreciate the helpful discussion and technical assistance from all members of Dr. Biao He's laboratory. This work was supported by grants (R01AI097368 and R01AI106307) from the National Institutes of Health.

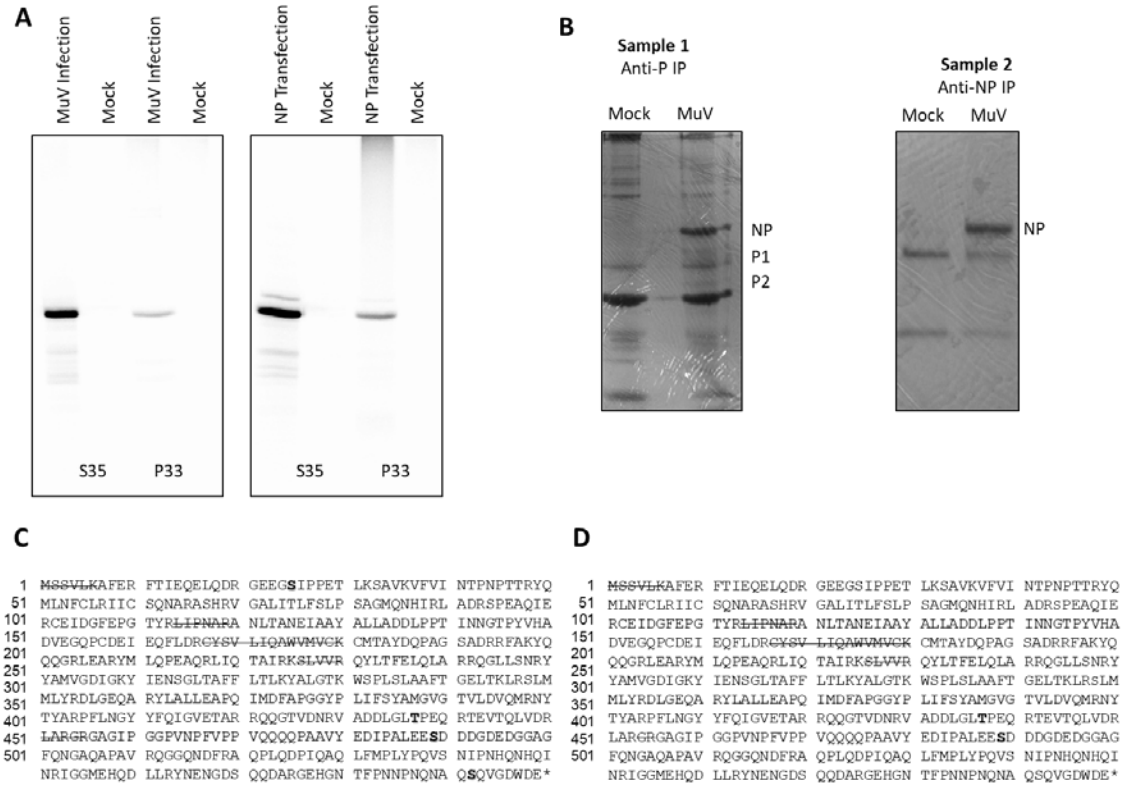

Figure 3.1. Analysis of NP phosphorylation by mass spectrometry. (A) Phosphorylation of NP in infected or transfected cells. Vero cells were infected with MuV-IA and HEK293T cells were transfected with NP and P. After 24 hr, proteins were labeled with ^{35}S-met or ^{33}P-Orthophosphoric acid. Cells were lysed and immunoprecipitated with anti-NP mAb. The samples were resolved by SDS-PAGE. (B) Immunoprecipitiation of NP by anti-NP and anti-P. Vero cells were infected by MuV-IA and lysate was immunoprecipitated with an anti-P mAb (sample 1). Unbound protein was immunoprecipiatated with and anti-NP mAb (sample 2). The samples were resolved by SDS-PAGE followed by visualization using Coomassie blue and NP band was excised for analysis by LC-MS/MS. The P1 and P2 bands of MuV P were excised for analysis in

another study. (C) Coverage of MS of NP after anti-P IP. (D) Coverage of MS of NP after anti-NP IP. Phosphorylated positions are in bold and positions not covered are struck through. Phosphorylation was considered significant with a random probability score of less than 5%.

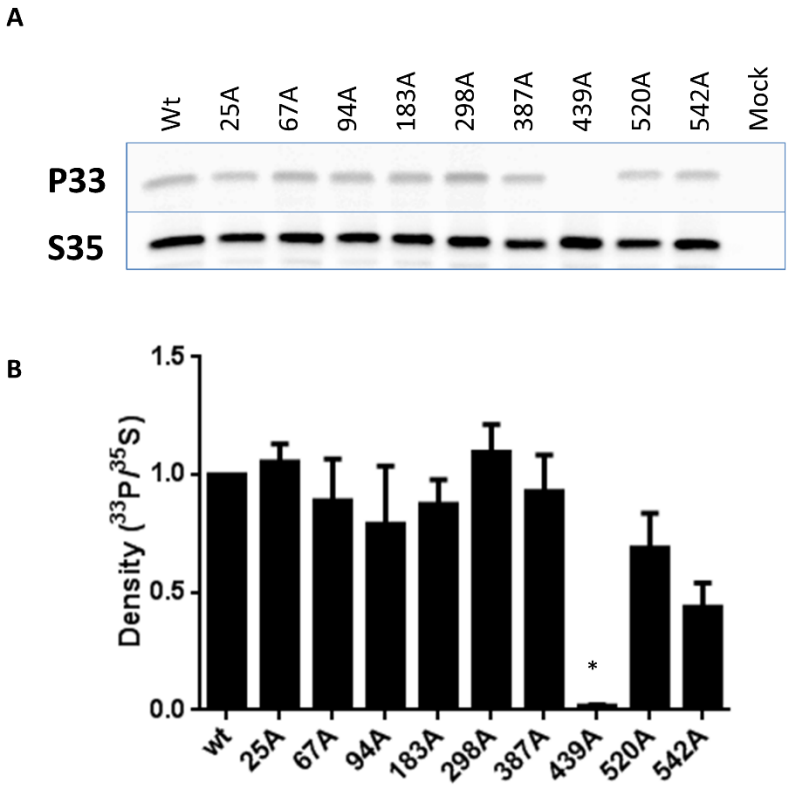

Figure 3.2. Phosphorylation of NP mutants in transfected cells. (A) Detection of NP mutant phosphorylation. Residue S439 was found to be the major phosphorylation site in NP. HEK293 cells were transfected with plasmids encoding either wt or NP with S/T residues mutated to A followed by ^{35}S-Met/Cys or ^{33}P-Orthophosphoric acid. Immunoprecipitation was performed with an anti-NP mAb and samples were resolved by SDS-PAGE. A representative gel is shown along with data from three separate experiments. (B) Summary of quantified NP phosphorylation. The relative density of

the phosphorylated versus total NP was calculated for each experiment. All data was normalized to *wt* NP. (One-way ANOVA with Holm-Sidak multiple comparison test, N=3, *p<0.001)

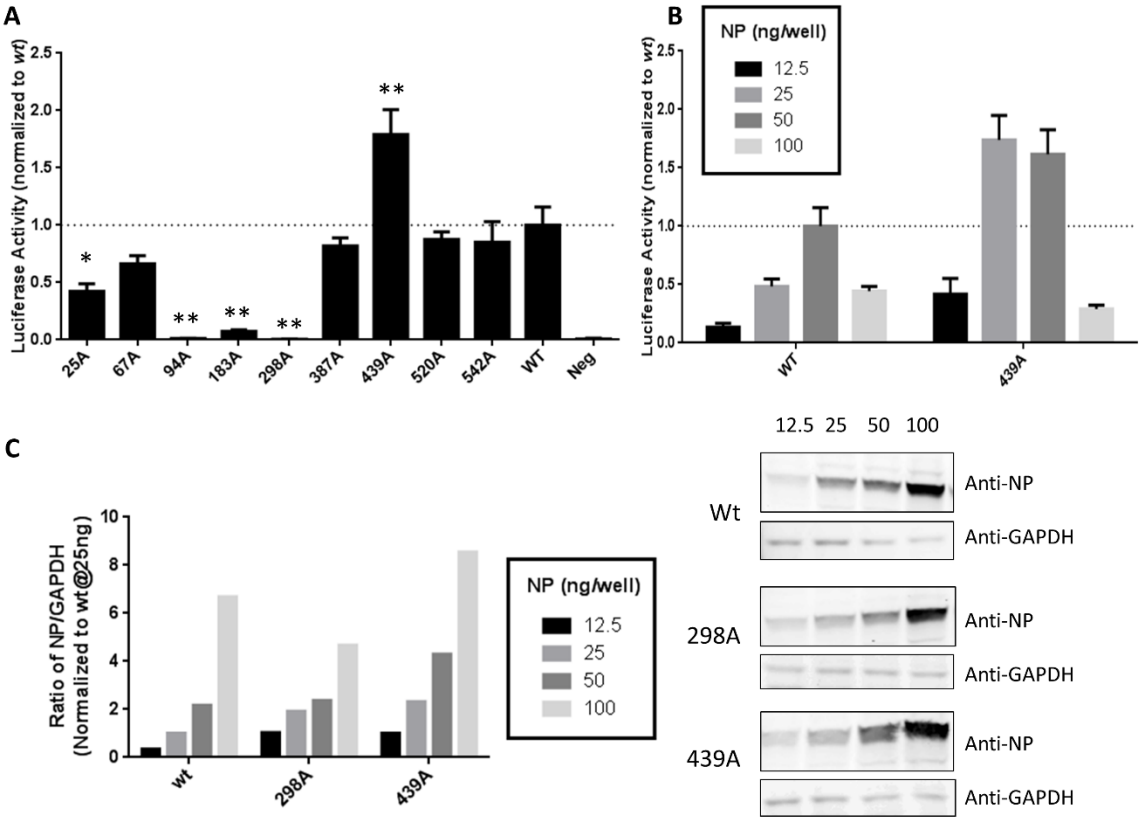

Figure 3.3. Effects of NP mutants on the MuV minigenome system. (A) Peak minigenome activity of the NP mutants. A MuV minigenome assay was performed using plasmids encoding NP with possible phosphorylation sites mutated to alanine. The amount of NP plasmid was varied (12.5, 25, 50, 100ng/well). The ratio of Renilla luciferase to firefly luciferase activity was normalized to wt for each sample and the peak titer is reported. Mutating position S439 was found to significantly increase minigenome activity. (n=3, ANOVA with Dunnett's multiple comparison test, *p<0.01, **p<0.001) (B) Representative activity curves for the minigenome assay. The minigenome activity

for *wt* and S439A NP are shown at each concentration tested. (C) The expression of NP was assessed by western blot. All mutant proteins were shown to be expressed at similar levels, as seen by blotting for NP using an NP specific mAb.

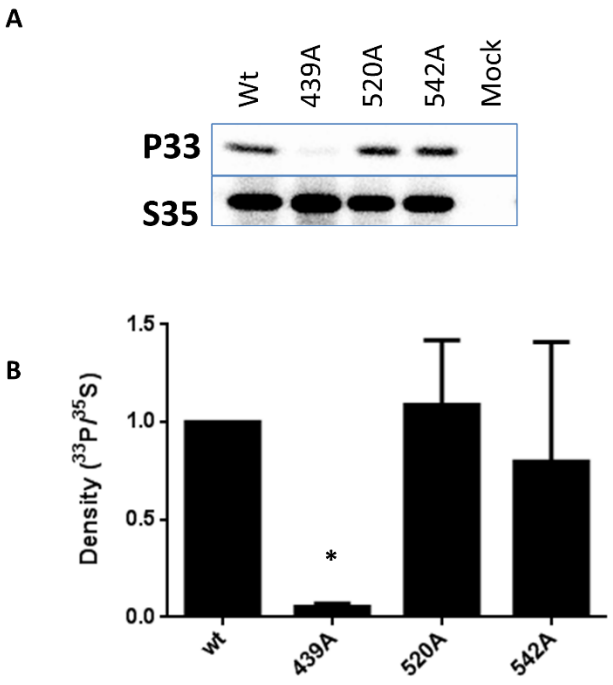

Figure 3.4. Phosphorylation of NP mutants in infected cells. (A) Detection of phosphorylation of NP mutants. Vero cells were infected with MuV (wt) or mutant viruses. Radioactive labeling was performed and lysates were immunoprecipitation with an anti-NP mAb. Samples were resolved by SDS-PAGE. A representative gel is shown. (B) Summary of NP phosphorylation in infected cells. MuV-NP-S439A was found the have significantly reduced phosphorylation in infected cells. (N=3, student t-test, *$p<0.01$)

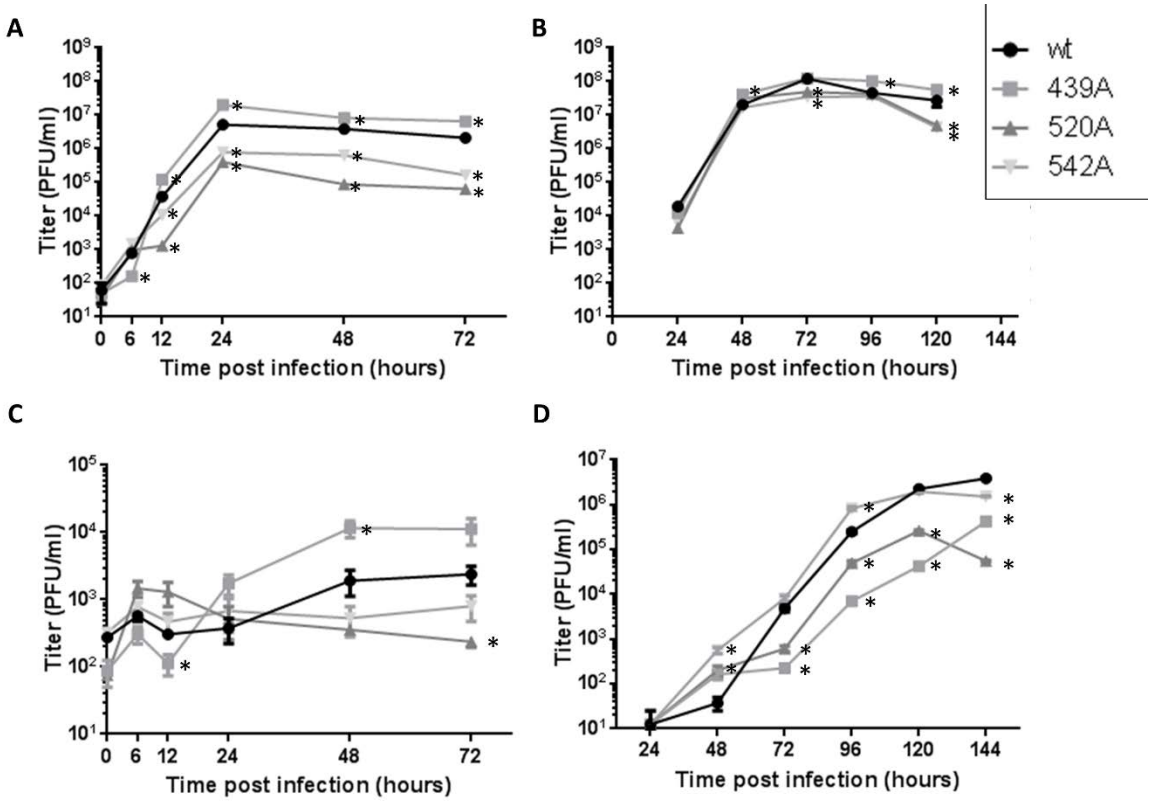

Figure 3.5. Growth kinetics of MuV mutants. In each experiment, cells were infected with MuV(wt), S439A, S520A, or S542A. Media was collected at various time points. The titer of virus in the media was determined by plaque assay using Vero cells (A) Vero cells infected at an MOI of 5. (B) Vero cells infected at an MOI of 0.01. (C) HeLa cells infected at an MOI of 5. (D) HeLa cells infected at an MOI of 0.01. (For all growth curves: n=3, ANOVA with Dunnett's multiple comparison test, *$p<0.05$)

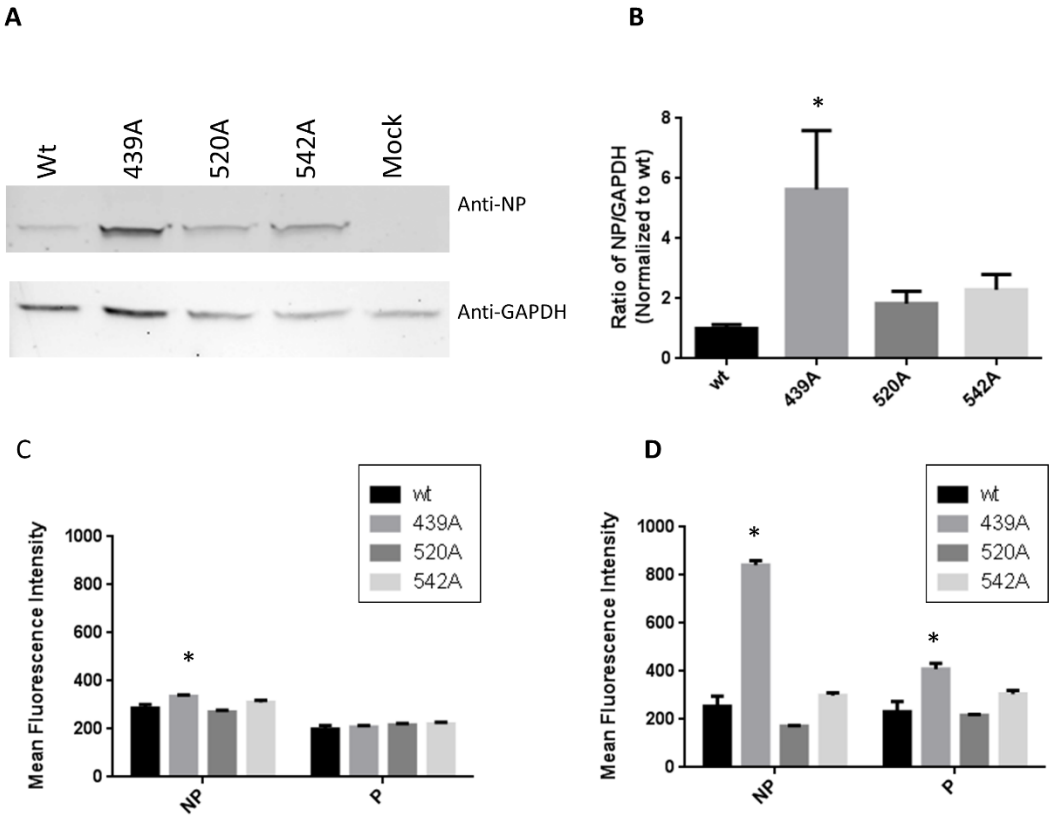

Figure 3.6. Protein production in infected Vero cells. In each experiment, cells were infected with MuV wt, S439A, S520A, or S542A. (A) Total protein production in Vero cells infected at an MOI of 5 after 24 hours. Samples were resolved by SDS-PAGE and NP was quantified by western blot. (B) Summary of total protein production in Vero cells infected at an MOI of 5. Average density was calculated over multiple experiments and 439A was found to have increased protein production. (C) Protein production in Vero cells infected at an MOI of 0.1 after 6 hours. Cells were collected and stained using anti-NP (A488) and anti-P (APC) for flow cytometry. The mean fluorescence intensity (MFI) was calculated for the stained population. (D) Protein production in Vero cells infected at an MOI of 5 after 24 hours. Cells were treated as in (C). (One-way ANOVA with Holm-Sidak multiple comparison test, n=3, *$p<0.05$)

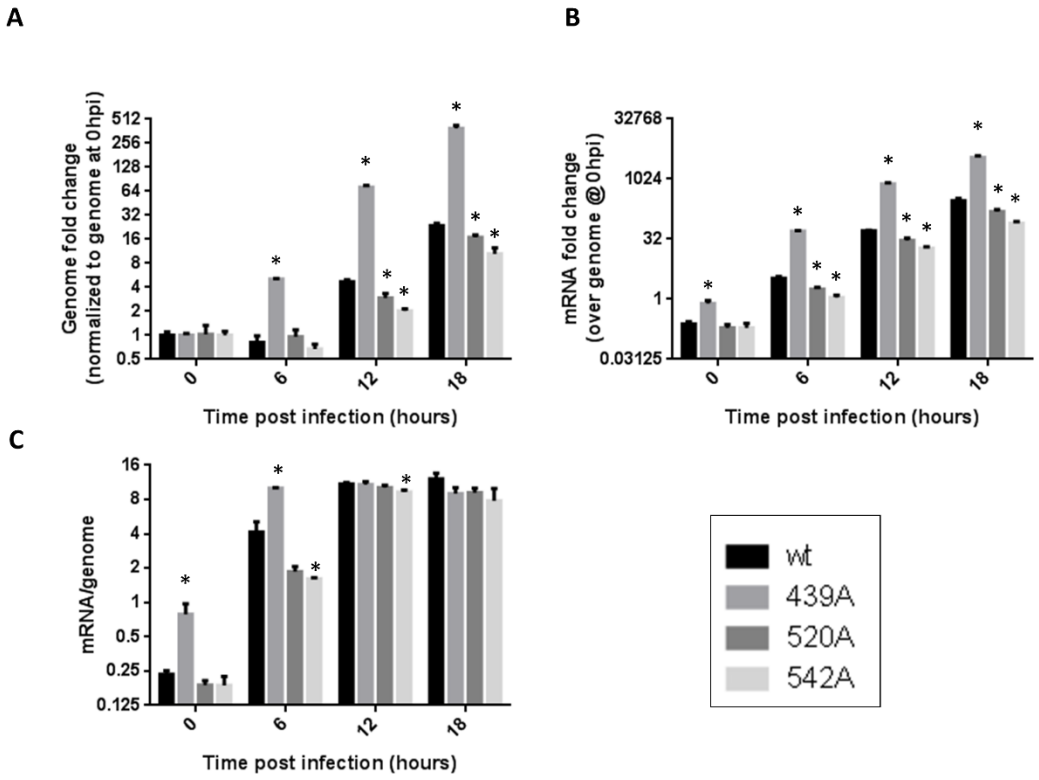

Figure 3.7. Genomic RNA and mRNA levels in infected Vero cells. Vero cells were infected at an MOI of 0.1 with MuV(wt), S439A, S520A, or S542A. Total RNA was extracted from biological replicates (n=3). Real-time PCR was performed on each sample using a using a MuV-F specific FAM-tagged probe. (A) Levels of genomic RNA. Genome replication was calculated after normalization to genomic RNA levels at 0 hpi. (B) Levels of viral mRNA. mRNA production was calculated after normalization to genomic RNA levels at 0 hpi. (C) Quantification of relative levels of mRNA to genomic RNA. The ratio of mRNA to genomic RNA was calculated at each timepoint. (Multiple T-tests with Holm-Sidak multiple comparison test, n=3, *$p<0.05$)

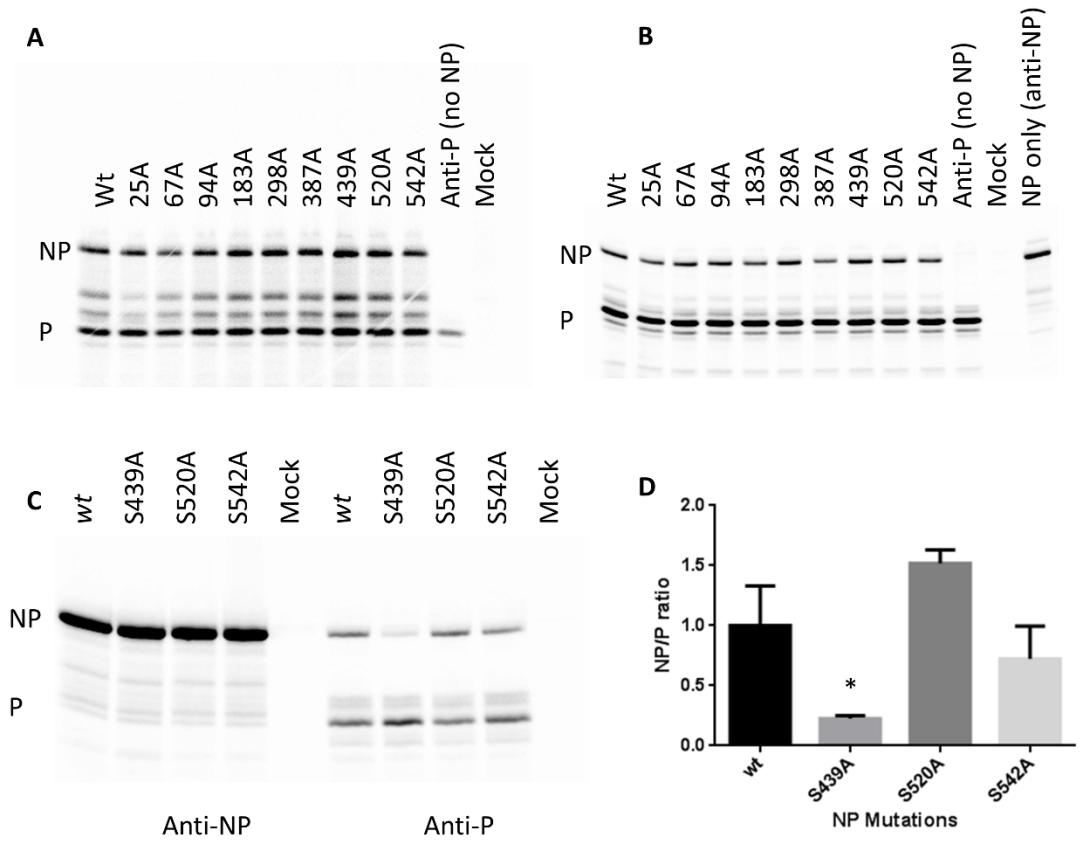

Figure 3.8. Interaction between MuV NP and P. (A) Interaction between NP and P in transfected cells. HEK293T cells were transfected with wt and mutant NPs and P. Proteins were labeled with ^{35}S-Met/Cys and co-immunoprecipitation was performed using antibodies specific to NP. No difference was detected in the amount of NP or P pulled down. (B) Interaction between NP and P in transfected cells. Using the same samples as (A), co-immunoprecipitation was performed using antibodies specific to P. No difference was detected in the amount of NP or P pulled down. (C) Interaction between NP and P in infected cells. Vero cells were infected with MuV (wt), S439A, S520A, S542A, or mock infected. Total protein was labeled with ^{35}S-Met/Cys and co-immunoprecipitation was performed using antibodies specific to NP or P. (D) The mean of the NP to P ratio for the anti-P immunoprecipitation is graphed with the SEM shown.

There was less NP co-immunoprecipitated with P, during infection with rMuV-NP-S439A. (n=3, student t-test, *p<0.05

Amino Acid	NetPhos (*in silico*)	LCMS Phos (anti-P IP)	LCMS Phos (anti-NP IP)
T12	**0.689**	N/A	N/A
S25	0.071	**0.0024**	29
T30	**0.950**	N/A	N/A
T42	**0.891**	N/A	N/A
S67	**0.990**	N/A	N/A
S94	**0.996**	0.28	0.29
T183	0.091	N/A	8.4
S191	**0.749**	N/A	N/A
S226	**0.510**	N/A	N/A
S298	0.042	N/A	0.059
T368	**0.816**	N/A	N/A
T387	**0.565**	**0.0004**	**0.0032**
T395	**0.500**	N/A	150
S439	**0.992**	**0.0074**	**0.00036**
S520	**0.979**	N/A	N/A
S542	**0.028**	**0.00015**	3.4

Table 3.1. Phosphorylation of MuV NP by *in silico* prediction and mass spectrometry. Phosphorylation site prediction was performed using the NetPhos 2.0 Server (http://www.cbs.dtu.dk/services/NetPhos/). Values >0.5 were considered to likely be phosphorylated and are highlighted. Phosphorylation sites found by mass spectrometry (as described in Fig. 3.1) are shown in the two right columns. The random probability score for each site is listed, with a score of <0.05 considered likely to be phosphorylated and are highlighted.

CHAPTER 4

MUMPS VIRUS NUCLEOPROTEIN ENHANCES PHOSPHORYLATION OF THE PHOSPHOPROTEIN BY POLO-LIKE KINASE 1[2]

[2]Pickar A*, Zengel J*, Xu P, Li Z, He B. J Virol 2015;90:1588–98. *Contributed equally to this work. Reprinted with the permission of the publisher.

Abstract

The RNA-dependent RNA polymerases (vRdRP) of non-segmented, negative-sense viruses (NNSV) consist of the enzymatic large protein (L) and the phosphoprotein (P). P is heavily phosphorylated and its phosphorylation plays a critical role in viral RNA synthesis. Since NNSVs do not encode kinases, P is phosphorylated by host kinases. In this study, we investigate the roles that viral proteins play in the phosphorylation of mumps virus (MuV) P. We found that NP enhances the phosphorylation of P. We have identified the serine/threonine kinase polo-like kinase 1 (PLK1) as a host kinase that phosphorylates P and that phosphorylation of P by PLK1 is enhanced by NP. The PLK1 binding site in MuV P was mapped to residues 146-148 within the S(pS/T)P motif and the phosphorylation site was identified as residues S292 and S294.

Significance

It has previously been shown that P acts as a chaperone for NP, which encapsidates viral genomic RNA to form the NP-RNA complex, the functional template for viral RNA synthesis. Thus, it is assumed that phosphorylation of P may regulate NP's ability to form the NP-RNA complex, thereby regulating viral RNA synthesis. Our work demonstrates that MuV NP affects phosphorylation of P, suggesting that NP can regulate viral RNA synthesis by regulating phosphorylation of P.

INTRODUCTION

Many human and animal pathogens such as mumps virus (MuV), Sendai virus (SeV), human respiratory syncytial virus (RSV), the parainfluenza viruses, Measles virus (MeV), J paramyxovirus (JPV), Hendra virus (HeV), and Nipah virus (NiV) are in the *Paramyxoviridae* family of the *Mononegavirales* [1]. The non-segmented, negative-stranded RNA genome of these viruses is encapsidated by the nucleoprotein (NP) to produce the helical nucleocapsid that functions as the template for viral RNA synthesis. The viral RNA dependent RNA polymerase (vRdRp), which minimally consists of the phosphoprotein (P) and the large protein (L), functions for both transcription and replication of the viral RNA genome. The enzymatic activities of the L protein are responsible for initiation, elongation, and termination of RNA synthesis, and the L protein functions to add the 5' cap and 3' poly(A) sequences to transcribed viral mRNA [1]. P protein interacts with NP to dock the vRdRp to the NP-RNA template.

The P proteins of paramyxoviruses are highly phosphorylated and phosphorylation of these proteins has been shown to play critical roles in regulating viral mRNA synthesis [2–7]. Phosphorylation of residues within the P protein of parainfluenza virus 5 (PIV5), a prototypical paramyxovirus, plays both negative and positive roles in mRNA synthesis [3–5]. A phosphorylation site at S157 was found in the P protein of PIV5-infected cells [3]. Further studies indicate that polo-like kinase 1 (PLK1) associates with S157 and phosphorylates the PIV5 P protein at S308 [3,4]. Phosphorylation of both of these residues reduces viral gene expression and prevents cytokine induction and cell death. This report shows that P phosphorylation negatively regulates viral gene expression, suggesting that PIV5 limits its gene expression to avoid induction of innate

immune responses [4]. Further studies of the PIV5 P protein by mass spectrometry have identified T286 as a phosphorylation site and mutation of this residue reduces mini-genome activity [5]. A recombinant virus containing the T286 mutation grows slower than wild-type PIV5 and has delayed viral mRNA synthesis and protein expression, demonstrating that phosphorylation at T286 plays a positive role in virus growth and viral gene expression by up-regulating viral mRNA transcription [5]. These studies suggest a role of P phosphorylation in viral mRNA synthesis.

It is commonly believed that phosphorylation of the P proteins is carried out by host kinases [8]. The main host kinases that have been identified so far to phosphorylate paramyxovirus P proteins are casein kinase II (CKII), protein kinase c isoform zeta (PKC-ζ), protein kinase B (AKT) and PLK1 [9–14]. The P proteins of RSV and measles virus are thought to be phosphorylated by CKII [9–11]. The P proteins of HPIV3 and Sendai virus are reported to be phosphorylated by PKC-ζ [12,13] The P protein of canine distemper virus is phosphorylated by both PKC-ζ and CKII [14]. Phosphorylation of the PIV5 P protein by AKT results in up regulation of viral gene expression whereas phosphorylation by PLK1 results in down regulation [15]. It has been proposed to target host kinases that are critical for viral RNA synthesis as an anti-viral strategy for these paramyxoviruses [15].

MuV is a human pathogen of the *Rubulavirus* genus of the family *Paramyxovidae*. MuV infection causes acute parotitis and it is a neurotropic agent with symptoms ranging from mild meningitis to severe encephalitis [16]. Phosphorylation of MuV P plays a role in viral RNA synthesis [7]. A systematic mutational analysis of MuV P has identified residue T101 of P important in viral RNA synthesis. Analysis of a

recombinant MuV containing this mutation (rMuV-P-T101A) indicates that phosphorylation at P-T101 plays a negative role in viral transcription [7]. Host kinases that are important for MuV phosphorylation have not been identified.

In this work, we examined the role of viral proteins in phosphorylation of P of MuV, identified a host kinase that is important for MuV replication and investigated the mechanism of activation of this host kinase.

Materials and Methods

Plasmids and cells

A plasmid containing the human PLK1 gene was obtained from Open Biosystems (AL, USA). A Flag tag was added to the N-terminus of PLK1 and cloned into pCAGGS vector. Kinase-deficient PLK1 (Flag-PLK1-K82M) was constructed using Flag-PLK1 as the template as previously described [4]. MuV NP, P, and L genes of the $MuV^{Iowa/US/06}$ strain were cloned into the pCAGGS expression vector [21]. Plasmids expressing P mutants were constructed using standard molecular cloning techniques. Plasmids containing the full-length genome for rMuV-P-T147A, rMuV-P-S292A/S294A, and rMuV-P-T147A/S292A/S294A viruses were made similarly to that of rMuV-P-T101A as described before [7]. The MuV mini-genome plasmid (BH526/ pMG-RLuc), containing *Renilla*, and a plasmid containing firefly-luciferase (pFF-Luc) were described previously [7]. Construction details and sequence files of the plasmids are available upon request.

HEK293T cells were maintained in Dulbecco's modified Eagle medium (DMEM) with 5% fetal bovine serum (FBS) and 1% penicillin-streptomycin (P/S) (Mediatech Inc., Manassas, VA). Vero and HeLa cells were maintained in DMEM supplemented with 10% FBS and 1% P/S. BSR-T7 cells were maintained in DMEM supplemented with 10%

FBS, 1% P/S, 10% tryptose phosphate broth (TPB), and 400 μg/ml G418 sulfate antibiotic (Mediatech Inc.). All cell lines were incubated at 37°C with 5% CO_2 and passed at an appropriate dilution one day prior to use, to achieve 80 to 90% confluence upon transfection or infection.

Transfections, infections, and virus rescue

Cells were transfected using JetPRIME® (Polyplus-transfection Inc., New York, NY) following the manufacturer's protocols. For virus infections, cells were inoculated with viruses at a multiplicity of infection (MOI) of 0.1 or 3 in DMEM plus 1% bovine serum albumin (BSA) and incubated at 37°C with 5% CO_2 for 1-2 hours. The inocula were then replaced with DMEM supplemented with 2% FBS and 1% P/S.

rMuV-P-T147A, rMuV-P-T204A, rMuV-P-S292A/S294A, rMuV-P-T147A/T204A, and rMuV-P-T147A/S292A/S294A were rescued from the plasmids containing their respective full-length genome as described before [7]. A plasmid containing the full-length genome (5 μg), along with plasmids pCAGGS-L (2 μg), pCAGGS-NP (100ng), and pCAGGS-P (320ng), were transfected into BSR-T7 cells. Three days later, transfected BSR-T7 cells were mixed with Vero cells at a 1:5 dilution. Four days later, media was transferred to fresh Vero cell monolayers and propagated further. When syncytia formation was observed, media was collected and used for plaque assays in Vero cells as previously described [5]. Single plaques were isolated 6-7 days later and cultured in fresh Vero cells to produce passage 1 (P1). After titer determination, P1 was passaged again at an MOI of 0.01 to produce P2. After 72 hrs, virus was collected, sucrose-phosphate-glutamate SPG (2.18 M sucrose, 37.6 mM potassium phosphate monobasic, 71 mM potassium phosphate dibasic, and 49 mM potassium

glutamate) was added to 1% final concentration, and aliquots were stored at -80°C. Titers were determined by plaque assay. Viral genomes were sequenced as previously described [27]. Viral RNA was isolated using QIAamp Viral RNA Mini Kit (Qiagen, Valencia, CA) followed by synthesis of DNA templates using SuperScript III One-Step RT-PCR System with Platinum Taq (Life Technologies, Grand Island, NY) and 5 sets of primers to amplify the entire genome. Fragments were sent to Genewiz (South Plainfield, NJ) for sequencing using 6-10 primers per fragment. Only viruses matching the full-length plasmid sequence were used for further experiments. Primer sequences are available upon request.

Phosphorylation of P

To examine phosphorylation of P, HeLa cells or HEK293T cells in 6-well plates were transfected with 1 μg of pCAGGS-P or pCAGGS-P mutants, 1 μg of pCAGGS-NP, and 1 μg of Flag-PLK1 or Flag-PLK1-K82M, or infected with MuV or a recombinant mutant MuV at an MOI of 0.1. After 18 hpt, the cells were starved with DMEM lacking cysteine-methionine and then labeled with 72.7 μCi/ml ^{35}S-EasyTagTM Express35S Protein Labeling (Perkin Elmer, Waltham, MA) for 3-8 hours (h) or starved with DMEM lacking sodium phosphate and then labeled with 100 μCi ^{33}P-Radionuclide Orthophosphoric acid (Perkin Elmer, Waltham) for 8 h. The cells were then lysed with whole-cell extraction buffer (WCEB) (50mM Tris-HCl [pH 8.0], 280 mM NaCl, 0.5% NP-40, 0.2 mM EDTA, 2 mM EGTA, and 10% glycerol) with a mixture of protease inhibitors as previously described [23].The lysate was immunoprecipitated using rec-protein G-sepharose 4B conjugate and mouse monoclonal anti-MuV-P, mouse monoclonal anti-MuV-NP, or mouse anti-Flag (M2 clone, Sigma-Aldrich, St. Louis, MO)

antibodies. After washing 3x with WCEB, the agarose beads were mixed with 3x SDS loading buffer (188 mM Tris-HCl [pH 6.8], 6% SDS, 30% glycerol, 0.03% w/v bromophenol blue, and 200 mM dithiothreitol [DTT]), heated at 95°C for 5 min, and resolved by 10% SDS-polyacrylamide gel electrophoresis (PAGE). Phosphorylation of the P protein of 4 individual experiments was calculated by densitometry analysis of the $^{33}P/^{35}S$ ratio using ImageQuant TL software (GE Healthcare Life Sciences).

PLK1 inhibitor

The highly selective PLK1 inhibitor, BI 2536, was purchased from Selleck Chemicals (Houston, TX). The compound was dissolved in ethanol. To study the effect of the PLK1 inhibitor on P phosphorylation in infected cells, Vero cells were infected with MuV at an MOI of 0.1 and incubated with 1 uM BI 2536. To study the effect of the PLK1 inhibitor on P phosphorylation in transfected cells, HEK293T cells were transfected with 1 μg of P or P mutants, 1 μg of NP, and 1 μg of Flag-PLK1. At 18 hours post infection (hpi) or transfection, cells were starved with DMEM lacking cysteine-methionine and then labeled with 72.7 μCi/ml ^{35}S-EasyTagTM Express35S Protein Labeling (Perkin Elmer) in the presence of 1 uM BI 2536 for 3 h. The cells were then lysed with WCEB and immunoprecipitated as described above.

To study the effect of PLK1 inhibitor on viral protein expression, Vero cells were infected with a recombinant virus expressing a *Renilla* luciferase protein (rMuV-Rluc) at an MOI of 0.01 and incubated with BI 2536 at various concentrations. After 24 hpi cells were lysed with *Renilla* luciferase assay lysis buffer (Promega) and vigorously mixed for 20 min to permit full lysis. *Renilla* luciferase activity was measured according to manufacturer's protocol (Promega) and light intensity was detected by a GloMax® 96

Microplate Luminometer (Promega). Aliquots of the cell lysates were used for Western blot analysis to detect P protein expression.

MuV mini-genome system and dual-luciferase assay.

The MuV mini-genome system used in this study was described previously [7]. BSR-T7 cells in 24-well plates were transfected with pCAGGS-P (80ng) pCAGGS-NP (25 ng), pCAGGS-L (500 ng), pMG-RLuc (100 ng), pFF-Luc (1 ng), and various amounts of Flag-PLK1 or Flag-PLK1 (K82M) (0, 16, 32, or 64 ng). Empty pCAGGS vector was used to normalize the amount of transfected DNA per sample. After 48 hpt, 2/5 of the lysate from each well was used to carry out the dual-luciferase assay according to the manufacturer's protocol (Promega, Madison, WI), and light intensity was detected using a GloMax 96 Microplate Luminometer (Promega). Relative luciferase activity was defined as the ratio of *Renilla* luciferase (R-Luc) to firefly luciferase (FF-Luc) activity. Six replicates of each sample were measured. Cell lysate aliquots from the dual luciferase assay were mixed with one-half volume of 3x SDS loading buffer and heated at 95°C for 5 min. Samples were resolved by 10% SDS-PAGE and transferred to a polyvinylidene difluoride membrane (GE Healthcare, Piscataway, NJ). The membrane was incubated with mouse anti-MuV-NP antibody (1:2000 dilution) or mouse anti-Flag (M2 clone, Sigma, 1:1000 dilution), followed by incubation with Cy3 conjugated goat anti-mouse IgG secondary antibody (1:2500 dilution) (Jackson ImmunoResearch, West Grove, PA) and scanned using a Typhoon 9700 imager (GE Healthcare Life Sciences, Piscataway, NJ).

Pulse-chase labeling

To examine the stability of P, HEK293T cells were transfected with 1 μg of P, 1 μg of NP, and 1 μg of Flag-PLK1. Empty pCAGGS vector was used to normalize the amount of transfected DNA per sample. After 18 hpt, the cells were starved with DMEM lacking cysteine-methionine and then labeled with 72.7 μCi/ml ^{35}S-EasyTagTM Express35S Protein Labeling for 30 min. The cells were then washed with PBS and the media was replaced with DMEM supplemented with 2% FBS and 1% P/S. After replacing the media (0 h) and after 4, 8, and 12 h, cells were lysed with WCEB and the lysate was immunoprecipitated using rec-protein G-sepharose 4B conjugate and mouse anti-MuV-P as described above. The P half-life of 4 individual experiments was calculated by normalization of P expression at 0 h using ImageQuant TL software (GE Healthcare Life Sciences).

Single-step growth curve

Vero cells in 10-cm dishes were infected with MuV, rMuV-P-T147A, rMuV-P-S292A/S294A, or rMuV-P-T147A/S292A/S294A at a MOI of 3 in triplicate. Media was collected at 0, 8, 16, 24, 48, 72 hpi and supplemented with 1% SPG, then stored at -80°C. Virus titers were determined in Vero cells by plaque assays, and completed in triplicate as previously described [5].

Phosphorylation of P in related viruses

Plasmids encoding NP and P for parainfluenza virus 5 (PIV5, W3A), J paramyxovirus (JPV, JPV-BH), respiratory syncytial virus (RSV, A2), and measles virus (MeV, Edmonston) were previously produced or cloning into pCAGGS vector for this study. Plasmids were transfected along with PLK1 or PLK1 (K82M) in different

combinations. After 24 hours, radioactive labeling was performed as previously described above. Immunoprecipitation was performed using monoclonal antibodiesAbs specific to P (PIV5: anti-P/V, JPV: rabbit anti-P, RSV: clone C1 MeV: clone 9H4). Samples were resolved by SDS-PAGE.

Statistical analysis

Statistical analysis was performed using GraphPad Prism version 5.00 for Windows (GraphPad Software, San Diego, CA). Student's *t* test was used to calculate *P* values when comparing two groups. When performing multiple comparisons, the Holm-Sidak method with alpha = 5% was used to determine statistical significance.

Results

Phosphorylation of MuV P is greater in virus-infected cells compared to cells transfected with P

Previous research shows that there is a difference in the phosphorylation of MuV P in MuV-infected cells versus cells transfected with plasmid encoding MuV P [7]. To confirm these results, HeLa cells were transfected with plasmids encoding MuV P or infected with MuV. The cells were radioactively labeled with either ^{35}S-Cys/Met or ^{33}P-orthophosphate and lysates were immunoprecipitated with a monoclonal anti-MuV-P antibody to determine the amount of phosphorylation (Fig. 4.1A). P phosphorylation was lower during transfection compared to virus infection. Most interestingly, there was a difference in the patterns of P bands associated with the P protein in infected cells versus transfected cells. This higher band was also the major phosphorylated species in infected cells. The major phosphorylated P species, the slower migrating band, was detected in MuV-infected cells but not in transfected cells.

To understand the discrepancy in phosphorylation of P in transfected cells versus infected cells, we examined phosphorylation of P in cells containing the mini-genome system components. The mini-genome system has been used to examine MuV RNA synthesis [7]. Plasmids encoding P, L, and NP were transfected along with a plasmid encoding the MuV mini-genome under a T7 promoter. When the mini-genome plasmid is transcribed by T7 RNAP, a negative-sense mini-genome RNA is produced, consisting of the leader and trailer of MuV flanking the negative sense coding sequence for Renilla luciferase. Since this system is able to model the transcriptional activity observed during infection, we reasoned that phosphorylation of P in this system should reflect that of P in infection. BSR-T7 cells are typically used for mini-genome experiments due to their stable expression of T7 RNAP. However, the expression level of transfected plasmids in BSR-T7 cells was not sufficient to examine phosphorylation using radioactive labeling. Instead, HEK293T cells were used. P was transfected alone, with the individual mini-genome components, or with all of the components together. Radioactive labeling and P immunoprecipitation was performed as before and samples were resolved by SDS-PAGE (Fig. 4.1B). The phosphorylation of MuV P was enhanced in the presence of MuV NP, while the other mini-genome components had no effect. The phosphorylation of transfected P was closer to that of P during infection when NP was co-transfected. Most importantly, the pattern of phosphorylated P looked similar between P+NP and MuV-infected samples.

MuV NP and PLK1 are both required for high levels of MuV P phosphorylation

To understand the mechanism of the enhanced phosphorylation of P by NP, it will be important to identify the host kinase that phosphorylates P during viral infection. It has

been shown that PLK1 is responsible for the phosphorylation of P for the closely related virus parainfluenza virus 5 (PIV5) [4]. PLK1 is a serine/threonine kinase that functions as the critical regulator in progression through mitosis [17]. PLK1 contains a polo-box domain (PBD) and a kinase activity domain. The PBD domain of PLK1 interacts with its target through the consensus binding motif (S p(S/T) P), where the second amino acid residue is phosphorylated for optimal binding [18]. Upon binding of PLK1 to its target within the STP motif, PLK1 phosphorylates the target itself or a protein associated with the target [19]. To determine if PLK1 was responsible for MuV P phosphorylation in infected cells, we treated MuV-infected cells with a PLK1 inhibitor (BI 2536) during radioactive labeling. Treatment of infected cells with BI 2536 resulted in an 80% reduction in P phosphorylation (Fig. 4.2A and 4.2B). The P_1 band (the major phosphorylated P species) was no longer visible in the BI 2536-treated sample. These results suggest that PLK1 phosphorylates P in infected cells.

To determine the role of PLK1 in phosphorylation of P in transfected cells, plasmids encoding P, NP and Flag-PLK1 were transfected in different combinations (Fig. 4.3A). As seen previously, the addition of NP resulted in greater P phosphorylation. There was also an increase in P phosphorylation when P and PLK1 were co-expressed. When all three plasmids were transfected together, there was a large increase in the amount of P phosphorylation and a shift to a dominant P_{1T} band. The increase was greater than the additive effect when adding NP or PLK1 alone, suggesting that the coordination of NP, P, and PLK1 results in synergistic enhancement of P phosphorylation.

PLK1 kinase activity is required for increased phosphorylation of MuV P

To confirm that PLK1 kinase activity was required for phosphorylation of MuV P, we used a plasmid encoding a PLK1 kinase deficient mutant (PLK1-K82M). The PLK1 kinase deficient mutant has a point mutation in the ATP binding motif (K82M) and lacks kinase activity [20]. We found that the enhanced phosphorylation phenotype and dominant P_{1T} band for the P+NP+PLK1 sample was absent when PLK1 was replaced with the kinase deficient mutant (Fig. 4.3B). This suggests that PLK1 kinase activity is required for enhanced P phosphorylation.

We confirmed that PLK1 activity is required for P phosphorylation by treating transfected samples with BI 2536 during radioactive labeling (Fig 4.3C). A band shift from P_{1T} to P_2 was observed in the inhibitor-treated sample. This band shift was consistent with a loss of phosphorylation observed in earlier experiments and suggests that BI 2536 prevents P phosphorylation during transfection. There was also an increase in the amount of PLK1 that co-immunoprecipitated with P in the inhibitor-treated samples. PLK1 may dissociate from the transient P-PLK1 complex following phosphorylation, therefore inhibiting PLK1 activity may result in retention of the P-PLK1 interaction.

We also wanted to understand if the enhanced phosphorylation of P during co-transfection with NP, but not PLK1, was dependent on endogenous PLK1activity. In order to do this, cells were transfected with P or P+NP followed by treatment with BI 2536 to inhibit endogenous PLK1 activity (Fig. 4.3D). We found that the enhance phosphorylation of P seen in the presence of NP was abolished when PLK1 activity was inhibited. The treated NP+P sample had phosphorylation at a similar level as P alone

(Fig. 4.3E). This confirms that the enhanced phosphorylation phenotype seen with NP/P co-transfection is PLK1 dependent.

Stability of MuV P in the presence of NP and PLK1

It is possible that NP increases stability of P, not phosphorylation of P. To examine stability of P in the presence of NP, P was transfected with NP, PLK1 or both NP and PLK1. After 18 hours post transfection (hpt), cells were pulsed with radioactive isotope, and the amount of P was determined over time (Fig. 4.4A). The half-life of P in transfected cells was determined for each condition (Fig. 4.4B). The half-life of P was similar when NP and PLK1 were also transfected. There was a significant decrease in the half-life of P when PLK1 was present (P=0.031). These results suggest increased phosphorylation of P in the presence of NP or PLK1 was not due to protein stability. Although there was no difference between half-lives of the total amount of P, the P_{1T} band appeared to be more stable than the P_2 band when P, NP, and PLK1 were co-transfected (Fig. 4.4C).

PLK1 inhibits MuV viral protein production

To understand the role of P phosphorylation by PLK1 in the MuV life cycle, we assessed the role of PLK1 inhibition using recombinant MuV expressing *Renilla* luciferase (rMuV-Rluc) [21]. When Vero cells infected (MOI=0.01) with rMuV-Rluc were treated with BI 2536, there was an increase in reporter expression (Fig. 4.5A). Similar increases were observed in HeLa cells and with a high MOI (data not shown). Viral protein levels were also increased after treatment with BI 2536, corroborating the results observed using the Renilla reporter (Fig. 4.5B).

To determine if treatment with PLK1 inhibitor had a direct effect on viral RNA synthesis, we examined the effects of the inhibitor on the MuV mini-genome system. BSR-T7 cells were transfected with plasmids required for optimal mini-genome activity followed by treatment with BI 2536. After 48 hpt, mini-genome activity was measured (Fig. 4.5C). There was an increase in mini-genome activity at all concentrations of BI 2536 ≥ 50nM. This result suggests that phosphorylation of P by PLK1 decreases MuV transcription and replication.

To determine if overexpression of PLK1 would have the converse effect, PLK1 or PLK1-K82M were transfected along with the mini-genome components. The addition of PLK1 resulted in a decrease in mini-genome activity in a dose dependent manner, while there was no significant difference in the mini-genome activity when the kinase deficient PLK1-K82M plasmid was added (Fig. 4.5D). This result confirms the role of PLK1 as a negative regulator of MuV transcription and replication.

Determining the critical residues in MuV P required for phosphorylation by PLK1

PLK1 has been shown to interact with its target through a highly conserved binding site motif (S-pS/pT-P), where the second amino acid residue, S or T, is phosphorylated for optimal binding and subsequent kinase activity [18,22]. MuV P contains two possible PLK1 binding sites: residues 146-148 (STP) and 203-205 (STP). The second residue of each binding motif was mutated to alanine (A) to produce plasmids encoding P-T147A and P-T204A, as well as a double mutant P-T147A/T204A. The P mutants were co-transfected with NP and PLK1 to determine if there was still enhanced phosphorylation of P, characterized by the presence of a strong P_{1T} band (Fig. 4.6). Cells transfected with NP, PLK1 and P showed the characteristic P_{1T} band, as did the P-T204A

mutant. When NP and PLK1 were co-transfected with P-T147A or P-T147A/T204A, the P_{1T} band was lost. When BI 2536 was included during labeling, P_{1T} was lost for all treated samples. As seen previously (Fig. 4.3C), a greater amount of PLK1 co-immunoprecipitated with P when treated with BI 2536. The amount of PLK1 co-immunoprecipitated was reduced for both mutants containing the T147A mutation. This data shows that PLK1 binding and subsequent phosphorylation of P is dependent on the motif at positions 146-148.

To determine the sites in P that are phosphorylated by PLK1 after PLK1 binding, a library containing the entire serine or threonine residues of P mutated to alanine was screened. Each P mutant was transfected with NP and PLK1, and P phosphorylation was determined based on the presence of the P_{1T} band (Fig. 4.7A). There were three mutants that had decreased P_{1T} band intensity: P-T147A, P-T145A/S146A/T150A, and P-T292A/S294A. To determine critical residues, the two clusters were separated into single site mutants and tested (Fig. 4.7B). As expected, P-T147A had decreased phosphorylation. While P-S292A/S294A had a very low level of phosphorylation, the individual mutations had little difference in phosphorylation. It is likely that these residues are a target for PLK1 phosphorylation and that both residues are compensating each other. The P-T145A/S146A/T150A mutant also had decreased phosphorylation. When split into individual mutations, P-T145A and P-T150A both had low levels of phosphorylation, while P-S146A was similar to wild-type P. Since these sites are close to the PLK1 binding site, it is possible that mutating these sites disrupted the PLK1 binding site. Changes around this site may modify a kinase target domain that is required for phosphorylation at position T147, which is required for efficient PLK1 binding.

We also wanted to determine if the T147 and S292/S294 sites were important for phosphorylation of P in the presence of NP without the addition of exogenous PLK1. In order to determine this, cells were transfected with P, P-T147A, or P-S292A/S294A with or without the addition of NP. We found, as before, that there was enhanced phosphorylation of P in the presence of NP, but that there was little to no increase in phosphorylation of either mutant in the presence of NP (Fig. 4.7C and 4.7D). This suggests that the enhanced phosphorylation of P in the presence of NP is disrupted by mutating the PLK1 binding motif at position T147 or the target motif at position S292/S294.

Determining the effects of point mutations in P of rMuV

To determine the effects of the mutations at the PLK1 binding site (P-T147A) and the target site (P-S292A/S294A), viruses were rescued (rMuV-P-T147A, rMuV-P-S292A/S294A, and rMuV-P-T147A/S292A/S294A). Following rescue, Vero cells were infected and P phosphorylation was determined (Fig. 4.8A). Relative P phosphorylation was decreased by approximately 60% for the mutants containing the T147A mutation (Fig. 4.8B). While total phosphorylated levels of rMuV-P-S292A/S294A were similar to wild-type MuV, the slower moving phosphorylated P was no longer detected.

Growth of rMuV P mutants in cell culture

To determine the effects of these mutations on viral growth, single-step growth curves were performed in Vero cells. Viral titers were determined up to 72 hours post-infection (hpi) (Fig. 4.9A). Each of the P mutations had a significant effect on the growth kinetics of MuV (Fig. 4.9B). rMuV-P-T147A and rMuV-P-T147A/S292A/S294A had increased titers at multiple time points. Mutations that decreased phosphorylation in the

transfection experiments had a positive effect on viral growth, thus this data suggests that P phosphorylation by PLK1 has a negative effect on viral growth.

The role of NP and PLK1 in the phosphorylation of P for related viruses

Since NP played an important role in the phosphorylation of MuV P, we thought that it may also play a role in related viruses. We tested this hypothesis for PIV5, J paramyxovirus (JPV), and respiratory syncytial virus (RSV). For each virus, the effects of NP and PLK1 on P phosphorylation were assessed. PIV5 had a similar phenotype to MuV, with P phosphorylation greatly increasing with the addition of both NP and PLK1 (Fig. 4.10A). The phosphorylation of JPV P was dependent on the presence of NP, but it was not dependent on PLK1 (Fig. 4.10B). For JPV, there was little or no P phosphorylation when NP was not present. For RSV (Fig. 4.10C), P was highly phosphorylated when transfected alone and NP or PLK1 had no effect. These results suggest that NP plays a role in the phosphorylation and function of the P protein in viruses other than MuV.

Discussion

In a previous publication, we observed that the banding pattern and the phosphorylation of MuV P differed in MuV-infected cells compared with transfected cells expressing MuV P alone [7]. We suspected that there were other viral proteins playing a role in the phosphorylation of P. Previous research on the closely related virus PIV5 shows that phosphorylation of PIV5 P is dependent on AKT1 and PIV5 L protein [15,23]. However, phosphorylation of P was not shown to be directly dependent on interaction with L. In our current study, we showed an increase in phosphorylation of P when NP and PLK1 were co-transfected with P for both MuV and PIV5. The degree of

phosphorylation and the banding pattern of P in co-transfected samples were similar in infected cells in contrast to when P was transfected alone. It is important to consider that there may be important interactions that are excluded in the simplified system when a single viral protein is expressed.

The major role of the NP-P interaction is to enable the vRdRP to dock the replication complex onto RNA encapsidated by NP. NP structure, solubility, and RNA binding, are all affected by NP interaction with P. Specifically, P keeps nascent NP soluble until it is ready to bind viral RNA genome [24–26]. Thus, P is thought of as a regulator of NP function. In this work, we have shown that NP can regulated P structure and function. MuV NP is required for enhanced and appropriate phosphorylation of MuV P. This work suggests that NP regulates the phosphorylation status of P, which in turn regulates the functions of P, since the phosphorylation state of P has a clear effect on the transcriptional and replicative activity of the MuV vRdRp complex in both the mini-genome system and during viral infection. The ratio of NP to P has been shown to be important for activity in the MuV minigenome assay [7, 18]. It is possible that increasing the amount of NP could decrease activity through affecting the phosphorylation status of P, which may explain the drop in activity when an excess of NP is transfected. The discovery that NP plays a role in determining the phosphorylation state of P adds complexity to the NP-P interaction.

We examined the mechanism behind the enhanced and appropriate phosphorylation phenotype, by determining the role that PLK1 plays in P phosphorylation and virus growth. It's know that PIV5 P is phosphorylated by PLK1 and that this phosphorylation down-regulates gene expression [4]. The same phenotype was

observed in our experiments with MuV. When we inhibited phosphorylation of MuV P by PLK1, we saw an increase in gene expression, protein production, and viral growth. Inhibition of PLK1 kinase activity using BI 2536 increased reporter readout during infection and in the mini-genome system. Over-expression of the kinase deficient mutant of PLK1 (K82M) did not inhibit mini-genome activity, while wild-type PLK1 did. Together, this data shows that PLK1 is a negative regulator of viral RNA synthesis of MuV through its binding and phosphorylation of the P protein.

The discovery that NP enhanced P phosphorylation and induced the P_2 to P_{1T} band shift was instrumental in identifying PLK1 phosphorylation sites on P. We used this band shift to find mutations in P that reduced phosphorylation. We found the PLK1 binding site in P was at 146-S(pT)P-148 and the target site was at residues S292 and S294. Mutating these sites resulted in increased viral growth, as expected. Our finding that rMuV-P-T147A has enhanced growth illustrates the limitations of the mini-genome system. When a P containing the T147A or S292A/S294A mutations were tested in the MuV mini-genome system, the activity was comparable to wild-type P [7]. The mini-genome system is critical for determining the roles of viral proteins in viral RNA synthesis if rescuing virus is not feasible, but there may be additional roles for P that cannot be assessed in this system.

In this work, we demonstrated NP plays a role in P phosphorylation for other paramyxoviruses. PIV5 shows a similar phenotype to MuV, with NP and PLK1 increasing phosphorylation of P and producing a slower migrating P band. We found that JPV, a currently unclassified paramyxovirus, required NP for enhanced P phosphorylation, but did not require PLK1. JPV P does not possess the PLK1 binding

motif found in MuV and PIV5 P, so this result is not surprising. RSV had highly phosphorylated P proteins, even when transfected alone, suggesting that the requirement for NP varies between viruses.

Acknowledgements

We appreciate the helpful discussion and technical assistance from all members of Dr. Biao He's laboratory. This work was supported by grants (R01AI097368 and R01AI106307) from National Institutes of Health.

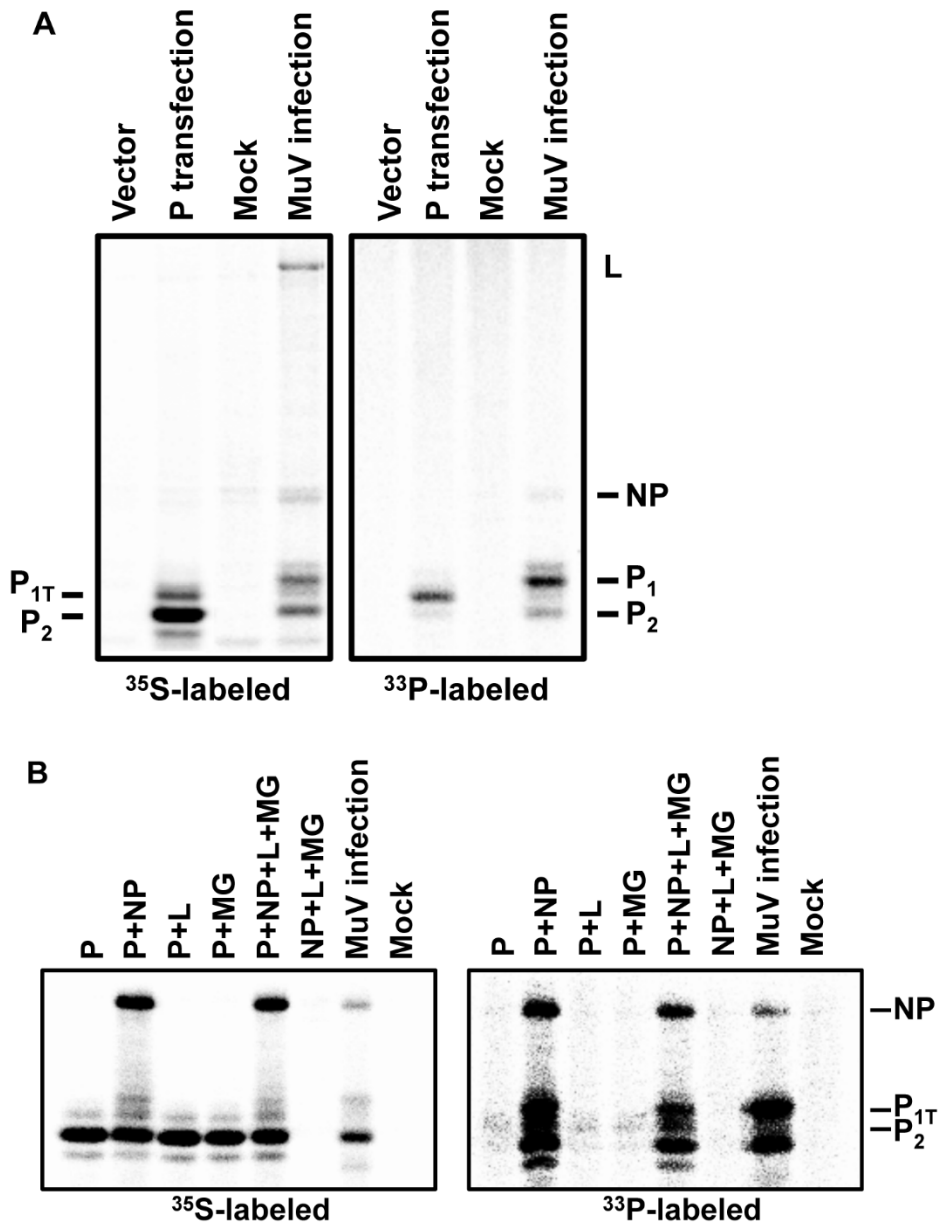

Figure 4.1. Banding pattern of phosphorylated MuV P in transfected and infected cells. (A) P phosphorylation in P-transfected cells. HeLa cells were transfected with empty vector or P or infected with MuV and radioactively labeled with [^{35}S]Met or [^{33}P]phosphate. The cells were lysed and immunoprecipitated with monoclonal anti-MuV-P antibody. The immunoprecipitated products were resolved by SDS-PAGE. The major (infection-P_1, transfection-P_{1T}) and minor (P_2) phosphorylated products are

defined. (B) P phosphorylation in minigenome-component-transfected HEK293T cells were transfected with P, NP, L, and MG-RLuc (MG) in various combinations and radioactively labeled with ^{35}S or ^{33}P. The cells were lysed, immunoprecipitated with anti-MuV-P, and resolved by SDS-PAGE.

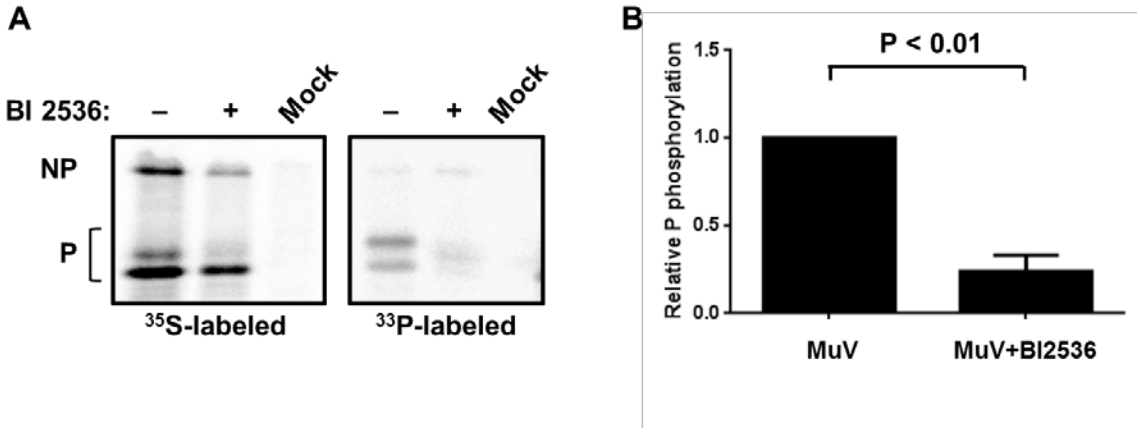

Figure 4.2. Effects of BI 2536 on P phosphorylation. (A) Effects of PLK1 inhibitor on P phosphorylation. Vero cells were mock infected or infected with MuV. At 18 hpi, the cells were radioactively labeled with ^{35}S or ^{33}P in the presence of 1 uM BI 2536. The cells were lysed and immunoprecipitated with anti-MuV-P. (B) Quantification of effects of BI 2536 on P phosphorylation. The relative level of P phosphorylation was calculated as the ratio of phosphorylated protein (^{33}P-labeled P) to total protein (^{35}S-labeled P) and standardized to that of MuV-infected without inhibitor. *P* value was calculated using Student's *t* test. Error bars represent the standard error of the mean (SEM) of 3 individual experiments.

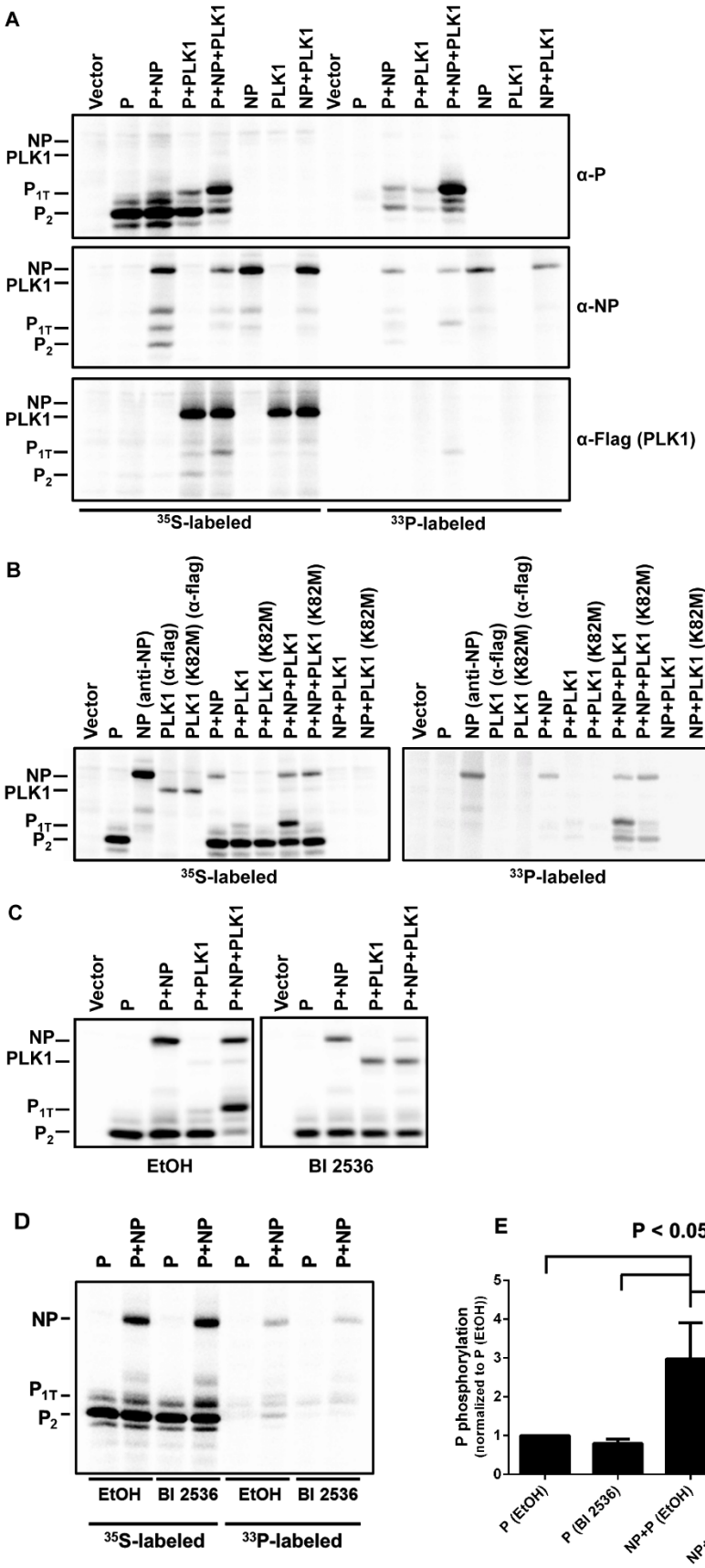
A
Vector
P
P+NP
P+PLK1
P+NP+PLK1
NP
PLK1
NP+PLK1
NP
PLK1
α-P
α-NP
α-Flag (PLK1)
P_{1T}
P_2
^{35}S-labeled
^{33}P-labeled
B
NP (anti-NP)
PLK1 (α-flag)
PLK1 (K82M) (α-flag)
P+PLK1 (K82M)
P+NP+PLK1
P+NP+PLK1 (K82M)
NP+PLK1 (K82M)
C
EtOH
BI 2536
D
E
P < 0.05
P phosphorylation
(normalized to P (EtOH))
P (EtOH)
P (BI 2536)
NP+P (EtOH)
NP+P (BI 2536)

Figure 4.3. PLK1 phosphorylates P. (A) PLK1 enhances P phosphorylation. HEK293T cells were transfected with P, NP and Flag-PLK1 in various combinations and radioactively labeled with ^{35}S or ^{33}P. The cells were lysed and split into fractions for immunoprecipitation with monoclonal anti-MuV-P, monoclonal anti-MuV-NP, or monoclonal anti-Flag antibodies. The immunoprecipitated products were resolved by SDS-PAGE. (B) PLK1 kinase activity required for P phosphorylation. HEK293T cells were transfected with P, NP, Flag-PLK1, and Flag-PLK1(K82M) in various combinations and radioactively labeled with ^{35}S or ^{33}P. The cells were lysed and immunoprecipitated with anti-MuV-P. (C) PLK1 inhibitor prevents P phosphorylation in transfected cells. HEK293T cells were transfected with P, NP and Flag-PLK1 in various combinations and radioactively labeled with ^{35}S in the presence of 1 uM BI 2536. The cells were lysed and immunoprecipitated with anti-MuV-P. (D) PLK1 inhibitor prevents P phosphorylation by endogenous PLK1 in the presence of NP. HEK293T cells were transfected with P or P+NP. Cells were labeled with ^{35}S or ^{33}P with or without BI 2536. The cells were lysed and immunoprecipitated with anti-MuV-P. (E) Quantification of P phosphorylation by endogenous PLK1. The phosphorylation of P was determined for each of the samples by finding the ratio of ^{33}P to ^{35}S. Significance was determined using the Holm-Sidak method with alpha = 5%.

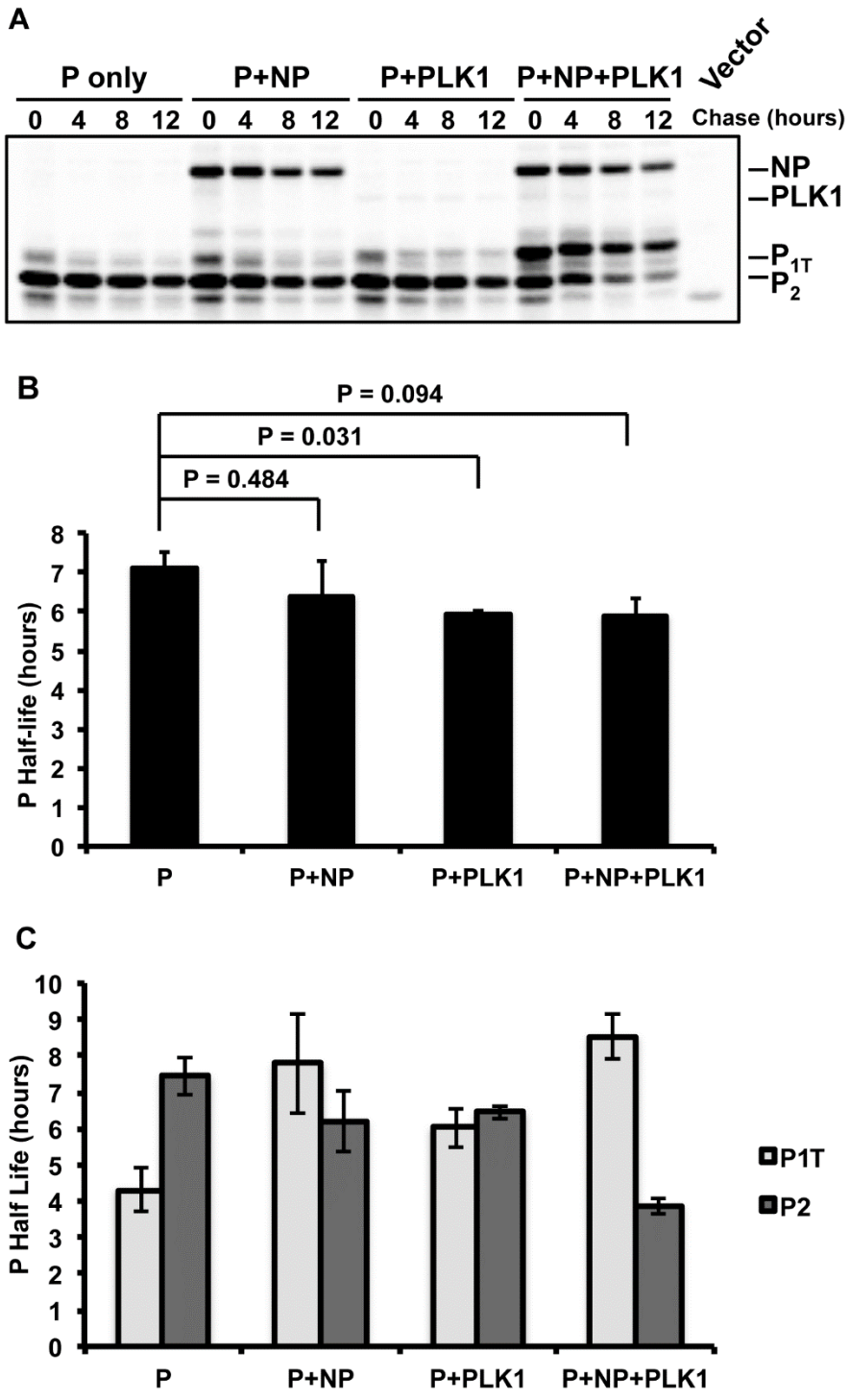

Figure 4.4. Pulse-chase analysis of P stability in the presence of NP and PLK1. (A) Stability of P in the presence of NP and PLK1. HEK293T cells were transfected with P, NP and Flag-PLK1 in various combinations. Cells were pulsed with ^{35}S for 30 min

followed by chase incubations in culture media. At 0, 4, 8, and 12 hours post chase (hpc), cells were lysed and immunoprecipitated with anti-MuV-P and resolved by SDS-PAGE. (B and C) Quantification of P half-life. The relative level of P was measured and standardized to that of 0 hpc for each group. The half-life of P was calculated for total P (B) or P_{1T} or P_2 (C) based on exponential trend lines for four individual experiments. *P* values were calculated using Student's *t* test.

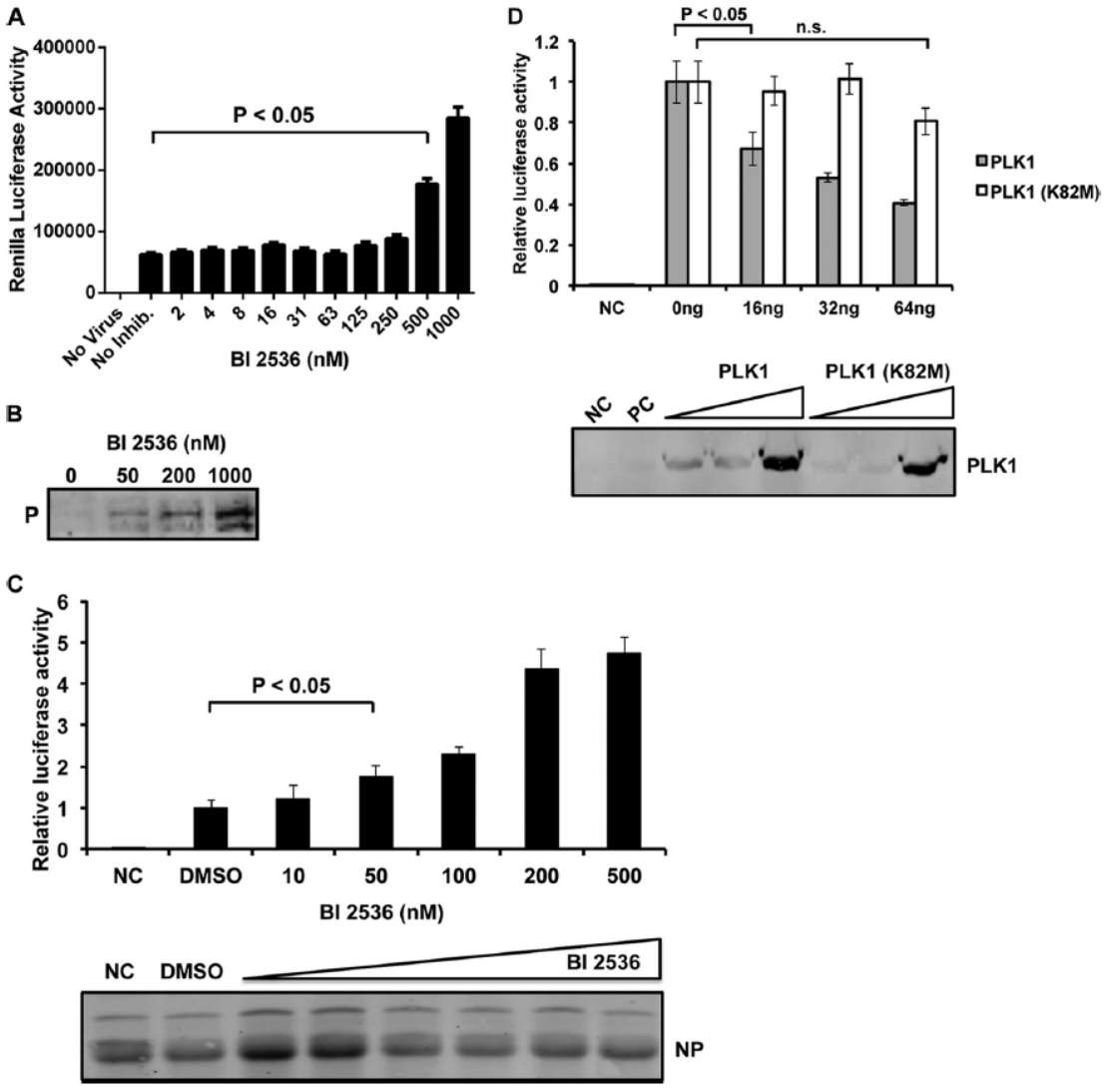

Figure 4.5. PLK1 inhibits viral protein production. (A and B) Effect of BI 2536 on recombinant MuV expressing *Renilla* luciferase (rMuV-Rluc). (A) Vero cells in 96-well

plates were infected with rMuV-Rluc at an MOI of 0.01 and incubated with BI 2536 at various concentrations. *Renilla* luciferase activity was measured at 24 hpi. Error bars represent the SEM of data from 4 replicates. (B) Immunoblotting of cell lysates was performed to detect the expression levels of P. (C) Effect of BI 2536 on MuV mini-genome activity. BSR-T7 cells in 24-well plates were transfected with P (80ng), NP (25 ng), L (500 ng), pMG-RLuc (100 ng), pFF-Luc (1 ng), and incubated with BI 2636 at various concentrations. Activity was measured at 48 hpt as described in Materials and Methods. *Renilla* luciferase was the reporter gene in the mini-genome and Firefly luciferase expression was used as a transfection control. The mini-genome activity was measured and normalized as the ratio of *Renilla* luciferase activity to firefly luciferase activity (relative luciferase activity). Immunoblotting of mini-genome cell lysates was performed to detect the expression levels of NP. (D) Effect of PLK1 and PLK1 (K82M) overexpression on mini-genome activity. BSR-T7 cells were transfected as described in (C) along with various amounts of Flag-PLK1 or Flag-PLK1 (K82M) (0, 16, 32, or 64 ng). Activity was measured at 48 hpt as described in Materials and Methods. *P* values were calculated using Student's *t* test. Error bars represent the SEM of data from six replicates. Immunoblotting of mini-genome cell lysates was performed to detect the expression levels of PLK1 and PLK1 (K82M).

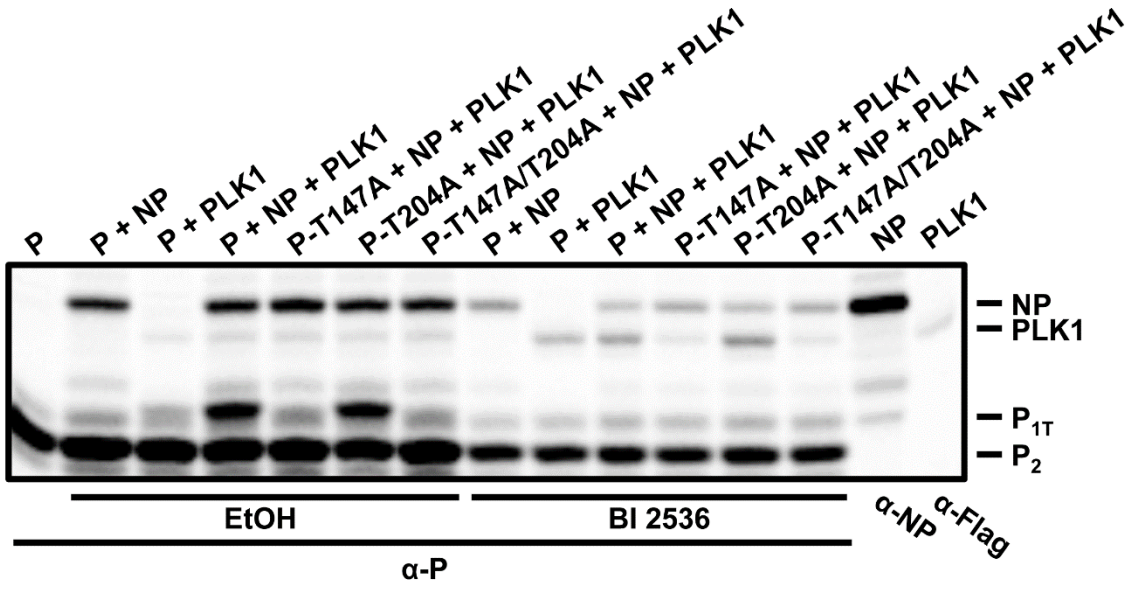

Figure 4.6. Interaction between PLK1 and P at P146-148 binding motif. HEK293T cells were transfected with P, P mutants, NP and Flag-PLK1 in various combinations and radioactively labeled with ^{35}S in the presence of solvent or 1 uM BI 2536. The cells were lysed and immunoprecipitated with anti-MuV-P, anti-MuV-NP, or anti-Flag antibodies and resolved by SDS-PAGE.

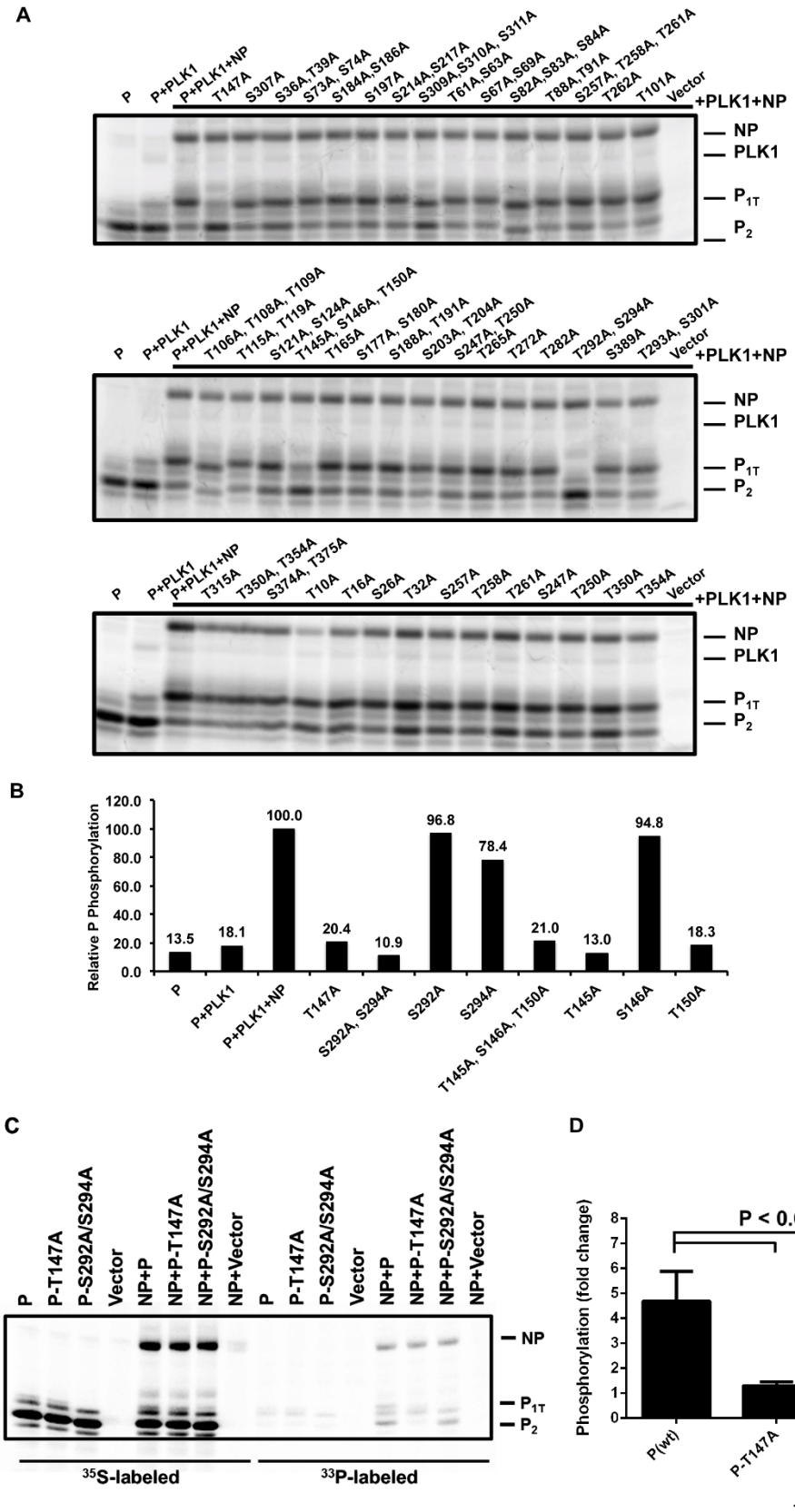
A
P
P+PLK1
P+PLK1+NP
T147A
S307A
S36A,T39A
S73A, S74A
S184A,S186A
S197A
S214A,S217A
S309A,S310A, S311A
T61A,S63A
S67A,S69A
S82A,S83A, S84A
T88A,T91A
S257A, T258A, T261A
T262A
T101A
Vector
+PLK1+NP
NP
PLK1
P1T
P2
P
P+PLK1
P+PLK1+NP
T106A, T108A, T109A
T115A, T119A
S121A, S124A
T145A, S146A, T150A
T165A
S177A, S180A
S188A, T191A
S203A, T204A
S247A, T250A
T265A
T272A
T282A
T292A, S294A
S389A
T293A, S301A
Vector
+PLK1+NP
NP
PLK1
P1T
P2
P
P+PLK1
P+PLK1+NP
T315A
T350A, T354A
S374A, T375A
T10A
T16A
S26A
T32A
S257A
T258A
T261A
S247A
T250A
T350A
T354A
Vector
+PLK1+NP
NP
PLK1
P1T
P2
B
Relative P Phosphorylation
120.0
100.0
80.0
60.0
40.0
20.0
0.0
13.5
18.1
100.0
20.4
10.9
96.8
78.4
21.0
13.0
94.8
18.3
P
P+PLK1
P+PLK1+NP
T147A
S292A, S294A
S292A
S294A
T145A, S146A, T150A
T145A
S146A
T150A
C
P
P-T147A
P-S292A/S294A
Vector
NP+P
NP+P-T147A
NP+P-S292A/S294A
NP+Vector
P
P-T147A
P-S292A/S294A
Vector
NP+P
NP+P-T147A
NP+P-S292A/S294A
NP+Vector
NP
P1T
P2
35S-labeled
33P-labeled
D
Phosphorylation (fold change)
P < 0.05
8
7
6
5
4
3
2
1
0
P(wt)
P-T147A
P-S292A/S294A

Figure 4.7. PLK1 phosphorylation site in MuV P. (A) Identification of critical residues for P phosphorylation by PLK1. HEK293T cells were transfected with P, P mutants, NP and Flag-PLK1 and radioactively labeled with ^{35}S. The cells were lysed and immunoprecipitated with anti-MuV-P. (B) Quantification of P phosphorylation. The relative level of P phosphorylation was calculated as the ratio of phosphorylated protein (P_{1T}) to total protein ($P_{1T}+P_2$) and standardized to that of wild-type P-transfected with PLK1 and NP. (C) Phosphorylation of P mutants by endogenous PLK1 in the presence of NP. HEK293T cells were transfected with P, P-T147A, or P-S292A/S294A with or without NP and radioactively labeled with ^{35}S or ^{33}P. The cells were lysed and immunoprecipitated with anti-MuV-P. (D) Quantification of P mutant phosphorylation by endogenous PLK1. The fold change in P phosphorylation with the addition of NP was calculated for wild-type P and each of the P mutants. Significance was determined using the Holm-Sidak method with alpha = 5%.

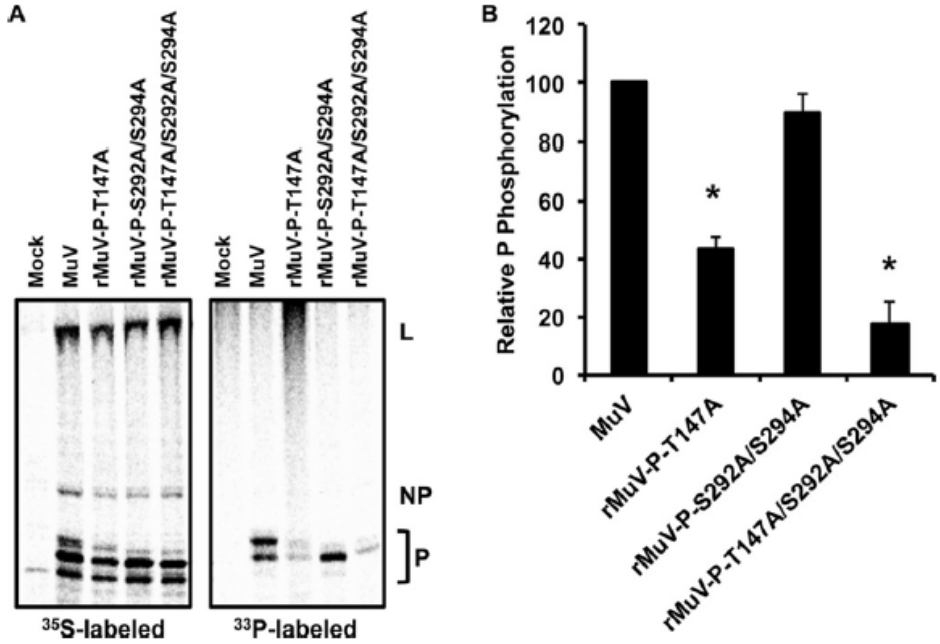

Figure 4.8. P phosphorylation in recombinant viruses. (A) P phosphorylation in infected cells. Vero cells were mock infected or infected with MuV, rMuV-P-T147A, rMuV-P-S292A/S294A, or rMuV-P-T147A/S292A/S294A at an MOI of 0.1 and radioactively labeled with ^{35}S or ^{33}P. The cells were lysed and immunoprecipitated with anti-MuV-P. (B) Quantification of P phosphorylation. The relative level of P phosphorylation was calculated as the ratio of phosphorylated protein (^{33}P-labeled P) to total protein (^{35}S-labeled P) and standardized to that of MuV-infected. *P* values were calculated using Student's *t* test. Error bars represent the standard error of the mean (SEM) of 4 individual experiments. *$P < 0.01$.

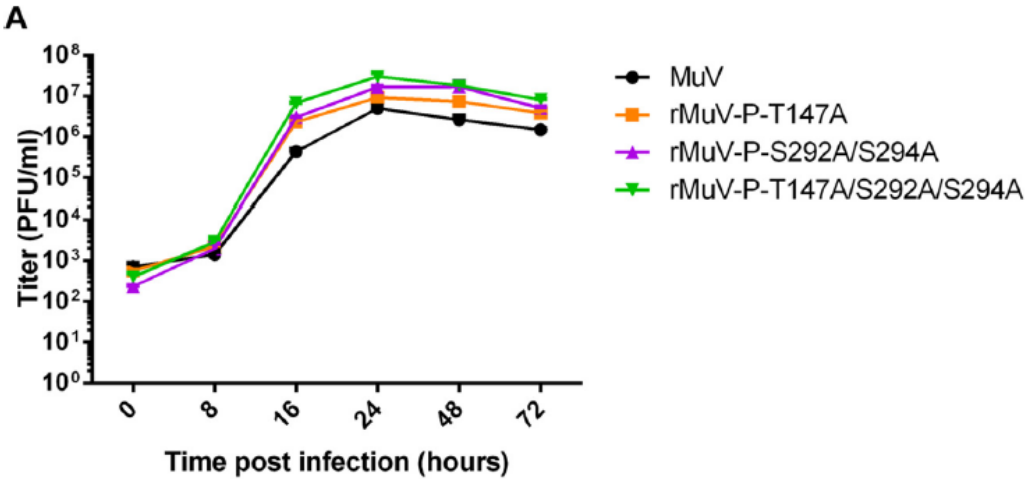

B

	Hours Post Infection					
Virus	0	8	16	24	48	72
rMuV-P-T147A	0.4029	0.0450	0.0188	**0.0067**	**0.0022**	0.0415
rMuV-P-S292A/S294A	0.0366	0.4818	**0.0001**	**0.0004**	0.0515	**0.0005**
rMuV-P-T147A/S292A/S294A	0.1586	0.0753	**< 0.0001**	0.0303	0.0147	**< 0.0001**

Figure 4.9. Growth kinetics of MuV mutants. (A) Single-step growth curve of recombinant viruses. In each experiment, cells were infected with MuV, rMuV-P-T147A, rMuV-P-S292A/S294A, or rMuV-P-T147A/S292A/S294A at an MOI of 3. Media was collected at various time points. The titer of virus in the media was determined by plaque

assay using Vero cells. (B) Each mutant virus was compared to wild-type MuV and statistical significance was determined using the Holm-Sidak method with alpha = 5%. The *P* values are provided with significant values in bold

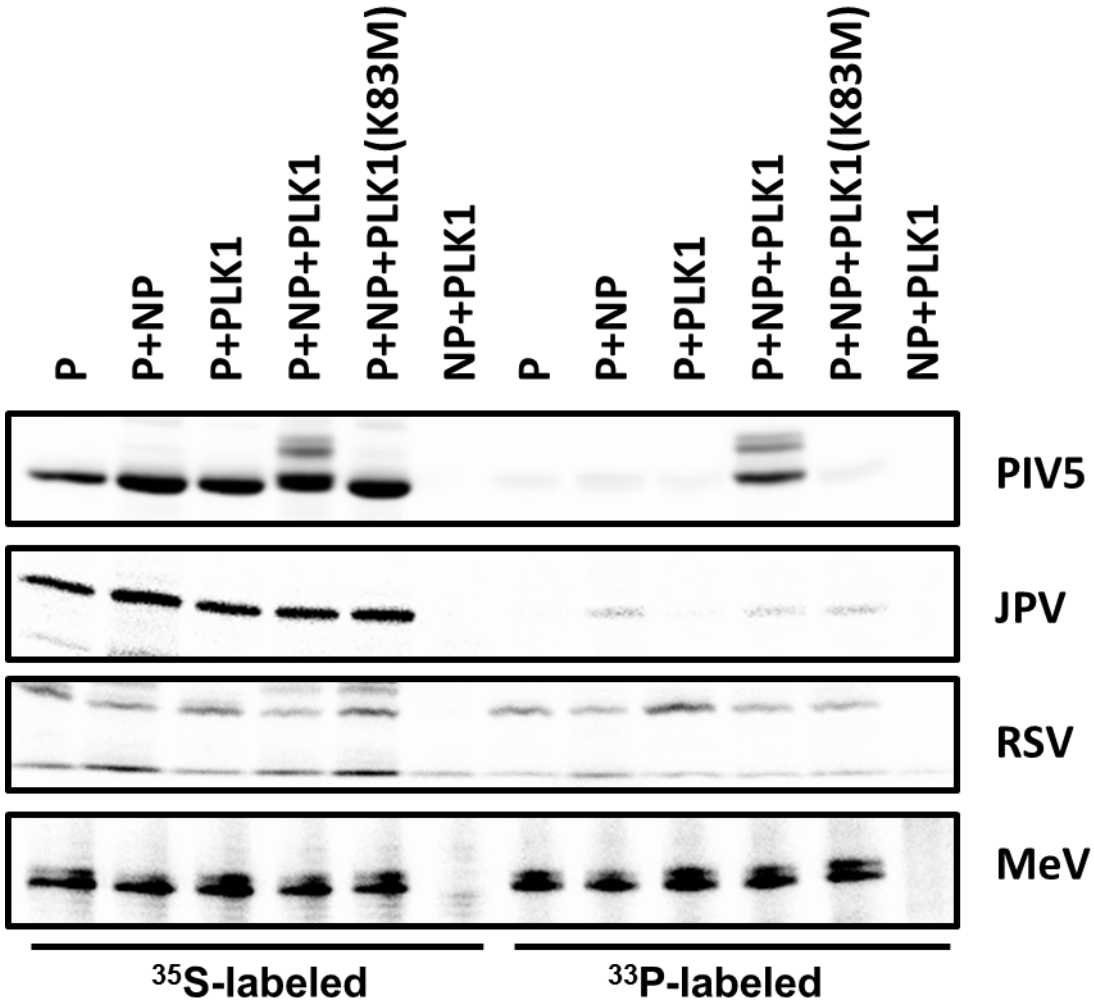

Figure 4.10. Effects of NP and PLK1 on phosphorylation of P in related viruses. P phosphorylation was assessed in transfected cells for PIV5 (A), JPV (B), and RSV (C). Plasmid encoding P of each virus was transfected along with various combinations of NP, PLK1, and PLK1 (K82M) and radioactively labeled with 35S or 33P. The cells were

lysed and immunoprecipitated with viral specific anti-P antibodies to determine phosphorylation of P for each transfection condition.

CHAPTER 5

IMMUNOGENICITY OF MUMPS VIRUS VACCINES MATCHING CIRCULATING GENOTYPES IN THE UNITED STATES AND CHINA[3]

Zengel J., Phan S.I., Pickar A., Xu P., He B. Vaccine. 2017 Jul 13;35(32):3988-3994.

Abstract

Mumps virus (MuV) causes acute infection in humans with characteristic swelling of the parotid gland. While vaccination has greatly reduced the incidence of MuV infection, there have been multiple large outbreaks of mumps virus (MuV) in highly vaccinated populations. The most common vaccine strain, Jeryl Lynn, belongs to genotype A, which is no longer a circulating genotype. We have developed two vaccine candidates that match the circulating genotypes in the United States (genotype G) and China (genotype F). We found that there was a significant decrease in the ability of the Jeryl Lynn vaccine to produce a neutralizing antibody response to non-matched viruses, when compared to either of our vaccine candidates. Our data suggests that an updated vaccine may allow for better immunity against the circulating MuV genotypes G and F.

Importance

In the past decade, there have been multiple large outbreaks of MuV in highly vaccinated populations. One factor contributing to these outbreaks may be antigenic drift in the circulating strains compared to the vaccine strain. In this work, we show that viruses from two circulating genotypes, G and F, are antigenically different than the genotype A vaccine strain. Using this information, we can produce a vaccine that is more antigenically similar to the circulating viruses, which may confer a better immune response.

Introduction

MuV is an enveloped, non-segmented, negative-sense RNA virus in family *Paramyxoviridae* and genus *Rubulavirus*. MuV is present in the saliva of infected patients [27] and can be transmitted between individuals through the upper respiratory tract or conjunctiva by droplet transmission. The characteristic symptom of mumps infection is the swelling of the parotid gland [55,56]. Although mumps is classically considered a disease of children, there are also many cases of infections in postpubertal individuals, causing orchitis occurs in many males [61,62]. Oophoritis and mastitis are less common, but can occur in postpubertal females [63,64]. Although sterility due to orchitis is considered rare [67], there are many cases of sterility or decreased sperm count described [68] and the cause of sterility is being investigated [69].

There is currently no effective treatment of mumps, with administration of mumps-specific immunoglobulins having limited success [70]. The best way to prevent mumps disease is to use a vaccine. The current mumps vaccines are live attenuated viruses. The most common vaccine worldwide is Jeryl Lynn. The vaccine was developed over 50 years ago by serially passaging virus isolated from a patient in hen's eggs and chick embryo cell culture [71]. There have been other vaccines produced by similar methods, including Leningrad-3 [72] and later L-Zagreb [73] in the former Soviet Union, Rubini in much of Europe [74], and Urabe in Japan, Europe, and Canada [75]. The use of many of these vaccines was halted or scaled back due to issues with aseptic meningitis after vaccination or a lack of vaccine efficacy [74,76–78,80].

Although the MuV have been very effective in decreasing the total number of mumps cases in vaccinated populations, there continues to be cases in these highly-vaccinated populations. The United States Department of Health and Human Services releases Healthy People objectives every ten years, looking forward at health goals in the United States over the next ten years. In 2000, the United States Department of Health and Human Services set a goal set to eliminate indigenous mumps cases by the year 2010 [81]. But, after numerous large outbreaks in the United States, this goal has now be updated to reduction of reported cases in the United States to under 500 per year [82]. In North America and parts of Europe, the most common circulating MuVs are genotype G, while the most common vaccine strain, Jeryl Lynn, is genotype A [84,85].

In Korea, where the Jeryl Lynn (genotype A) and Urabe AM9 (genotype B) strains are used for vaccination, the most common circulating MuV are genotype H [86]. The genotype C virus circulating in India may not be neutralized effectively after immunization with their L-Zagreb vaccine (genotype N) [87]. In China, there is still circulating MuV in the population, even with widespread vaccination [88], most of which appears to be of genotype F [89]. The vaccine used in China is S_{79} strain (genotype A), which was derived from the Jeryl Lynn vaccine strain [66].

Previously in our lab, a MuV vaccine candidate based on a genotype G virus was generated [9]. This vaccine was based on a clinical isolate from a large outbreak in Iowa in 2006. Attenuation was introduced by preventing the transcription of the V gene and deleting the SH ORF. This vaccine was shown to be safe and effective in generating an immune response in mice [9]. In this work, we further characterize this vaccine, as well as produce and test a chimeric vaccine to match the genotype F viruses circulating in

China. The immunogenicity and antigenicity were assessed among the Jeryl Lynn vaccine and our genotype G and F vaccines.

Materials and Methods

Phylogenetics

All available full length genome sequences were obtained from the Virus Pathogen Resource [169]. Of these, a representative set was selected by removing sequences isolated during the same outbreak or duplicate vaccine strains. Using MEGA 7 [170], the Maximum Likelyhood method based on the JTT matrix-based model [171] was used to generate trees for the F and HN protein sequences. The trees were drawn to scale with the branch lengths measured in the number of substitutions per site.

Plasmids and Cells

All plasmids were constructed using standard molecular cloning techniques. Plasmid sequences were based on the sequence of a mumps virus isolated during an outbreak in Iowa from 2006 (GenBank: JN012242.1). MuV NP, P, and L were previously cloned into the pCAGGS expression vector (24, 25). The plasmid encoding the MuV(ΔVΔSH) virus sequence was previously generated [9]. The MuV(ΔVΔSH, gen-F) rescue plasmid was generated by replacing the F and HN ORFs with the sequence from PZH0804 genotype F strain. The DNA for PZH0804 replacement was generated by gene synthesis (GenScript), and inserted into the genome using standard cloning techniques. Plasmids and sequences are available upon request.

BSR-T7 cells were maintained in DMEM supplemented with 10% FBS, 1% P/S, 10% tryptose phosphate broth (TPB), and 400 μg/ml G418 to maintain T7 RNA polymerase (RNAP) expression. Vero cells were maintained in DMEM with 10% FBS

and 1% P/S. All cells were cultured at 37°C and 5% CO_2. Cells were passaged the day before to achieve about 85-95% confluence for infection and 60-80% confluence for transfection.

Virus Rescue and Sequencing

BSR-T7 cells (1 day, 60-80% confluent, 6-well plate) were transfected with pCAGGS-NP (100 ng), pCAGGS-P (160 ng), pCAGGS-L (2000 ng), and full-length genome (2500 ng) using JetPRIME (Polyplus, Illkirch, France). After 48-72hr, transfected BSR-T7 cells were trypsinized and co-cultured with Vero cells at a ratio of 1:5 in a 10-cm dish. When CPE was observed (2-7 days), the media was collected and a plaque assay was performed using Vero cells. Single plaques were isolated 6-7 days later and cultured in fresh Vero cells in 6-well plates to produce passage 1 (P1). After titer determination, P1 was passaged again in T75 or T150 flasks at an MOI of 0.01 to produce P2. After 72hrs, virus was collected, BSA was added to 1% final concentration, and aliquots were stored at -80°C. Titer was determined by plaque assay. Viral RNA was isolated using QIAamp Viral RNA Mini Kit (Qiagen, Valencia, CA) followed by synthesis of DNA templates using SuperScript III One-Step RT-PCR System with Platinum Taq (Life Technologies, Grand Island, NY) and 5 sets of primers were used to amplify the entire genome. Fragments were sent to Genewiz (South Plainfield, NJ) for sequencing using 8 primers per fragment. Virus was confirmed to match plasmid sequence. Primer sequences are available upon request.

Viruses

The genotype G vaccine is based on a strain isolated from a patient during the 2006 outbreak in Iowa. This virus was attenuated through insertion of two nucleotides in

the RNA editing region of P/V to prevent V expression and deletion of the SH ORF, as previously described [9]. The Jeryl Lynn vaccine strain was isolated from the measles, mumps, and rubella vaccine, as previously described [9]. The genotype F vaccine was generated by rescuing an Iowa/06(ΔVΔSH) virus that has the F and HN ORFs replaced with that of PZH0804.

Western Blotting

To measure total protein, cells were infected at an MOI of 0.1. After 48 hours, cells were lysed with 2x Laemmli Sample Buffer (Bio-Rad), and heated at 95°C for 5 min. Samples were then resolved on a 10% acrylamide gel by SDS-PAGE and transferred to Amersham Hybond LFP PVDF membranes (GE Healthcare Life Sciences). Immunoblotting was performed by incubating the membranes with anti-NP and anti-P or anti-F mAbs generated in our lab and mouse anti-actin (Sigma) in 5% milk+PBS+0.1% Tween 20 (PBST) overnight at 4°C, followed by three washes with PBST, followed by incubation with Cy3-conjugated goat anti-mouse IgG diluted 1:2500 (Jackson ImmunoResearch,West Grove, PA) in 5% milk+PBST for 1hr at room temperature. After the incubation, the membrane was washed four times with PBST and dried. The blot was visualized on the Typhoon FLA 7000 (GE Healthcare Life Sciences) and the densitometry analysis was performed using ImageQuant TL software (GE Healthcare).

Growth Curves

Vero cells in 6-well plates were infected with MuV at an MOI of 0.01 in 1 ml of DMEM+2% FBS+1% P/S for 1 hr in triplicate. Cells were washed with PBS and 2 ml of DMEM+2% FBS+1% P/S was added to the cells. Samples were collected at 24, 48, 72, and 96 hours post-infection (hpi). All samples were supplemented with 1% BSA after

collection and stored at -80°C. Virus titers were determined by plaque assay on Vero cells. Results were confirmed in a second experiment. Significance was determined by two-way ANOVA using the Holm-Sidak method to correct for multiple comparisons.

Cell-cell fusion assay

Vero cells (24-well plate, 70% confluent) were transfected with plasmids encoding F and HN from either Iowa/06 or PZH0804, along with a plasmid encoding firefly luciferase under a T7 promoter and a plasmid encoding Renilla luciferase as a transfection control. A second set of Vero cells (10 cm dish, 70% confluent) was transfected with a plasmid encoding the T7 polymerase. After 24 hours, the T7-transfected cells were trypsinized and overlaid onto the 24-well plate. After an additional 24 hours, cells were lysed and a dual luciferase assay was performed according to the manufacturer's instructions (Lonza). The fusion activity was determined by dividing the firefly luciferase activity by the Renilla luciferase activity.

Mouse Experiments

6-8 week old BALB/c mice were used for all experiments. Mice were infected intranasally (i.n.) with 10^5 PFU of each vaccine candidate in 100µl of virus in PBS or sham immunized with PBS only. At day 21 post vaccination, mice were boosted in the same manner. At day 14 post-boost (day 35), mice were humanely euthanized, blood was collected to assess MuV-specific ELISA titers and neutralization titers, and splenocytes were isolated to determine MuV-specific cell-mediated immune responses. All animal studies were conducted under guidelines approved by the Institutional Animal Care and Use Committee (IACUC) of the University of Georgia.

ELISA

To generate antigen for ELISA, Vero cells were infected with each of the vaccine viruses or mock infected with PBS. After 48 hours, cells were washed twice with PBS and scraped off. The cells were resuspended in PBS followed by three freeze and thaw cycles at -80°C and 37°C, respectively, to lyse the cells. This was followed by sonication to disrupt the cell membrane and release viral antigen into solution. Protein amounts were standardized to the amount of F protein in each preparation. Immunlon high binding polystyrene plates (Thermo Scientific) were coated overnight at 4°C with MuV genotype A, G, and F or Vero cell lysate. The next day, plates were washed and blocked with 300 µl of diluent/blocking solution (KPL) with 5% nonfat milk for 1 hour at room temperature. Serum was diluted in KPL diluent/blocking solution and added to each plate. Secondary antibody incubation was performed using a goat anti-mouse HRP antibody (SouthernBiotech) diluted in KPL buffer at 1:1000. Plates were developed with SureBlue Reserve TMB substrate (KPL). Absorbance was determined using the BioTek Epoch reader, and dilution cutoffs were determined based on the 0.5 absorbance.

Interferon-gamma ELISpot

ELISpot was performed using the Mouse IFN-gamma BD ELISpot Set using the manufacturer's protocol. In short, plates were coated with IFN-gamma-specific capture antibody overnight at 4°C. The next day, the plates were blocked with RPMI containing 10% FBS and 1% Penicillin-Streptomycin-L-Glutamine. Spleens were removed from mice and cells were isolated through mechanical disruption followed by red blood cell lysis using ACK lysis buffer. Cells were resuspended in RPMI containing 10% FBS and 1% Penicillin-Streptomycin-L-Glutamine to a concentration of 250,000 cells per 100 µl.

Cells were added to the blocked ELISpot plate in triplicate for each condition. Cell were stimulated with the same Vero cell lysates used for the ELISA, as well as with PMA/ionomycin and media only controls for 48 hours at 37°C in a 5% CO_2 incubator. Plates were developed using an anti-IFN-gamma antibody conjugated to biotin, followed by incubation with Streptavidin-HRP. This was followed by incubation with AEC from the AEC substrate set (BD). Spots were visualized using the Cellular Technology Ltd. IMMUNOSPOT reader.

Plaque Reduction Neutralization Assay

Heat-inactivated serum was diluted in DMEM between 1:20 and 1:640 in 2-fold increments. 50µl of diluted serum was incubated with 80 PFU of virus in 50 µl of DMEM for 1 hour at 37°C. After incubation, the mixture was added to 1 ml of DMEM + 2% FBS + Penicillin/Streptomycin and added to confluent Vero cells in a 6-well plate. Cells were incubated at 37°C for 1 hr with rocking every 15 minutes. After this, media was removed and a solid overlay was added containing DMEM+ 2% FBS + Penicillin/Streptomycin + 1% Low-melt agarose. The number of plaques was determined at 6-7 days post infection. The plaque reduction titer was determined based on the dilution of serum that was able to reduce the number of plaque by one half.

Modeling of MuV F and HN

Models were generated with Iowa/06 F and HN sequences using the SWISS-MODEL Workspace [172]. The PIV5 crystal structures for F (4WSG) [125] and HN (4JF7) [120] were used as the backbone for the models. Models were visualized using PyMol Version 1.8.2.0 [173]. Each monomer was colored and sites that differed between

Jeryl Lynn and both Iowa/06 and PZH0804 were labeled and highlighted with magenta spheres.

Results

Phylogenetic assessment of MuV isolates

To compare the genome sequences among virus isolates in different locations over time, full length virus sequences were obtained from the Virus Pathogen Resource [169]. There were 94 complete genomes available at the time of analysis. Sequences isolated from the same outbreak or vaccine background were removed to avoid bias, leaving 54 sequences for further analysis. Maximum Likelihood trees were generated for F (Fig. 5.1A) and HN (Fig. 5.1B). We have selected three representative viruses to represent these groups: Jeryl Lynn (A), PZH0804/China/2008 (F), and Iowa/USA/2006 (G).

The similarity of the viruses chosen for the vaccine studies were assessed among the open reading frame (ORF) and encoded protein sequences (Fig. 5.1C). We found that Iowa/06 and PZH0804 had the highest percentage similarity for both ORF and protein sequences. Jeryl Lynn still a high degree of similarity for both the F and HN ORFs (92.8-93.9%) and protein sequences (95.2-96.1%).

Construction of chimera virus

The genotype G vaccine was previously generated in our lab [9]. This vaccine is a recombinant virus based on a virus isolated during a 2006 mumps outbreak at a college in Iowa. It was attenuated through the removal of the immunomodulatory proteins V and SH, and will be referred to as MuV(ΔVΔSH). The genotype F vaccine was generated by replacing F and HN ORFs in the genotype G vaccine with those of the

PZH0804/China/2008 virus, which was isolated in Panzhihua in the Sichuan province of China in 2008 [174]. We chose to replace F and HN because neutralizing antibodies against the surface antigens of MuV are thought the be important for protection [175]. This chimeric virus will be referred to as MuV(ΔVΔSH, gen-F) (Fig. 5.2).

Rescue and characterization of vaccine viruses

Vaccine viruses were rescued using a MuV reverse genetics system previously developed in our lab [49]. After rescue, a plaque assay was performed and single plaques were isolated. Larger stock viruses were grown from a single plaque isolate, and the sequence was confirmed to match the expected sequence. The protein expression of wild-type Iowa/06, MuV(ΔVΔSH), and MuV(ΔVΔSH, gen-F) in Vero cells was determined (Fig. 5.3A). Blotting for NP showed similar levels of expression, while there was increased expression of P for both vaccine strains. The increased expression of P is likely due to the lack of V transcription, as previously reported [44].

The expression of F was similar for all viruses, but there was an increase in fusion of cells infected with MuV(ΔVΔSH, gen-F) (Fig. 5.3C). Larger syncytia can be seen 24 hours after infection with MuV(ΔVΔSH, gen-F), when compared to MuV(ΔVΔSH). By 48 hours post infection, most cells are fused when infected with MuV(ΔVΔSH, gen-F). To determine if the F protein of PZH0804 caused this increase in fusion, we performed a cell-cell fusion assay (Fig. 5.3D). We found that there was an increase in fusion when the F protein of PZH0804 was co-transfected with either PZH0804 or Iowa/06 HN, suggesting that the increase in cell-cell fusion during viral infection is due to differences in the F proteins.

Antibody responses after MuV vaccination

To compare immunogenicity of the vaccine candidates, BALB/c mice were immunized intranasally (i.n.) with 10^5 PFU of each vaccine candidate and boosted at 21 days post-vaccination. At day 14 post-boost (day 35), mice were euthanized, blood was collected to assess MuV-specific ELISA titers and neutralization titers, and splenocytes were isolated to determine MuV-specific cell-mediated immune responses.

To compare humoral immune responses, MuV-specific serum IgG titers were measured. The average absorbance is reported for plates coated with antigen from Jeryl Lynn (Fig. 5.4A), MuV(ΔVΔSH) (Fig. 5.4B), and MuV(ΔVΔSH, gen-F) (Fig. 5.4C). The titer was determined using a cutoff absorbance of 0.5 for each sample, and reported for Jeryl Lynn (Fig. 5.4D), MuV(ΔVΔSH) (Fig. 5.4E), and MuV(ΔVΔSH, gen-F) (Fig. 5.4F). The ELISA titer trended higher for the Jeryl Lynn in each case, but the only significant difference was between Jeryl Lynn and MuV(ΔVΔSH) serum titers against Jeryl Lynn ($p=0.0016$). The results from the ELISAs suggest that there are similar amounts of antibody produced from vaccination with each of the vaccine candidates, and that there is little difference in antibody specificity among the genotypes. This data is consistent with the trend seen using a commercial ELISA kit coated with antigen produced from the Enders strain of MuV, another genotype A virus (data not shown).

We next determined the cross neutralization between the different genotypes. Mice immunized with Jeryl Lynn had neutralization titers against genotype A virus that were significantly greater than those produced with either the Iowa/06 or PZH0804 vaccines (Fig. 5.5A). Mice immunized with either MuV(ΔVΔSH) or MuV(ΔVΔSH, gen-F) produced significantly higher neutralizing titers against genotype F virus than Jeryl

Lynn (Fig. 5.5B). A significantly lower neutralizing titer produced in mice immunized with Jeryl Lynn, while mice immunized with MuV(ΔVΔSH) or MuV(ΔVΔSH, gen-F) produced similar neutralizing titers (Fig. 5.5C). This data shows that there is a difference in the neutralizing antibodies between genotype A viruses and genotype F and G viruses.

Cellular immune response after MuV vaccination

Since cellular immunity may also be important in preventing disease caused by MuV [176,177], we measured the cellular immune responses after vaccination. The number of interferon-gamma (IFNγ)-secreting cells in the spleen of vaccinated mice was assessed at 14 days post-boost by ELISpot (Fig. 5.6). While we found that Jeryl Lynn consistently produced more IFNγ-secreting cells for each of the antigens, there was no significant difference. This result suggests that there is no genotype-specific difference in the cellular immune response between the vaccines.

Enhancing vaccine growth in cell culture

One of the drawbacks of the current vaccine candidate is the low titers that are achieved when grown in cell culture. In order to try to increase the titer of the MuV(ΔVΔSH) virus, we introduced an alanine substitution mutation at P(T147) in the MuV(ΔVΔSH) rescue plasmid to rescue the virus MuV(ΔVΔSH, P-T147A). This mutation was previously shown to increase the growth of wild-type MuV in vero cells [178]. After the virus was rescued, the growth kinetics were determined in vero cells (Fig. 5.7A). The virus had a peak titer that was about 10-fold higher than that of the parent MuV(ΔVΔSH) vaccine candidate, but was still about 10-fold lower than that of MuV(wt).

The ability of the new virus to produce a similar immune response in mice was also tested. Mice were immunized twice as in the previous experiments and serum was collected 14 days after the boost. The ELISA titer of the serum generated in mice was determined using a commercial MuV ELISA kit coated with antigen form the Enders vaccine strain (genotype A) (Fig. 5.7B). There was no significant difference in titer among the various vaccination groups. We also determined the neutralization titer using a plaque reduction assay. The neutralization titer was determined against both genotype G (Fig. 5.7C) and genotype A (Fig. 5.7D) viruses. There was no significant difference between the neutralization of the genotype G virus for serum isolated form mice immunized with either MuV(ΔVΔSH) or MuV(ΔVΔSH, P-T147A). There was a significant decrease in the neutralizing titer of the genotype a virus for the mice immunized with the MuV(ΔVΔSH, P-T147A) virus compared to those immunized with MuV(ΔVΔSH). Overall, this shows that the mutation was able to increase vaccine yield in cell culture and give similar immune responses against the circulating strain of MuV.

Discussion

The MuV vaccine was able to greatly reduce the number of mumps cases after its introduction in the late 1960's. There was a resurgence of mumps cases in the late 1980's in the vaccinated population [179], which prompted the recommendation of a second dose of the MMR vaccine [180]. Two doses of MMR reduced the number of mumps cases to under 300 annually in the United States from 2001-2005 [181]. However, mumps outbreaks have occurred in the United States in the last decade, including the large outbreak centered around a university in Iowa, which had over 5,000 cases in 2006 [2,4,5,182]. Mumps outbreaks have also been reported in vaccinated

populations in Europe and Asia [85–88,183,184]. None of these outbreaks were associated with the genotype A, which was the Jeryl Lynn vaccine genotype.

Both of our vaccine candidates could generate a robust immune response against the circulating genotype G and F viruses. While Jeryl Lynn vaccination could generate a good immune response against genotype A virus, there was a significant decrease in the ability of serum from these mice to neutralize genotype G or F viruses. It is possible that this decrease may contribute to some of the recent outbreaks. It has been shown that there is variation in serum neutralizing antibodies among people over time [86,91,184,185]. Poor immune responses or waning immunity may result in some individuals dropping below a protective threshold. This may be exacerbated by a vaccine that does not match the circulating strains.

Although there was a significant difference in neutralizing antibody titers between Jeryl Lynn and the two vaccine candidates, vaccination with Jeryl Lynn produced higher or similar serum ELISA titers and cellular immune responses. It is known that NP is an immunodominant antigen during MuV infection [186,187]. Antibodies against NP may mask a decrease in antibodies specific to F and HN. The lack of differences in the cellular immune response may be due to NP or common T-cell epitopes in F and HN. We do not currently know what the dominant T-cell epitopes are for MuV, but this data would suggest they are shared between these viruses.

Our results also allow us to start exploring the reasons for the differences in the neutralizing antibodies produced after vaccination. Since no antigenic difference between the genotype G and F vaccine candidates was observed using the neutralization assay, we propose that there is likely a common difference between the HN and/or F of

these viruses and Jeryl Lynn that accounts for the difference in neutralization titers. Using the structures of PIV5 F [125] and HN [120], we modeled the structure of MuV F and HN (Fig. 5.8). We compared the common variation compared to sites that may be targeted by neutralizing antibodies [115,188]. We found that 7 of these sites in HN differed in Iowa/06 and PZH0804 viruses compared to Jeryl Lynn. Two of the mutated residues, 354 and 356, have been shown to escape neutralization by neutralizing monoclonal antibodies [111]. The sites proposed to be important for F-specific neutralizing antibodies did not differ, but all epitopes may not have been mapped [188]. We also found many differences in the F and HN interacting domains. Antibodies recognizing this region may prevent F-HN interaction after receptor binding. Mutating these residues and testing their antigenicity will help with determining what sites are important for the differential neutralization between genotypes.

During these studies, we observed increased fusogenicity of the PZH0804 F protein in both infected and transfected cells when compared to Iowa/06 F. There is a total of 17 differences between the F protein sequences. It is likely that the differences in fusion are due to a difference at position 195. Previous research has shown that an aromatic residue at this position reduces fusion in COS7 cells [127]. Another residue that was known to effect fusogenicity in MuV at postion 383 was the same in both viruses [126]. We also considered sites known to affect PIV5 fusion, but no differences were found between PZH0804 and Iowa/06 F proteins [189–191]. It appears that the change at position 195 is responsible for the change in fusion.

One of the drawbacks of MuV(ΔVΔSH) that we tested previously and in this paper is the low peak titers that are achieved in vero cells, which would likely be used for

vaccine production in the future. In order to address this, we introduced a mutation into the MuV(ΔVΔSH) backbone, which we previously identified to increase the peak titers of MuV(wt) that was grown in vero cells [178]. The MuV(ΔVΔSH, P-T147A) virus was rescued and shown to also have increase peak titers in cell culture with a 10-fold increase in peak titer compared to MuV(ΔVΔSH), but with a peak titer still about 10-fold lower than MuV(wt). We believe that work is a good example of how basic research can be used to enhance translational research. The information that we obtained when studying the role of phosphorylation of the P proteins resulted in finding a residue that could be mutated to increase the titer of or candidate vaccine virus.

Although there are changes in the genotype, MuV is still considered to have only one serotype [192]. Previously, differences in neutralizing titer against a range of viruses was examined after a second vaccination with Jeryl Lynn [91]. Six weeks post-immunization, there was at least a 2-fold decrease in the titer when neutralizing genotype G virus compared to neutralization of homologous virus, consistent with our results. While the definitive role of antibody in protection has not been proven, it is possible that the observed decrease is responsible for the increase in infections seen in the United States over the past decade. Our Iowa/06 based vaccine produced a good immune response specific to both genotype F and G viruses. A vaccine matching the circulating genotypes may better protect against MuV infection.

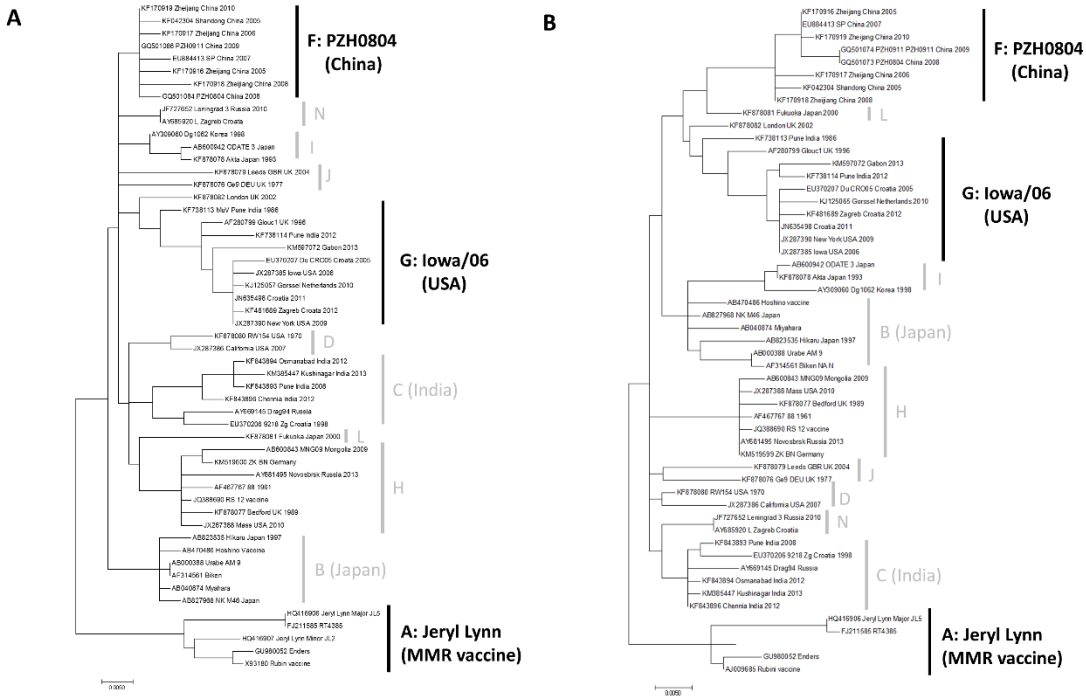

C

F

	Iowa/06	Jeryl Lynn
Jeryl Lynn	1518/1617 (93.9%)	
PZH0804	1543/1617 (95.4%)	1512/1617 (93.5%)

F

	Iowa/06	Jeryl Lynn
Jeryl Lynn	513/539 (95.2%)	
PZH0804	521/539 (96.7%)	512/539 (95.0%)

HN

	Iowa/06	Jeryl Lynn
Jeryl Lynn	1623/1749 (92.8%)	
PZH0804	1651/1749 (94.4%)	1628/1749 (93.1%)

HN

	Iowa/06	Jeryl Lynn
Jeryl Lynn	555/583 (95.2%)	
PZH0804	567/538 (97.3%)	560/583 (96.1%)

Figure 5.1. Phylogenetic tree of mumps virus (MuV) fusion (F) and hemagglutinin (HN) amino acid sequences from available full length sequences. Full length MuV sequences were obtained from the Virus Pathogen Resource (viprbrc.org), and duplicate or highly similar sequences were removed. The remaining sequences were used to compare the protein sequences for F (**A**) and HN (**B**). We generated Maximum Likelihood trees using a method based on the JTT matrix-based model [1]. The tree is drawn to scale, with

branch lengths measured in the number of substitutions per site. Evolutionary analyses were conducted in MEGA7 [2]. Labels for the established MuV genotypes were added to the right of the trees. The genotypes studied in the paper (A, F, and G) are highlighted. (**C**) Comparison of F and HN gene and protein sequences for the vaccine viruses. The number of matched nucleotides or amino acids in the coding sequence for F and HN was determined for each of the vaccine viruses, and the % similarity was calculated.

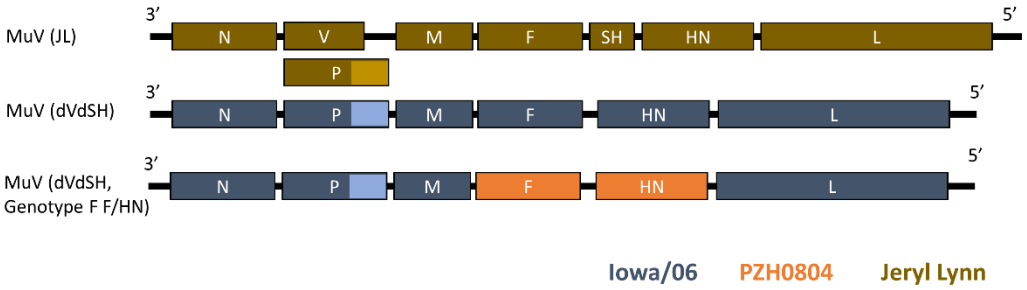

Figure 5.2: Schematics of vaccines viruses. NP, nucleoprotein; V, V protein; P, phosphoprotein; M, matrix protein; F, fusion protein; SH, small hydrophobic protein; HN, hemagglutinin-neuraminidase protein; L, large protein/RNA-dependent polymerase. Vaccine candidates are based on sequences for Iowa/USA/2006 (genotype G), Jeryl Lynn vaccine (genotype A), and PZH0804/China/2008 (genotype F). The Iowa/USA/2006 vaccine candidate was generated by inserting two alanine residues in the RNA editing site to prevent V transcription and by removing of the SH ORF. The Jeryl Lynn vaccine strain was isolated from the measles, mumps, and rubella (MMR) vaccine.

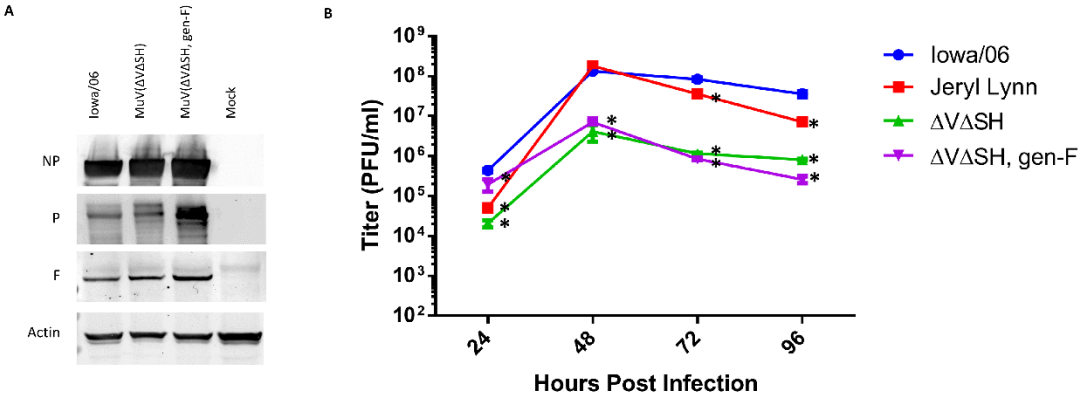

Figure 5.3: Characterization of vaccine viruses. (A) Expression of viral proteins. Vero cells were infected at an MOI=0.1 for 48 hours with wild-type Iowa/USA/2006, MuV (ΔVΔSH), MuV (ΔVΔSH, gen-F), or mock infected. Cell lysates were analyzed by Western blotting after SDS-PAGE using antibodies specific for MuV NP, P, or F. (B) Vaccine virus growth in cell culture. Vero cells were infected with viruses at an MOI = 0.01. The titer of virus in the media was determined at 24, 48, 72, and 92 h.p.i. The growth rate of each of the viruses was compared to the clinical isolate, Iowa/06. The titer of Jeryl Lynn was lower at 24, 72, and 96 hours post infection (h.p.i), but there was no difference in the peak titer at 48 h.p.i. Both MuV(ΔVΔSH) and MuV(ΔVΔSH, gen-F) had decreased titers at all time points, and had about a 20-fold decrease in peak titer at 48 hours post infection. (*n* is 3; 2-way ANOVA with Dunnett's multiple-comparison test comparing to Iowa/06; *, $P < 0.05$).

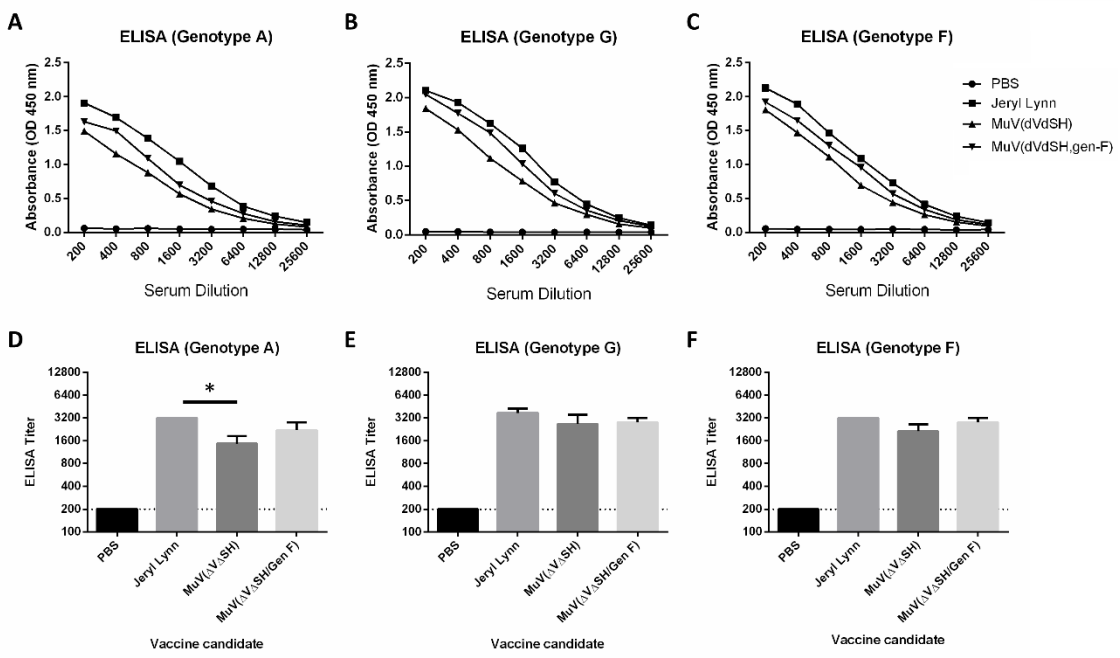

Figure 5.4: Cross-reactive antibody titers in mice after immunization. Serum was collected from mice 14 days after boosting. Serum antibody titers were determined by ELISA. Dilution curves were generated using serum from each of the vaccination groups using plates coated with Jeryl Lynn (**A**), MuV (ΔVΔSH) (**B**), or MuV (ΔVΔSH, gen-F) (**C**). Titers were determined by using the dilution at which the OD at 450nm was >0.5. The mean titer and SEM are reported for each vaccination group for plate coated with Jeryl Lynn (**D**), MuV (ΔVΔSH) (**E**), or MuV (ΔVΔSH, gen-F) (**F**). (*n* is 4-6; 1-way ANOVA with Fisher's LSD post hoc comparisons to homologous group; *, P<0.05)

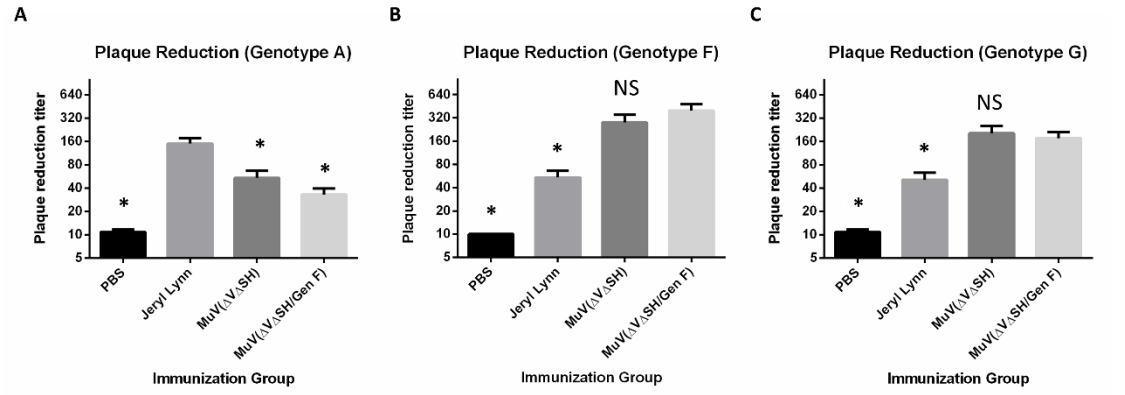

Figure 5.5: Cross-neutralization titers in mice after immunization. Serum was collected from mice 14 days after boosting. A plaque reduction assay was used to determine the neutralization titer for each vaccination group. The plaque reduction titer for each vaccination group was determined using Jeryl Lynn (**A**), MuV (ΔVΔSH) (**B**), and MuV (ΔVΔSH, gen-F) (**C**). The mean 50% plaque reduction titer and SEM are reported. (*n* is 4-6; 1-way ANOVA with Fisher's LSD post hoc comparisons to homologous group; *, $P<0.05$)

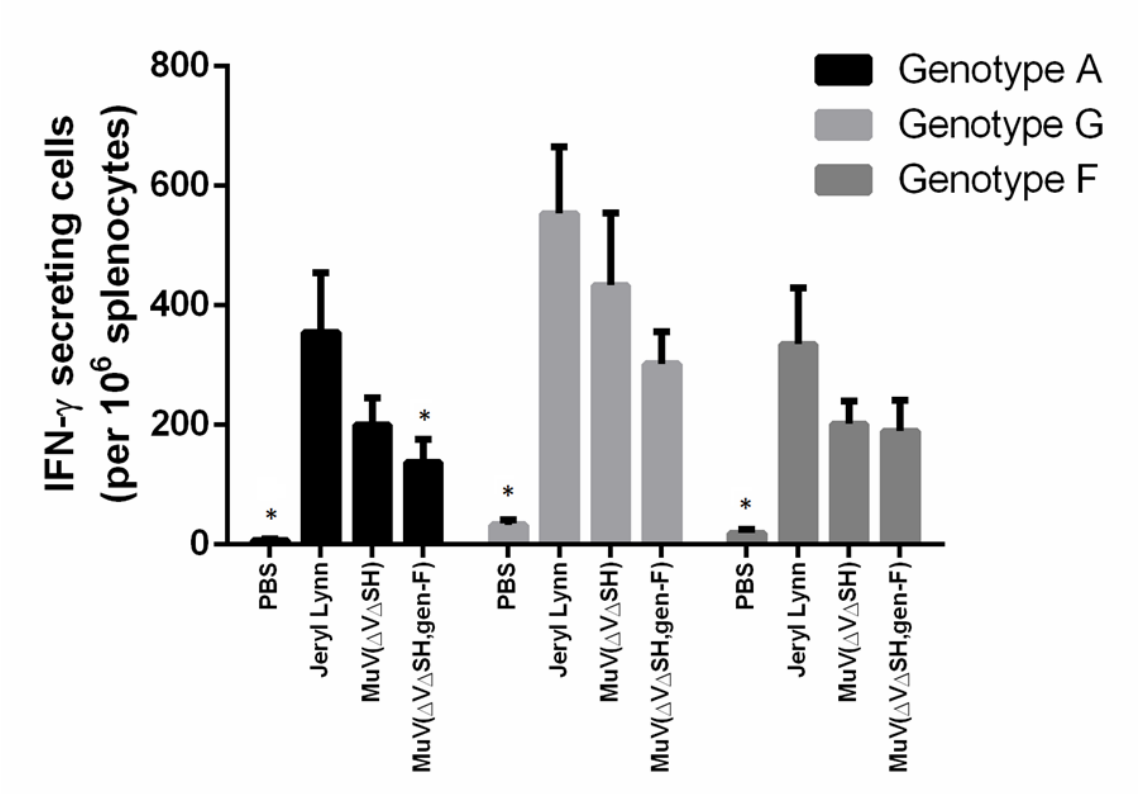

Figure 5.6: Cellular immunity in mice after immunization. Spleens were removed from mice and splenocytes were isolated 14 days after boosting. ELISpot was used to determine the number of interferon-γ secreting cells. Splenocytes were stimulated with antigen from Jeryl Lynn, MuV (ΔVΔSH), or MuV (ΔVΔSH, gen-F). The mean and SEM were reported for the number of interferon-γ secreting cells per 10^6 splenocytes. (*n* is 4-6; 1-way ANOVA with Fisher's LSD post hoc comparisons to homologous group; *, $P<0.05$)

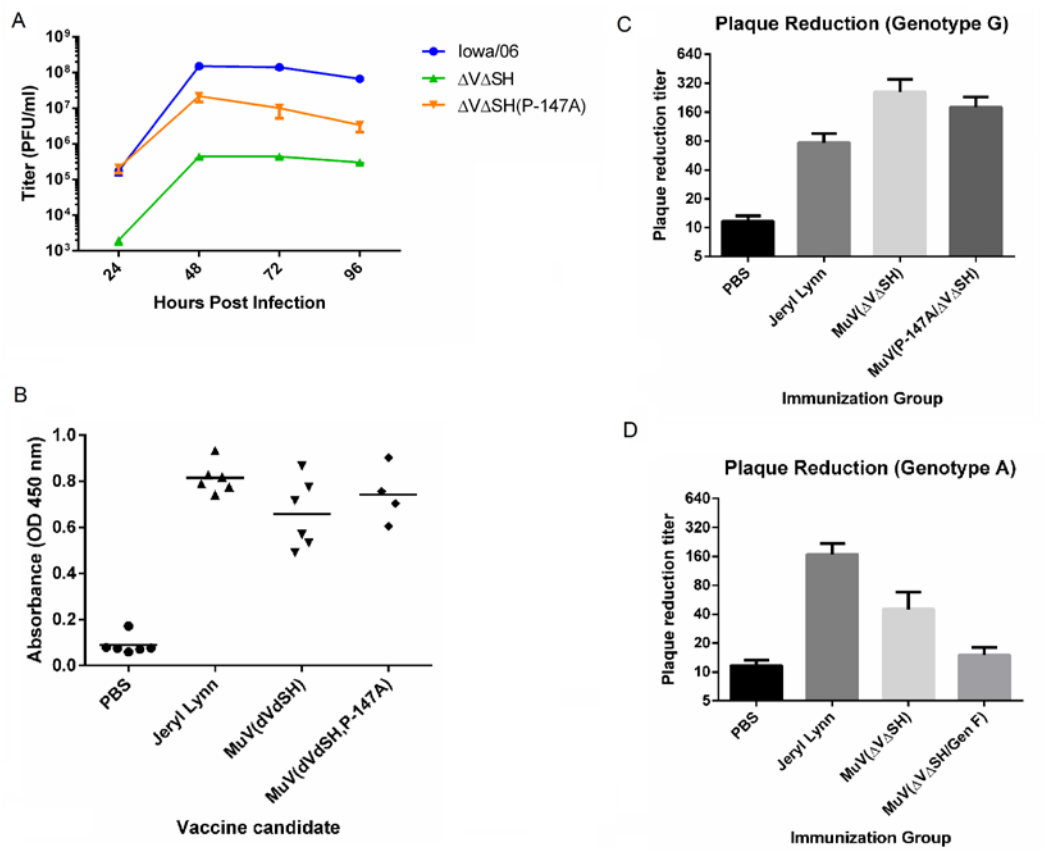

Figure 5.7. Enhancing the yield of the genotype G vaccine candidate in cell culture. (A) Vaccine virus growth in cell culture. Vero cells were infected with viruses at an MOI = 0.01. The titer of virus in the media was determined at 24, 48, 72, and 92 h.p.i. The growth rate of the MuV(ΔVΔSH, P-T147A) was compared to MuV(ΔVΔSH) and MuV(wt). The peak titer was found to be significantly higher for the MuV(ΔVΔSH, P-T147A virus) compared to MuV(ΔVΔSH), but it was still significantly lower than MuV(wt). (B) ELISA titer after two doses of vaccine. ELISA titers were determined using a commercial kit coated with antigen from the Enders strain (genotype A). The differences in ELISA titer were not significant different between the groups. (C, D) Neutralization titer in mice after immunization. Serum was collected from mice 14 days after boosting. A plaque reduction assay was used to determine the neutralization titer

for each vaccination group. The plaque reduction titer for each group was determined using MuV (ΔVΔSH) (C) or Jeryl Lynn (D). The neutralizing titers produced from vaccination with the MuV (ΔVΔSH, P-T147A) vaccine candidate were no significantly different from MuV (ΔVΔSH) against the homologous virus, but there was a decrease in the neutralizing titer against the genotype A virus.

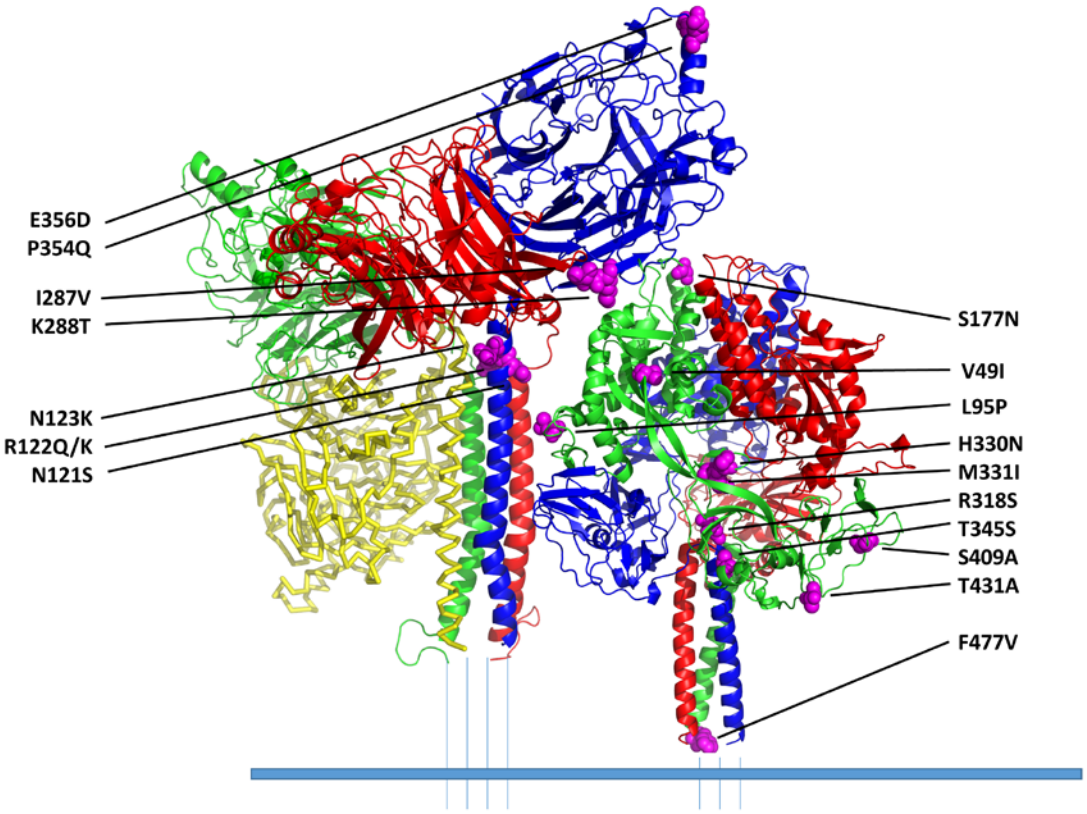

Figure 5.8. Model of MuV F and HN protein structures. The MuV F (right) and HN (left) were modeled based on the crystal structure of PIV5 F (3WSG) and HN (4JF7). Residues that differ between Jeryl Lynn and both Iowa/06 and PZH0804 were mapped onto each structure and labeled with magenta spheres. Labels were added showing the mutation from Jeryl Lynn to Iowa/06 and PZH0804. There are multiple differences

found in the F-HN interacting domain. There are also changes at residues 354 and 356 that are known to escape neutralization by some monoclonal antibodies.

CHAPTER 6

CONCLUSIONS

The use of vaccination to prevent mumps has been a great success over the last 50 years. Before widespread vaccination in the late 1960's, over 40% of the population would have been infected by MuV by the age of 10 [193]. Those that did not get mumps as children would often get infected when in the military , possibly due to living in close quarters [194]. Since the introduction of the vaccine, there was a decrease of over 99% in the incidence of mumps in the United States for many years. The availability of an effective vaccine also decreased research interest. Priorities changed when there were large outbreaks in both Europe and the United States, included cases of infection in fully vaccinated individuals [2–4,6]. Because of these outbreaks, it has become clear that basic research is required to better understand basic details of MuV infection, replication, pathogenicity, and the correlates of vaccine protection. The goal of the research comprising this thesis was to determine the role of phosphorylation in MuV infection and replication. Previous work in our lab showed that the phosphorylation of P played an important role in regulating viral RNA synthesis [8]. We hypothesized that the transcription and replication of MuV is controlled by the phosphorylation of NP and the NP-dependent phosphorylation of P. To address this hypothesis, we proposed the following specific aims:

Specific Aim 1: To determine the phosphorylated residues in MuV NP that are critical for viral transcription and replication. The working hypothesis is that phosphorylation of residues in MuV NP play a role in viral RNA transcription and replication. To determine what residues were phosphorylated in MuV virus and MuV-infected cells, we used various purification methods followed by mass spectrometry along with *in silico* prediction. Although our original goal was to determine the role of NP phosphorylation, we found several phosphorylation residues in MuV proteins including the two major sites that were discussed in this both of work at position NP-S439 and P-T147.

We confirmed using radioactive labeling that NP-S439 was the major phosphorylation site in MuV NP. Preventing the phosphorylation of NP-S439 resulted in an increase in RNA synthesis in both the minigenome system and in rescued virus. This suggests that phosphorylation of this residue may play a role in regulating RNA synthesis. We also found that the amount of NP associated with P was decreased cells infected with MuV(NP-S439A), suggesting that this interaction may be phosphorylation dependent. An interesting observation in viruses containing the NP-S439A mutation was that there was a slight lag in virus replication at 6 hours post infection. We hypothesized that this may be due to differences in the ratio of genomic RNA to mRNA and protein, which may cause a decrease in the production of infections virus at very early time points. This would explain why a mutation at this site does not naturally occur, since early replication would be very important in an infected host.

The discovery of phosphorylation of MuV P at residues T147 allowed us to build on previous research relating to the role of P in MuV RNA synthesis [8], as well how

phosphorylation of P is related between various paramyxoviruses, including PIV5, where phosphorylation of P on homologous residues was previously reported [152]. The overall findings on the role of P phosphorylation were similar to those found with PIV5, including the kinase involved. The major new finding that NP plays an important role in the phosphorylation of P. We found that without NP, P phosphorylation was greatly reduced for MuV, PIV5, and JPV. This demonstrates that context can be very important for phosphorylation, which can inform future experiments with a goal of identifying phosphorylated proteins.

Together these results suggest that phosphorylation is an important regulator of RNA replication. The two phosphorylation events may also be related, since it was shown that removal of the major phosphorylation site resulted in decreased P association. This may result in a decrease in P phosphorylation. This is supported by our findings that a decrease in phosphorylation through either the NP(S439A) or P(T147A) mutations results in increased RNA synthesis. This new understanding of how phosphorylation effects MuV growth may allow for the development of treatments for mumps or directed mutagenesis to increase vaccine virus yield.

Specific Aim 2: To determine host factors that are involved in the phosphorylation of MuV proteins. We hypothesized that we could use kinase motif prediction algorithms and siRNA screening to determine which host kinases are important for viral replication and transcription. In specific aim 1, we determined that there were multiple instances when phosphorylation had a significant effect on MuV replication and virion production. In this aim, we wanted to determine host proteins that

were involved in these processes. This included host kinases that are responsible for the phosphorylation of the MuV proteins or host proteins that have interactions that require a certain phosphorylation state.

After determining that P was phosphorylated, we wanted to determine the kinase that was responsible for this phosphorylation. The site that we confirmed by mass spec at T147 cause this site to be an S/pT/P motif, which is known to be a PLK1 binding site [162]. We went on to confirm that most the P phosphorylation was due to phosphorylation of PLK1. This was done by showing that inhibitors of PLK1 greatly reduced P phosphorylation in infected or transfected cells and that transfection of PLK1 increased P phosphorylation in transfected cells. It was found that preventing phosphorylation by the host kinase PLK1 resulted in an increase in viral protein production and growth. While we were originally hoping to find a kinase that has a positive effect on viral growth, which would allow for the possible use of a kinase inhibitor to help treat MuV infection, this new information may allow for increase yield of vaccine viruses.

Combining the research of the first two aims allows us to propose a possible mechanism for how NP, P, and PLK1 interact, and the phosphorylation that occurs (Fig. 6.1). In this model, we propose that P is first phosphorylated at T147 in the STP binding motif by a yet unknown kinase. This allows for PLK1 binding, but not phosphorylation at the secondary phosphorylation sites at S292 and S294. For phosphorylation at these sites to occur, NP needs to bind P. Since we demonstrate that NP-P interaction is impacted by NP phosphorylation, it is possible that phosphorylation at S439 will also result in increased NP-P association, and therefore increase P phosphorylation.

Phosphorylation of both NP and P has a negative impact on RNA synthesis, although there are likely other roles for phosphorylation that have yet to be assessed.

Specific Aim 3: To improve the lead MuV vaccine candidate previously developed in our lab using directed mutagenesis of the MuV genome based on the finding from Specific Aims 1 and 2. The working hypothesis is that growth of the vaccine candidate may be enhanced through the incorporation of mutations in NP and P, which increase virus growth in cell culture, while maintaining attenuation of pathogenesis *in vivo*.

A sub aim for this project is to determine if vaccination with MuV-dVdSH can produce an immune response to currently circulating mumps genotype better than vaccination with the current Jeryl Lynn vaccine. The working hypothesis was that the MuV-dVdSH vaccine candidate based on the genotype G virus, MuV/Iowa/06, will produce a better immune response to currently circulating strains in the United States and China when compared to the Jeryl Lynn vaccine.

To address this aim, we continued the work previously performed in our lab in the development of a specifically attenuated MuV vaccine based on the outbreak strain from Iowa in 2006 [9]. The vaccine virus was created by preventing the expression of the V protein through mutation of the RNA editing site and deletion of the SH ORF producing MuV(ΔVΔSH). This virus was previously shown to be immunogenic in mice and safe in a rat neurotoxicity model. Although the genotype G virus this vaccine was based on is the major circulating virus in both the United States and much of Europe, we wanted to see if we could use our vaccine strain as a platform for other MuV genotype vaccines.

We decided to test this by producing a vaccine specific to the genotype F viruses currently circulating in China. We demonstrate that vaccination with a virus expressing the F and HN or genotype G or F MuV results in increased neutralization titer against either genotype G or F compared to vaccination with the genotype A Jeryl Lynn strain. Our results from this work suggest that while a new vaccine may be required to better match circulating strains, it is possible that we would not need a vaccine against each individual genotype. This could streamline the production of new vaccine candidates against currently circulating MuV strains.

The main drawback was that this vaccine did not grow well in cell culture, growing to peak titers that were about 100-fold lower that the parent strain. To improve the growth of the vaccine virus, we attempted to introduce mutation at phosphorylation sites that were shown to increase wild-type virus growth, specifically NP-S439A and P-T147A. We were unable to rescue a vaccine virus containing the NP-S439A mutation, but we were able to rescue the MuV(ΔVΔSH, P-T147A) vaccine virus. The inclusion of the P-T147A mutation resulted in peak cell culture titers to be increased 10-fold, although this was still less than MuV(wt) peak titers. The new vaccine virus was also shown to be effective in eliciting an immune response in mice.

In this body of work, we identify multiple phosphorylation sites in MuV proteins that had not previously been described. We were then able to show how phosphorylation at these sites affected viral RNA synthesis and replication. This basic research was then able to enhance the production of a next generation mumps vaccine candidate that was developed in our lab. Continuing this research may also allow for us to find inhibitors

that can be used to treat patients with mumps. This research shows how basic research is an important for translational research that could help prevent or cure infectious diseases in humans.

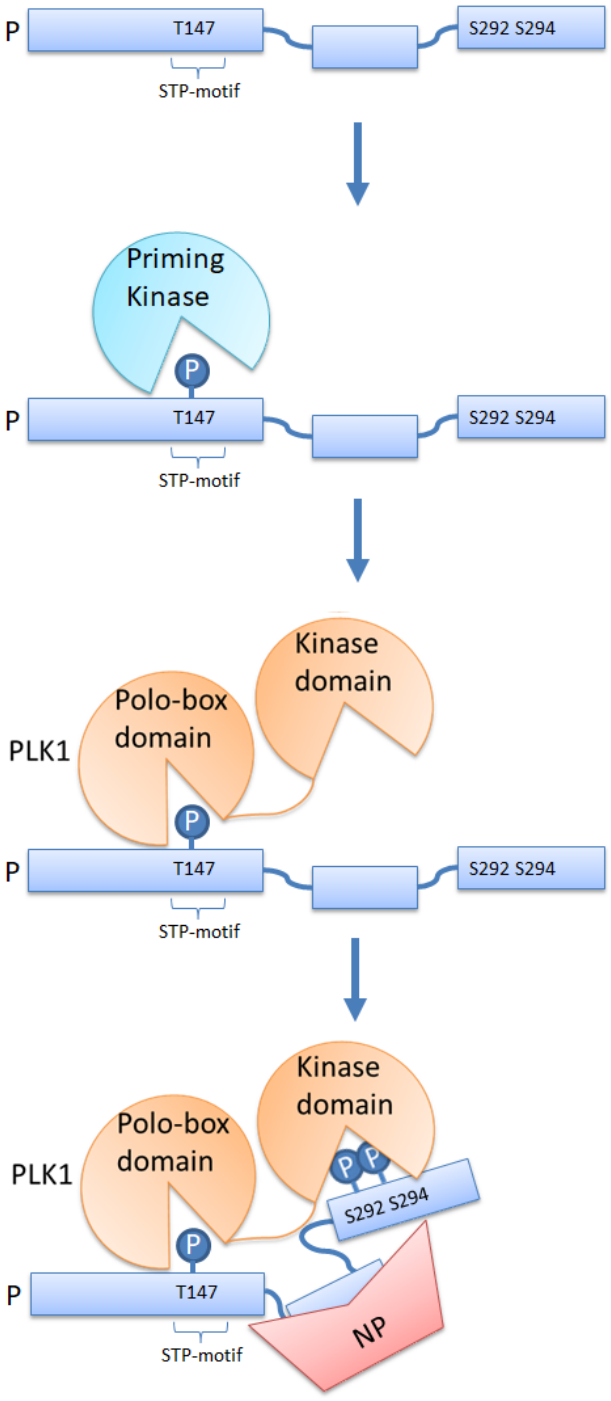

Figure 6.1. Proposed model for NP, P, and PLK1 interactions. The phosphorylation of P requires phosphorylation by an unknown priming kinase, association with PLK1, and interaction with NP. This results in phosphorylation at residues T147, S292, and S294. The phosphorylation of P has a negative impact on RNA synthesis in a minigenome system or infected cells.

REFERENCES

[1] Pellet PE, Roizmann B. Field Virology. 5th edition. New York Lippencott-Raven 2007;2:2479–500.

[2] Dayan GH, Quinlisk MP, Parker A a, Barskey AE, Harris ML, Schwartz JMH, et al. Recent resurgence of mumps in the United States. N Engl J Med 2008;358:1580–9. doi:10.1056/NEJMoa0706589.

[3] Dayan GH, Rubin S. Mumps outbreaks in vaccinated populations: are available mumps vaccines effective enough to prevent outbreaks? Clin Infect Dis 2008;47:1458–67. doi:10.1086/591196.

[4] CDC. Update: multistate outbreak of mumps--United States, January 1-May 2, 2006. MMWR Morb Mortal Wkly Rep 2006;55:559–63.

[5] Bouyer D. Mumps outbreak - New York, New Jersey, Quebec, 2009. MMWR Morb Mortal Wkly Rep 2009;58:1270–4.

[6] Marin M, Quinlisk P, Shimabukuro T, Sawhney C, Brown C, Lebaron CW. Mumps vaccination coverage and vaccine effectiveness in a large outbreak among college students--Iowa, 2006. Vaccine n.d.;26:3601–7.

[7] Naruse H, Nagai Y, Yoshida T, Hamaguchi M, Matsumoto T, Isomura S, et al. The polypeptides of mumps virus and their synthesis in infected chick embryo cells. Virology 1981;112:119–30.

[8] Pickar A, Xu P, Elson A, Li Z, Zengel J, He B. Roles of serine and threonine residues of mumps virus P protein in viral transcription and replication. J Virol 2014;88:4414–22. doi:10.1128/JVI.03673-13.

[9] Xu P, Chen Z, Phan S, Pickar A, He B. Immunogenicity of novel mumps vaccine candidates generated by genetic modification. J Virol 2014;88:2600–10. doi:10.1128/JVI.02778-13.

[10] Strauss JH, Strauss EG. Viruses and human disease 2002:383. doi:10.1007/978-3-642-38965-8.

[11] Hamilton R. IX. An account of a distemper, by the common people in England vulgarly called the mumps. Earth Environ Sci Trans R Soc Edinburgh 1790;2:59–72. doi:10.1017/S0263593300027280.

[12] Bruyn HB, Sexton HM, Brainerd HD. MUMPS MENINGOENCEPHALITIS—A Clinical Review of 119 Cases with One Death. Calif Med 1957;86:153–60.

[13] BANG HO, BANG J. Involvement of the Central Nervous System in Mumps. Acta Med Scand 1943;113:487–505. doi:10.1111/j.0954-6820.1943.tb09179.x.

[14] Wollstein M. An experimental study of parotitis (mumps). J Exp Med 1916;23:353–75. doi:10.1001/jama.1918.02600340031009.

[15] Wollstein M. A further study of experimental parotitis. J Exp Med 1918;28:377–85.

[16] Wollstein M. Experimental mumps meningitis. J Exp Med 1921;34:537–43.

[17] Gordon MH. No Title. Rep Loc Govt Bd Publ Heal 1914;96.

[18] Conseil CN and E. No Title. Compt Rend Acad 1916;157:340–3.

[19] Granata S. Sulla etiologia degli orecchioni da virus filtrable. Med Ital 1908;6:647–9.

[20] GN A. Parotitis complicated with meningitis. Am J Dis Child 1913;VI:399–407.

[21] RL H. The cerebral complications of mumps: With report of nine cases. Arch Intern Med 1919;23:737–44.

[22] Kermorgant Y. No Title. Ann l'Inst Pasteur 1925;39:565.

[23] Is mumps caused by a spirochete? J Am Med Assoc 1925;85:748–9.

[24] BÉNARD R. Mumps Meningitis and Kermorgant's Spiroehaete. Bull Mem la Soc Medicale des Hop Paris 1927;51:918–20.

[25] Johnson CD, Goodpasture EW. an Investigation of the Etiology of Mumps. J Exp Med 1934;59:1–19. doi:10.1084/jem.59.1.1.

[26] Xu P, Huang Z, Gao X, Michel FJ, Hirsch G, Hogan RJ, et al. Infection of Mice, Ferrets, and Rhesus Macaques with a Clinical Mumps Virus Isolate. J Virol 2013;87:8158–68. doi:10.1128/JVI.01028-13.

[27] Johnson CD, Goodpasture EW. The etiology of mumps. Am J Hyg 1935:46–57.

[28] LEVENS JH, ENDERS JF. THE HEMOAGGLUTINATIVE PROPERTIES OF AMNIOTIC FLUID FROM EMBRYONATED EGGS INFECTED WITH MUMPS VIRUS. Sci 1945;102:117–20. doi:10.1126/science.102.2640.117.

[29] Habel K. Cultivation of Mumps Virus in the Developing Chick Embryo and Its Application to Studies of Immunity to Mumps in Man. Public Heal Reports 1945;60:201–12. doi:10.2307/4585189.

[30] ENDERS JF, LEVENS JH. Attenuation of virulence with retention of antigenicity of mumps virus after passage in the embryonated egg. J Immunol 1946;54:283–91.

[31] Paterson RG, Lamb R a. RNA editing by G-nucleotide insertion in mumps virus P-gene mRNA transcripts. J Virol 1990;64:4137–45. doi: .

[32] Bernard JP, Northrop RL. RNA polymerase in mumps virion. J Virol 1974;14:183–6.

[33] Takeuchi K, Hishiyama M, Yamada A, Sugiura A. Molecular cloning and sequence analysis of the mumps virus gene encoding the P protein : mumps virus P gene is monocistronic. J Gen Virol 1988;69:2043–9.

[34] Okazaki K, Tanabayashi K, Takeuchi K, Hishiyama M, Okazaki K, Yamada A. Molecular cloning and sequence analysis of the mumps virus gene encoding the L protein and the trailer sequence. Virology 1992;188:926–30.

[35] Takeuchi K, Hishiyama M, Yamada A, Sugiura A. Molecular cloning and sequence analysis of the mumps virus gene encoding the P protein: mumps virus P gene is monocistronic. J Gen Virol n.d.;69 (Pt 8):2043–9.

[36] Cox R, Green TJ, Purushotham S, Deivanayagam C, Bedwell GJ, Prevelige PE, et al. Structural and functional characterization of the mumps virus phosphoprotein. J Virol 2013;87:7558–68.

[37] Li M, Schmitt PT, Li Z, McCrory TS, He B, Schmitt AP. Mumps virus matrix, fusion, and nucleocapsid proteins cooperate for efficient production of virus-like particles. J Virol 2009;83:7261–72.

[38] Waxham MN, Merz DC, Wolinsky JS. Intracellular maturation of mumps virus hemagglutinin-neuraminidase glycoprotein: conformational changes detected with monoclonal antibodies. J Virol 1986;59:392–400.

[39] Choppin PW, Scheid A. The Role of Viral Glycoproteins in Adsorption, Penetration, and Pathogenicity of Viruses. Rev Infect Dis 1980;2:40–61.

[40] Tanabayashi K, Takeuchi K, Okazaki K, Hishiyama M, Yamada A. Expression of mumps virus glycoproteins in mammalian cells from cloned cDNAs: Both F and HN proteins are required for cell fusion. Virology 1992;187:801–4. doi:10.1016/0042-6822(92)90482-5.

[41] Waxham MN, Server AC, Goodman HM, Wolinsky JS. Cloning and sequencing of the mumps virus fusion protein gene. Virology 1987;159:381–8.

[42] Merz DC, Server AC, Waxham MN, Wolinsky JS. Biosynthesis of mumps virus F glycoprotein: non-fusing strains efficiently cleave the F glycoprotein precursor. J Gen Virol 1983;64 (Pt 7):1457–67. doi:10.1099/0022-1317-64-7-1457.

[43] Kubota T, Yokosawa N, Yokota S-I, Fujii N, Tashiro M, Kato A. Mumps virus V protein antagonizes interferon without the complete degradation of STAT1. J Virol 2005;79:4451–9. doi:10.1128/JVI.79.7.4451-4459.2005.

[44] Xu P, Luthra P, Li Z, Fuentes S, D'Andrea JA, Wu J, et al. The V protein of mumps virus plays a critical role in pathogenesis. J Virol 2012;86:1768–76.

[45] Yang Y, Zengel J, Sun M, Sleeman K, Timani KA, Aligo J, et al. Regulation Of Viral RNA Synthesis By The V Protein Of Parainfluenza Virus 5. J Virol 2015. doi:10.1128/JVI.01832-15.

[46] Pickar A, Elson A, Yang Y, Xu P, Luo M, He B. Oligomerization of Mumps Virus Phosphoprotein. J Virol 2015;89:11002–10. doi:10.1128/JVI.01719-15.

[47] Takeuchi K, Tanabayashi K, Hishiyama M, Yamada a. The mumps virus SH protein is a membrane protein and not essential for virus growth. Virology 1996;225:156–62. doi:10.1006/viro.1996.0583.

[48] Wilson RL, Fuentes SM, Wang P, Taddeo EC, Klatt A, Henderson AJ, et al. Function of small hydrophobic proteins of paramyxovirus. J Virol 2006;80:1700–9. doi:10.1128/JVI.80.4.1700-1709.2006.

[49] Xu P, Li Z, Sun D, Lin Y, Wu J, Rota PA, et al. Rescue of wild-type mumps virus from a strain associated with recent outbreaks helps to define the role of the SH ORF in the pathogenesis of mumps virus. Virology 2011;417:126–36.

[50] MEYER MB. AN EPIDEMIOLOGIC STUDY OF MUMPS; ITS SPREAD IN SCHOOLS AND FAMILIES. Am J Epidemiol 1962;75:259–81.

[51] CDC. Mumps: For Healthcare Providers 2015. http://www.cdc.gov/mumps/hcp.html (accessed December 2, 2015).

[52] Utz JP, Kasel JA, Cramblett HG, Szwed CF, Parrott RH. Clinical and Laboratory Studies of Mumps: Laboratory Diagnosis by Tissue-Culture Technics. N Engl J Med 1957;257:497–502.

[53] Utz JP, Szwed CF, Kasel JA. Clinical and laboratory studies of mumps II. Detection and duration of excretion of virus in urine. Exp Biol Med 1958;99:259–61.

[54] Utz JP, Houk VN, Alling DW. Clinical and Laboratory Studies of Mumps. N Engl J Med 1964;270:1283–6. doi:10.1056/NEJM196406112702404.

[55] DEWAR RS. Mumps meningitis and orchitis without parotitis. Lancet (London, England) 1950;1:256.

[56] KILHAM L. Mumps meningoencephalitis with and without parotitis. Am J Dis Child 1949;78:324–33.

[57] Brown JW, Kirkland HB, Hein GE. CENTRAL NERVOUS SYSTEM INVOLVEMENT DURING MUMPS. Am J Med Sci 1948;215.

[58] Russell RR, Donald JC. Neurological Complications of Mumps. Br Med J 1958;2:27–30.

[59] Everberg BG. Deafness Following Mumps. Acta Otolaryngol 1957;48:397–403. doi:10.3109/00016485709126900.

[60] Mizushima N, Murakami Y. Deafness following mumps: the possible pathogenesis and incidence of deafness. Auris Nasus Larynx 1986;13 Suppl 1:S55-7.

[61] WERNER CA. Mumps orchitis and testicular atrophy; occurrence. Ann Intern Med 1950;32:1066–74.

[62] AC R. Mumps: Use of convalescent serum in the treatment and prophylaxis of orchitis. Am J Dis Child 1946;71:1–13.

[63] Morrison JC, Givens JR, Wiser WL, Fish SA. Mumps oophoritis: a cause of premature menopause. Fertil Steril 1975;26:655–9.

[64] LEE CM. Primary virus mastitis from mumps. Va Med Mon (1918) 1946;73:327.

[65] Enders M, Biber M, Exler S. Masern, Mumps und R{ö}teln in der Schwangerschaft. Bundesgesundheitsblatt - Gesundheitsforsch - Gesundheitsschutz 2007;50:1393–8. doi:10.1007/s00103-007-0195-9.

[66] Fu C, Liang J, Wang M. Matched Case-Control Study of Effectiveness of Live, Attenuated S(79) Mumps Virus Vaccine against Clinical Mumps . Clin Vaccine Immunol 2008;15:1425–8. doi:10.1128/CVI.00122-08.

[67] WERNER CA. MUMPS ORCHITIS AND TESTICULAR ATROPHY. II. A FACTOR IN MALE STERILITY*. Ann Intern Med 1950;32:1075–86.

[68] Wong WY, Zielhuis GA, Thomas CMG, Merkus HMWM, Steegers-Theunissen RPM. New evidence of the influence of exogenous and endogenous factors on sperm count in man. Eur J Obstet Gynecol Reprod Biol 2003;110:49–54. doi:10.1016/S0301-2115(03)00162-3.

[69] Wang X-X, Ying P, Diao F, Wang Q, Ye D, Jiang C, et al. Altered protein prenylation in Sertoli cells is associated with adult infertility resulting from childhood mumps infection. J Exp Med 2013;210:1559–74. doi:10.1084/jem.20121806.

[70] Copelovici Y, Strulovici D, Cristea AL, Tudor V, Armasu V. Data on the efficiency of specific antimumps immunoglobulins in the prevention of mumps and of its complications. Virologie 1979;30:171–7.

[71] Buynak EB, Hilleman MR. Live attenuated mumps virus vaccine. 1. Vaccine development. Proc Soc Exp Biol Med 1966;123:768–75.

[72] Smorodintsev AA, Nasibov MN, Jakovleva N V. Experience with live rubella virus vaccine combined with live vaccines against measles and mumps. Bull World Health Organ 1970;42:283–9.

[73] Beck M, Welsz-Malecek R, Mesko-Prejac M, Radman V, Juzbasic M, Rajninger-Miholic M, et al. Mumps vaccine L-Zagreb, prepared in chick fibroblasts. I. Production and field trials. J Biol Stand 1989;17:85–90.

[74] Chamot E, Toscani L, Egger P, Germann D, Bourquin C. [Estimation of the efficacy of three strains of mumps vaccines during an epidemic of mumps in the Geneva canton (Switzerland)]. Rev Epidemiol Sante Publique 1998;46:100–7.

[75] Popow-Kraupp T, Kundi M, Ambrosch F, Vanura H, Kunz C. A controlled trial for evaluating two live attenuated mumps-measles vaccines (Urabe Am 9-Schwarz and Jeryl Lynn-Moraten) in young children. J Med Virol 1986;18:69–79.

[76] Cizman M, Mozetic M, Radescek-Rakar R, Pleterski-Rigler D, Susec-Michieli M. Aseptic meningitis after vaccination against measles and mumps. Pediatr Infect Dis J 1989;8:302–8.

[77] Tešović G, Begovac J, Baće A. Aseptic meningitis after measles, mumps, and rubella vaccine. Lancet 1993;341:1541. doi:http://dx.doi.org/10.1016/0140-6736(93)90684-9.

[78] Sugiura A, Yamada A. Aseptic meningitis as a complication of mumps vaccination. Pediatr Infect Dis J 1991;10:209–13.

[79] Black S, Shinefield H, Ray P, Lewis E, Chen R, Glasser J, et al. Risk of hospitalization because of aseptic meningitis after measles-mumps-rubella vaccination in one- to two-year-old children: an analysis of the Vaccine Safety Datalink (VSD) Project. Pediatr Infect Dis J 1997;16:500–3.

[80] Gluck R, Hoskins JM, Wegmann A, Just M, Germanier R. Rubini, a new live attenuated mumps vaccine virus strain for human diploid cells. Dev Biol Stand 1986;65:29–35.

[81] US Department of Health and Human Services. Healthy People 2010. Washington DC: US Deparment of Health and Human Services; 2000.

[82] US Department of Health and Human Services. Healthy People 2020. Washington DC: 2010.

[83] Mumps virus nomenclature update: 2012. Wkly Epidemiol Rec 2012;87:217–24.

[84] Peltola H, Kulkarni PS, Kapre S V, Paunio M, Jadhav SS, Dhere RM. Mumps Outbreaks in Canada and the United States: Time for New Thinking on Mumps Vaccines. Clin Infect Dis 2007;45:459–66. doi:10.1086/520028.

[85] Gouma S, Sane J, Gijselaar D, Cremer J, Hahne S, Koopmans M, et al. Two major mumps genotype G variants dominated recent mumps outbreaks in the Netherlands (2009-2012). J Gen Virol 2014;95:1074–82. doi:10.1099/vir.0.062943-0.

[86] Park SH. Resurgence of Mumps in Korea. Infect Chemother 2015;47:1–11. doi:10.3947/ic.2015.47.1.1.

[87] Malayan, Jeevan; Warrier, Aparna; Venkat Ramanan, Padmasani; Reddy N, Sanjeeva; Manickan E. Unnoticeable Mumps Infection in India: Does MMR Vaccine Protect against Circulating Mumps Virus Genotype C? World Acad Sci Eng Technol n.d.:1416.

[88] Wang Z, Yan R, He H, Li Q, Chen G, Yang S, et al. Difficulties in Eliminating Measles and Controlling Rubella and Mumps: A Cross-Sectional Study of a First Measles and Rubella Vaccination and a Second Measles, Mumps, and Rubella Vaccination. PLoS One 2014;9:e89361. doi:10.1371/journal.pone.0089361.

[89] Liu Y, Hu Y, Deng X, Wang Z, Lu P, Ma F, et al. Seroepidemiology of mumps in the general population of Jiangsu province, China after introduction of a one-dose measles-mumps-rubella vaccine. Sci Rep 2015;5:14660. doi:10.1038/srep14660.

[90] Hindiyeh MY, Aboudy Y, Wohoush M, Shulman LM, Ram D, Levin T, et al. Characterization of Large Mumps Outbreak among Vaccinated Palestinian Refugees . J Clin Microbiol 2009;47:560–5. doi:10.1128/JCM.01756-08.

[91] Rubin SA, Link MA, Sauder CJ, Zhang C, Ngo L, Rima BK, et al. Recent Mumps Outbreaks in Vaccinated Populations: No Evidence of Immune Escape. J Virol 2012;86:615–20. doi:10.1128/JVI.06125-11.

[92] Emerson SU, Yu Y. Both NS and L proteins are required for in vitro RNA synthesis by vesicular stomatitis virus. J Virol 1975;15:1348–56.

[93] Abraham G, Banerjee AK. Sequential transcription of the genes of vesicular stomatitis virus. Proc Natl Acad Sci U S A 1976;73:1504–8.

[94] Ball LA, White CN. Order of transcription of genes of vesicular stomatitis virus. Proc Natl Acad Sci U S A 1976;73:442–6.

[95] Emerson SU. Reconstitution studies detect a single polymerase entry site on the vesicular stomatitis virus genome. Cell 1982;31:635–42.

[96] Iverson LE, Rose JK. Sequential synthesis of 5'-proximal vesicular stomatitis virus mRNA sequences. J Virol 1982;44:356–65.

[97] Cox R, Pickar A, Qiu S, Tsao J, Rodenburg C, Dokland T, et al. Structural studies on the authentic mumps virus nucleocapsid showing uncoiling by the phosphoprotein. Proc Natl Acad Sci U S A 2014;111:15208–13.

[98] Kingston RL, Gay LS, Baase WS, Matthews BW. Structure of the nucleocapsid-binding domain from the mumps virus polymerase; an example of protein folding induced by crystallization. J Mol Biol 2008;379:719–31.

[99] Kingston RL, Baase WA, Gay LS. Characterization of nucleocapsid binding by the measles virus and mumps virus phosphoproteins. J Virol 2004;78:8630–40.

[100] Bhella D, Ralph A, Murphy LB, Yeo RP. Significant differences in nucleocapsid morphology within the Paramyxoviridae. J Gen Virol 2002;83:1831–9. doi:10.1099/0022-1317-83-8-1831.

[101] Cox R, Green TJ, Qiu S, Kang J, Tsao J, Prevelige PE, et al. Characterization of a Mumps Virus Nucleocapsidlike Particle . J Virol 2009;83:11402–6. doi:10.1128/JVI.00504-09.

[102] Alayyoubi M, Leser GP, Kors CA, Lamb RA. Structure of the paramyxovirus parainfluenza virus 5 nucleoprotein-RNA complex. Proc Natl Acad Sci U S A 2015;112:E1792-9. doi:10.1073/pnas.1503941112.

[103] Severin C, Terrell JR, Zengel JR, Cox R, Plemper RK, He B, et al. Releasing the genomic RNA sequestered in the mumps virus nucleocapsid. J Virol 2016. doi:10.1128/JVI.01422-16.

[104] Ding H, Green TJ, Lu S, Luo M. Crystal structure of the oligomerization domain of the phosphoprotein of vesicular stomatitis virus. J Virol 2006;80:2808–14. doi:10.1128/JVI.80.6.2808-2814.2006.

[105] Tarbouriech N, Curran J, Ruigrok RWH, Burmeister WP. Tetrameric coiled coil domain of Sendai virus phosphoprotein. Nat Struct Mol Biol 2000;7:777–81.

[106] Liang B, Li Z, Jenni S, Rahmeh AA, Morin BM, Grant T, et al. Structure of the L Protein of Vesicular Stomatitis Virus from Electron Cryomicroscopy. Cell 2015;162:314–27. doi:10.1016/j.cell.2015.06.018.

[107] Tanabayashi K, Takeuchi K, Okazaki K, Hishiyama M, Yamada A. Expression of mumps virus glycoproteins in mammalian cells from cloned cDNAs: both F and HN proteins are required for cell fusion. Virology 1992;187:801–4.

[108] Li M, Schmitt PT, Li Z, McCrory TS, He B, Schmitt AP. Mumps virus matrix, fusion, and nucleocapsid proteins cooperate for efficient production of virus-like particles. J Virol 2009;83:7261–72. doi:10.1128/JVI.00421-09.

[109] Kulkarni-Kale U, Ojha J, Manjari GS, Deobagkar DD, Mallya AD, Dhere RM, et al. Mapping antigenic diversity and strain specificity of mumps virus: A bioinformatics approach. Virology 2007;359:436–46. doi:http://dx.doi.org/10.1016/j.virol.2006.09.040.

[110] Alsheikhly AR, Orvell C, Andersson T, Perlmann P. The role of serologically defined epitopes on mumps virus HN-glycoprotein in the induction of virus-dependent cell-mediated cytotoxicity. Analysis with monoclonal antibodies. Scand J Immunol 1985;22:529–38.

[111] Örvell C, Alsheikhly AR, Kalantari M, Johansson B. Characterization of genotype-specific epitopes of the HN protein of mumps virus. J Gen Virol 1997;78:3187–93.

[112] Yates PJ, Afzal MA, Minor PD. Antigenic and genetic variation of the HN protein of mumps virus strains. J Gen Virol 1996;77 (Pt 10:2491–7. doi:10.1099/0022-1317-77-10-2491.

[113] Reyes-Leyva J, Banos R, Borraz-Arguello M, Santos-Lopez G, Rosas N, Alvarado G, et al. Amino acid change 335 E to K affects the sialic-acid-binding and neuraminidase activities of Urabe AM9 mumps virus hemagglutinin-

neuraminidase glycoprotein. Microbes Infect 2007;9:234–40. doi:10.1016/j.micinf.2006.11.011.

[114] Sauder CJ, Zhang CX, Link MA, Duprex WP, Carbone KM, Rubin SA. Presence of lysine at aa 335 of the hemagglutinin-neuraminidase protein of mumps virus vaccine strain Urabe AM9 is not a requirement for neurovirulence. Vaccine 2009;27:5822–9. doi:http://dx.doi.org/10.1016/j.vaccine.2009.07.051.

[115] Santos-Lopez G, Scior T, Borraz-Arguello M del T, Vallejo-Ruiz V, Herrera-Camacho I, Tapia-Ramirez J, et al. Structure-function analysis of two variants of mumps virus hemagglutinin-neuraminidase protein. Braz J Infect Dis 2009;13:24–34.

[116] Sauder CJ, Zhang CX, Ngo L, Werner K, Lemon K, Duprex WP, et al. Gene-specific contributions to mumps virus neurovirulence and neuroattenuation. J Virol 2011;85:7059–69. doi:10.1128/JVI.00245-11.

[117] Cui A, Brown DWG, Xu W, Jin L. Genetic Variation in the HN and SH Genes of Mumps Viruses: A Comparison of Strains from Mumps Cases with and without Neurological Symptoms. PLoS One 2013;8:e61791.

[118] Crennell S, Takimoto T, Portner A, Taylor G. Crystal structure of the multifunctional paramyxovirus hemagglutinin-neuraminidase. Nat Struct Biol 2000;7:1068–74. doi:10.1038/81002.

[119] Yuan P, Thompson TB, Wurzburg BA, Paterson RG, Lamb RA, Jardetzky TS. Structural studies of the parainfluenza virus 5 hemagglutinin-neuraminidase tetramer in complex with its receptor, sialyllactose. Structure 2005;13:803–15. doi:10.1016/j.str.2005.02.019.

[120] Welch BD, Yuan P, Bose S, Kors CA, Lamb RA, Jardetzky TS. Structure of the Parainfluenza Virus 5 (PIV5) Hemagglutinin-Neuraminidase (HN) Ectodomain. PLoS Pathog 2013;9:e1003534.

[121] Kubota M, Takeuchi K, Watanabe S, Ohno S, Matsuoka R, Kohda D, et al. Trisaccharide containing α2,3-linked sialic acid is a receptor for mumps virus. Proc Natl Acad Sci 2016;113:11579–84. doi:10.1073/pnas.1608383113 .

[122] Wolinsky JS, Stroop WG. Virulence and persistence of three prototype strains of mumps virus in newborn hamsters. Arch Virol 1978;57:355–9. doi:10.1007/BF01320075.

[123] McCarthy M, Jubelt B, Fay DB, Johnson RT. Comparative studies of five strains of mumps virus in vitro and in neonatal hamsters: evaluation of growth, cytopathogenicity, and neurovirulence. J Med Virol 1980;5:1–15. doi:10.1002/jmv.1890050102.

[124] Yin H-S, Wen X, Paterson RG, Lamb RA, Jardetzky TS. Structure of the parainfluenza virus 5 F protein in its metastable, prefusion conformation. Nature 2006;439:38–44.

[125] Welch BD, Liu Y, Kors CA, Leser GP, Jardetzky TS, Lamb RA. Structure of the cleavage-activated prefusion form of the parainfluenza virus 5 fusion protein. Proc Natl Acad Sci U S A 2012;109:16672–7. doi:10.1073/pnas.1213802109.

[126] Yoshida N, Nakayama T. Leucine at Position 383 of Fusion Protein Is Responsible for Fusogenicity of Wild-Type Mumps Virus in B95a Cells. Intervirology 2010;53:193–202.

[127] Tanabayashi K, Takeuchi K, Okazaki K, Hishiyama M, Yamada A. Identification of an amino acid that defines the fusogenicity of mumps virus. J Virol 1993;67:2928–31.

[128] Waning DL, Schmitt AP, Leser GP, Lamb RA. Roles for the Cytoplasmic Tails of the Fusion and Hemagglutinin-Neuraminidase Proteins in Budding of the Paramyxovirus Simian Virus 5. J Virol 2002;76:9284–97. doi:10.1128/JVI.76.18.9284-9297.2002.

[129] Dutch RE, Lamb RA. Deletion of the cytoplasmic tail of the fusion protein of the paramyxovirus simian virus 5 affects fusion pore enlargement. J Virol 2001;75:5363–9. doi:10.1128/JVI.75.11.5363-5369.2001.

[130] Oomens AGP, Bevis KP, Wertz GW. The Cytoplasmic Tail of the Human Respiratory Syncytial Virus F Protein Plays Critical Roles in Cellular Localization of the F Protein and Infectious Progeny Production . J Virol 2006;80:10465–77. doi:10.1128/JVI.01439-06.

[131] Stone R, Takimoto T. Critical Role of the Fusion Protein Cytoplasmic Tail Sequence in Parainfluenza Virus Assembly. PLoS One 2013;8:e61281.

[132] Hagiwara K, Sato H, Inoue Y, Watanabe A, Yoneda M, Ikeda F, et al. Phosphorylation of measles virus nucleoprotein upregulates the transcriptional activity of minigenomic RNA. Proteomics 2008;8:1871–9.

[133] Yang J, Koprowski H, Dietzschold B, Fu ZF. Phosphorylation of rabies virus nucleoprotein regulates viral RNA transcription and replication by modulating leader RNA encapsidation. J Virol 1999;73:1661–4.

[134] Huang M, Sato H, Hagiwara K, Watanabe A, Sugai A, Ikeda F, et al. Determination of a phosphorylation site in Nipah virus nucleoprotein and its involvement in virus transcription. J Gen Virol 2011;92:2133–41.

[135] Sugai A, Sato H, Yoneda M, Kai C. Phosphorylation of measles virus nucleoprotein affects viral growth by changing gene expression and genomic RNA stability. J Virol 2013;87:11684–92.

[136] Becker S, Huppertz S, Klenk HD, Feldmann H. The nucleoprotein of Marburg virus is phosphorylated. J Gen Virol 1994;75 (Pt 4):809–18.

[137] Gombart AF, Hirano A, Wong TC. Nucleoprotein phosphorylated on both serine and threonine is preferentially assembled into the nucleocapsids of measles virus. Virus Res 1995;37:63–73.

[138] Lenard J. Host cell protein kinases in nonsegmented negative-strand virus (mononegavirales) infection. Pharmacol Ther 1999;83:39–48.

[139] Mazumder B, Adhikary G, Barik S. Bacterial expression of human respiratory syncytial viral phosphoprotein P and identification of Ser237 as the site of phosphorylation by cellular casein kinase II. Virology 1994;205:93–103.

[140] Das T, Schuster A, Schneider-Schaulies S, Banerjee AK. Involvement of cellular casein kinase II in the phosphorylation of measles virus P protein: identification of phosphorylation sites. Virology 1995;211:218–26.

[141] De BP, Gupta S, Banerjee AK. Cellular protein kinase C isoform zeta regulates human parainfluenza virus type 3 replication. Proc Natl Acad Sci U S A 1995;92:5204–8.

[142] Huntley CC, De BP, Banerjee AK. Phosphorylation of Sendai virus phosphoprotein by cellular protein kinase C zeta. J Biol Chem 1997;272:16578–84.

[143] Liu Z, Huntley CC, De BP, Das T, Banerjee AK, Oglesbee MJ. Phosphorylation of canine distemper virus P protein by protein kinase C-zeta and casein kinase II. Virology 1997;232:198–206.

[144] Sun M, Fuentes SM, Timani K, Sun D, Murphy C, Lin Y, et al. Akt plays a critical role in replication of nonsegmented negative-stranded RNA viruses. J Virol 2008;82:105–14.

[145] Hirsch AJ. The use of RNAi-based screens to identify host proteins involved in viral replication. Future Microbiol 2010;5:303–11. doi:10.2217/fmb.09.121.

[146] Ivancic-Jelecki J, Santak M, Forcic D. Variability of hemagglutinin-neuraminidase and nucleocapsid protein of vaccine and wild-type mumps virus strains. Infect Genet Evol 2008;8:603–13. doi:10.1016/j.meegid.2008.04.007.

[147] Alirezaie B, Aghaiypour K, Shafyi A. Genetic characterization of RS-12 (S-12), an Iranian isolate of mumps virus, by sequence analysis and comparative genomics of F, SH, and HN genes. J Med Virol 2008;80:702–10. doi:10.1002/jmv.21087.

[148] Odisseev H, Gacheva N. Vaccinoprophylaxis of mumps using mumps vaccine, strain Sofia 6, in Bulgaria. Vaccine 1994;12:1251–4.

[149] Lamb RA, Kolakofsky D. Paramyxoviridae: The viruses and their replication. In: Knipe DM, Howley PM, Griffin DE, Lamb RA, Martin MA, Roizman B, et al., editors. Fields Virol. 4th Ed, Philadelphia: Lippincott Williams and Wilkins; 2001, p. 1305–40.

[150] Asenjo A, Calvo E, Villanueva N. Phosphorylation of human respiratory syncytial virus P protein at threonine 108 controls its interaction with the M2-1 protein in the viral RNA polymerase complex. J Gen Virol n.d.;87:3637–42.

[151] Timani KA, Sun D, Sun M, Keim C, Lin Y, Schmitt PT, et al. A single amino acid residue change in the P protein of parainfluenza virus 5 elevates viral gene expression. J Virol n.d.;82:9123–33.

[152] Sun D, Luthra P, Li Z, He B. PLK1 down-regulates parainfluenza virus 5 gene expression. PLoS Pathog n.d.;5:e1000525.

[153] Sun D, Luthra P, Xu P, Yoon H, He B. Identification of a phosphorylation site within the P protein important for mRNA transcription and growth of parainfluenza virus 5. J Virol n.d.;85:8376–85.

[154] Sugai A, Sato H, Yoneda M, Kai C. Phosphorylation of measles virus phosphoprotein at S86 and/or S151 downregulates viral transcriptional activity. FEBS Lett n.d.;586:3900–7.

[155] Lenard J. Host cell protein kinases in nonsegmented negative-strand virus (mononegavirales) infection. Pharmacol Ther 1999;83:39–48. doi:10.1016/S0163-7258(99)00016-9.

[156] Villanueva N, Navarro J, Méndez E, García-Albert I. Identification of a protein kinase involved in the phosphorylation of the C-terminal region of human respiratory syncytial virus P protein. J Gen Virol n.d.;75 (Pt 3):555–65.

[157] Huntley CC, De BP, Banerjee AK. Phosphorylation of Sendai virus phosphoprotein by cellular protein kinase C ζ. J Biol Chem 1997;272:16578–84. doi:10.1074/jbc.272.26.16578.

[158] Carbone KM, Wolinsky JS. Mumps virus. In: Knipe DM, Howley PM, editors. Fields Virol. 4th Ed, New York: Lippincott Williams and Wilkins; 2001, p. 1381–441.

[159] Zengel J, Pickar A, Pei X, Lin A, He B. The roles of phosphorylation of the nucleocapsid protein of mumps virus in regulating viral RNA transcription and replication. J Virol 2015;89:7338–47. doi:10.1128/JVI.00686-15.

[160] Luthra P, Sun D, Wolfgang M, He B. AKT1-dependent Aativation of NF-κB by the L protein of parainfluenza virus 5. J Virol 2008;82:10887–95. doi:10.1128/JVI.00806-08.

[161] Eckerdt F, Strebhardt K. Polo-like kinase 1: target and regulator of anaphase-promoting complex/cyclosome-dependent proteolysis. Cancer Res 2006;66:6895–8. doi:10.1158/0008-5472.CAN-06-0358.

[162] Elia AEH, Cantley LC, Yaffe MB. Proteomic screen finds pSer/pThr-binding domain localizing Plk1 to mitotic substrates. Science n.d.;299:1228–31.

[163] Silljé HHW, Nigg EA. Signal transduction. Capturing polo kinase. Science n.d.;299:1190–1.

[164] Wu Z-Q, Liu X. Role for Plk1 phosphorylation of Hbo1 in regulation of replication licensing. Proc Natl Acad Sci U S A n.d.;105:1919–24.

[165] Lowery DM, Lim D, Yaffe MB. Structure and function of Polo-like kinases. Oncogene n.d.;24:248–59.

[166] Curran J, Marq JB, Kolakofsky D. An N-terminal domain of the Sendai paramyxovirus P protein acts as a chaperone for the NP protein during the nascent chain assembly step of genome replication. J Virol n.d.;69:849–55.

[167] Horikami SM, Curran J, Kolakofsky D, Moyer SA. Complexes of Sendai virus NP-P and P-L proteins are required for defective interfering particle genome replication in vitro. J Virol n.d.;66:4901–8.

[168] Fuentes SM, Sun D, Schmitt AP, He B. Phosphorylation of paramyxovirus phosphoprotein and its role in viral gene expression. Future Microbiol n.d.;5:9–13.

[169] Pickett BE, Greer DS, Zhang Y, Stewart L, Zhou L, Sun G, et al. Virus pathogen Database and Analysis Resource (ViPR): A comprehensive bioinformatics Database and Analysis Resource for the Coronavirus research community. Viruses 2012;4:3209–26. doi:10.3390/v4113209.

[170] Kumar S, Stecher G, Tamura K. MEGA7: Molecular Evolutionary Genetics Analysis version 7.0 for bigger datasets. Mol Biol Evol 2016:msw054. doi:10.1093/molbev/msw054.

[171] Jones DT, Taylor WR, Thornton JM. The rapid generation of mutation data matrices from protein sequences. Bioinformatics 1992;8:275–82. doi:10.1093/bioinformatics/8.3.275.

[172] Arnold K, Bordoli L, Kopp J, Schwede T. The SWISS-MODEL workspace: A web-based environment for protein structure homology modelling. Bioinformatics 2006;22:195–201. doi:10.1093/bioinformatics/bti770.

[173] Schrödinger, LLC. The {PyMOL} Molecular Graphics System, Version~1.8. 2015.

[174] Shi H, Liu L, Ma S, Chen J, Che Y, Wang J, et al. Molecular epidemiology of mumps virus strains circulating in south-west China from 2007 to 2009. J Med Microbiol 2011;60:1496–501. doi:10.1099/jmm.0.021907-0.

[175] Ennis R. The Possibility Of Neutrality. Educ Theory 1969;19.

[176] Mahon BP, Flynn MA. Cell Mediated and Humoral Immune responses to Mumps Virus: Recent Developments. Recent Res Dev Virol 2003;5:97–115.

[177] Speel LF, Osborn JE, Walker DL. An Immuno-Cytopathogenic Interaction between Sensitized Leukocytes and Epithelial Cells Carrying a Persistent Noncytocidal Myxovirus Infection. J Immunol 1968;101:409–17.

[178] Pickar A, Zengel J, Xu P, Li Z, He B. Mumps Virus Nucleoprotein Enhances Phosphorylation of the Phosphoprotein by Polo-Like Kinase 1. J Virol 2015;90:1588–98. doi:10.1128/JVI.02160-15.

[179] Hersh BS, Fine PE, Kent WK, Cochi SL, Kahn LH, Zell ER, et al. Mumps outbreak in a highly vaccinated population. J Pediatr 1991;119:187–93.

[180] ACIP. Measles prevention: supplementary statement. MMWR 1989;38:4.

[181] CDC. Notifiable Diseases/Deaths in Selected Cities Weekly Information. MMWR 2006;55:316–27.

[182] Albertson JP, Clegg WJ, Reid HD, Arbise BS, Pryde J, Vaid A, et al. Mumps Outbreak at a University and Recommendation for a Third Dose of Measles-Mumps-Rubella Vaccine - Illinois, 2015-2016. MMWR Morb Mortal Wkly Rep 2016;65:731–4. doi:10.15585/mmwr.mm6529a2.

[183] Zamir CS, Schroeder H, Shoob H, Abramson N, Zentner G. Characteristics of a large mumps outbreak: Clinical severity, complications and association with vaccination status of mumps outbreak cases. Hum Vaccin Immunother 2015;11:1413–7. doi:10.1080/21645515.2015.1021522.

[184] Vygen S, Fischer A, Meurice L, Mounchetrou Njoya I, Gregoris M, Ndiaye B, et al. Waning immunity against mumps in vaccinated young adults, France 2013. Euro Surveill Bull Eur Sur Les Mal Transm = Eur Commun Dis Bull 2016;21. doi:10.2807/1560-7917.ES.2016.21.10.30156.

[185] Rubin SA, Qi L, Audet SA, Sullivan B, Carbone KM, Bellini WJ, et al. Antibody Induced by Immunization with the Jeryl Lynn Mumps Vaccine Strain Effectively Neutralizes a Heterologous Wild-Type Mumps Virus Associated with a Large Outbreak. J Infect Dis 2008;198:508–15.

[186] Latner DR, McGrew M, Williams NJ, Sowers SB, Bellini WJ, Hickman CJ. Estimates of Mumps Seroprevalence May Be Influenced by Antibody Specificity and Serologic Method. Clin Vaccine Immunol 2014;21:286–97. doi:10.1128/CVI.00621-13.

[187] Brgles M, Bonta M, Šantak M, Jagušić M, Forčić D, Halassy B, et al. Identification of mumps virus protein and lipid composition by mass spectrometry. Virol J 2016;13:1–10. doi:10.1186/s12985-016-0463-0.

[188] Santak M, Orvell C, Gulija TK. Identification of conformational neutralization sites on the fusion protein of mumps virus. J Gen Virol 2015;96:982–90. doi:10.1099/vir.0.000059.

[189] Russell CJ, Jardetzky TS, Lamb RA. Conserved glycine residues in the fusion peptide of the paramyxovirus fusion protein regulate activation of the native state. J Virol 2004;78:13727–42. doi:10.1128/JVI.78.24.13727-13742.2004.

[190] Bose S, Heath CM, Shah PA, Alayyoubi M, Jardetzky TS, Lamb RA. Mutations in the parainfluenza virus 5 fusion protein reveal domains important for fusion

triggering and metastability. J Virol 2013;87:13520–31. doi:10.1128/JVI.02123-13.

[191] Gardner AE, Martin KL, Dutch RE. A Conserved Region between the Heptad Repeats of Paramyxovirus Fusion Proteins is Critical for Proper F Protein Folding. Biochemistry 2007;46:5094–105. doi:10.1021/bi6025648.

[192] WHO. Mumps 2016. http://www.who.int/biologicals/areas/vaccines/mmr/mumps/en/ (accessed September 17, 2016).

[193] Collins SD. Age Incidence of the Common Communicable Diseases of Children: A Study of Case Rates among All Children and among Children Not Previously Attacked and of Death Rates and the Estimated Case Fatality. Public Heal Reports 1929;44:763–826. doi:10.2307/4579202.

[194] Brooks H. Epidemic parotitis as a military disease. Med Clin North Am 1918;2:492–505.